

Protective Effects of Substituted 1(Benzyl)1-H-1,2,3 Triazole Compounds on the Dissolution of Iron in HCl Solution

by

Abdullatif Ibrahim Al-Abdulahdi

A Thesis Presented to the

FACULTY OF THE COLLEGE OF GRADUATE STUDIES

KING FAHD UNIVERSITY OF PETROLEUM & MINERALS

DHAHRAN, SAUDI ARABIA

In Partial Fulfillment of the
Requirements for the Degree of

MASTER OF SCIENCE

In

CHEMISTRY

January, 1995

INFORMATION TO USERS

This manuscript has been reproduced from the microfilm master. UMI films the text directly from the original or copy submitted. Thus, some thesis and dissertation copies are in typewriter face, while others may be from any type of computer printer.

The quality of this reproduction is dependent upon the quality of the copy submitted. Broken or indistinct print, colored or poor quality illustrations and photographs, print bleedthrough, substandard margins, and improper alignment can adversely affect reproduction.

In the unlikely event that the author did not send UMI a complete manuscript and there are missing pages, these will be noted. Also, if unauthorized copyright material had to be removed, a note will indicate the deletion.

Oversize materials (e.g., maps, drawings, charts) are reproduced by sectioning the original, beginning at the upper left-hand corner and continuing from left to right in equal sections with small overlaps. Each original is also photographed in one exposure and is included in reduced form at the back of the book.

Photographs included in the original manuscript have been reproduced xerographically in this copy. Higher quality 6" x 9" black and white photographic prints are available for any photographs or illustrations appearing in this copy for an additional charge. Contact UMI directly to order.

UMI

**A Bell & Howell Information Company
300 North Zeeb Road, Ann Arbor, MI 48106-1346 USA
313:761-4700 800:521-0600**

**TO MY FAMILY
&
PARENTS**

ACKNOWLEDGMENT

Acknowledgment is due to King Fahd University Of Petroleum and Minerals for support of this research.

I wish to express my appreciation to Dr. Abdallah Abdennabi who served as my major advisor. I also wish to thank the other members of my Thesis Committee Dr. H. Saricimen, Prof. S. M. Sultan, and Dr. S. Abu Orabi who helped in synthesizing the compounds used in this work.

Finally, I would like to thank my company, Saudi ARAMCO, for giving me the opportunity to pursue the MS degree.

TABLE OF CONTENTS

	Page
LIST OF TABLES	viii
LIST OF FIGURES	x
ABSTRACT	xv
CHAPTER 1 INTRODUCTION	1
Objectives	2
Methodology	3
Summary of the results	5
CHAPTER 2 BASICS OF ELECTROCHEMICAL CORROSION	
2.1 Electrochemical Reactions	7
2.2 Electrode Thermodynamics and kinetics	9
2.2.1 Nernst Equation	9
2.2.2 Activation Polarization	10
2.2.3 Concentration polarization	12
2.2.4 Mixed Potential Theory	12
2.3 Corrosion Rate Expressions	13
2.4 Equilibrium and Non-equilibrium Aspects of Electrochemistry	14

2.5	Corrosion Rate Measurements	17
2.5.1	Tafel Plot Technique	18
2.5.1.1	Effect of Concentration Polarization	22
2.5.1.1	Effect of Solution Resistance	23
2.5.2	Linear Polarization Technique	24
2.5.3	On-line Corrosion Monitoring Technique	28
2.5.4	AC impedance Technique	30
2.5.4.1	Analysis of ACIS Data	32
CHAPTER 3	CORROSION INHIBITORS	37
3.1	Definition and Introduction	37
3.2	Types of Inhibitors	38
3.3	Inhibition Mechanisms	39
3.4	Structure/ Inhibition Relationship	42
3.5	Triazole as Organic Inhibitors	44
3.6	Mild steel Inhibition by Triazole Compounds	46
CHAPTER 4	MATERIALS AND EXPERIMENTAL APPROACHES	
4.1	Materials	51
4.2	Structural Background of the Studied Chemicals	52
4.3	Synthesis of the Studied Chemicals	54
4.3.1	1(Substituted of benzyl) 4,5 dibenzoyl 1,2,3 triazole	54
4.3.2	Dimethyl 1(benzyl & 4-bromobenzyl) 1-H-1,2,3 triazole 4,5 dicarboxylate	55
4.3.3	Methyl & ethyl 1(benzyl) 1-H- 1,2,3 triazole 4- carboxylate	55
4.4	Experimental Procedure	56
4.4.1	Instrumentation	56
4.4.2	Solution Preparation	58
4.5	System Reproducibility	59
4.6	Cleaning Procedure	61

4.7	Chemical Applications	61
4.8	Optimization of Some experimental conditions	62
	4.8.1 Purging Time	62
	4.8.2 Solvent Effects	64
	4.8.3 Dosage Optimization	68
CHAPTER 5	RESULTS AND DISCUSSION	71
5.1	Uninhibited Solution	71
5.2	Inhibited Solution	75
	5.2.1 Substituents at the para- position of 1(benzyl) 4,5 dibenzoyl 1,2,3 triazole	75
	5.2.1.1 Results of Initial & Final ACIS	76
	5.2.1.2 Results of Continuous Polarization	82
	5.2.1.3 Results of Tafel Polarization	92
	5.2.1.4 Discussion	95
	5.2.2 Substituents at 4,5- Positions of the Triazole Cycle	98
	5.2.2.1 Results of Continuous Polarization	99
	5.2.2.2 Results of Tafel Polarization	109
	5.2.2.3 Discussion	113
5.3	Film Persistence test of 1(benzyl) 4,5 dibenzoyl 1,2,3 triazole	118
CHAPTER 6	CONCLUSION	121
6.1	Triazole Evaluation	121
6.2	Proposed Mechanism	123
6.3	Factors Influencing the Inhibition of the Triazole	123
	APPENDIX	125
	NOMENCLATURE	132
	REFERENCES	134

LIST OF TABLES

Table		Page
1	AC impedance equivalent circuit elements representation	33
2	Results of on-line polarization of the blank and in the presence of toluene and ethanol	67
3	Results of Tafel plots of the blank, toluene, and ethanol	67
4	Corrosion rate data for the blank obtained during the continuous monitoring	74
5	Polarization results of 1(benzyl)-1-H-4,5 dibenzoyl 1,2,3 triazole	83
6	Polarization results of 1(4-bromobenzyl)-1-H-4,5 dibenzoyl 1,2,3 triazole	84
7	Polarization results of 1(4-methylbenzyl)-1-H-4,5 dibenzoyl 1,2,3 triazole	84
8	Polarization results of 1(4-nitrobenzyl)-1-H-4,5 dibenzoyl 1,2,3 triazole	84
9a	Tafel plot results of 1(benzyl)-1-H-4,5 dibenzoyl 1,2,3 triazole	92
9b	Tafel plot results of 1 (4-bromobenzyl)-1-H- 4,5 dibenzoyl 1,2,3 triazole	93
9c	Tafel plot results of 1 (4- methylbenzyl)-1-H- 4,5 dibenzoyl 1,2,3 triazole	93

Table	Page
10 Results of dimethyl 1 (benzyl)1-H- 1,2,3 triazole 4,5 dicarboxylate	99
11 Results of dimethyl 1(4-bromobenzyl)1-H-1,2,3 triazole 4,5 dicarboxylate	99
12 Results of methyl 1 (4- bromobenzyl)1-H-1,2,3 triazole 4- carboxylate	100
13 Results of ethyl 1 (4- bromobenzyl)1-H-1,2,3 triazole 4- carboxylate	100
14a Results of Tafel plots of dimethyl 1(benzyl)1-H- 1,2,3 triazole 4,5 dicarboxylate	111
14b Results of Tafel plots of dimethyl 1(4-bromobenzyl) 1-H- 1,2,3 triazole 4,5 dicarboxylate	112
14c Results of Tafel plots of methyl 1(4-bromobenzyl) 1-H-1,2,3 triazole 4- carboxylate	112
14d Results of Tafel plots of ethyl 1(4-bromobenzyl) 1-H- 1,2,3 triazole 4- carboxylate	112
15 Inhibition comparison of the keto and ester groups of 1(benzyl) 1-H-1,2,3 triazole compounds	114
16 Results of chain length effect of 1(4-bromobenzyl) -1-H- 1,2,3 triazole 4- carboxylate	115

LIST OF FIGURES

Figure		Page
1	Schematic representation of Tafel plot	22
2	Current - potential scan for calculating corrosion rate	29
3	Equivalent electrical circuit for bare metal specimen	33
4	Circuit that models impedance under diffusion process	34
5	Nyquist plot representation	35
6	Bode plot representation	36
7	Octet and sextet resonance structures	53
8	Schematic representation of a rotating electrode	57
9	Typical electrochemical corrosion test cell	57
10	Block diagram of the testing instrument	58
11	Corrosion rate Vs. time of 10 mpy prover	60
12	Statistical fit of the corrosion rate measurements of 10 mpy prover	60
13	Effect of purging rate and time on the corrosion rate	63

Figure	Page
14 Effect of addition of toluene and ethanol on the corrosion rate of carbon steel electrode	65
15 Potential behavior of the blank solution in the presence of toluene and ethanol	66
16 Tafel polarization scans of the blank solution in the presence of toluene and ethanol	68
17 Tafel plot of 1(benzyl)-1-H-4,5 dibenzoyl 1,2,3 triazole at 100 ppm	69
18 Corrosion rate and potential measurements of 1(benzyl) -1-H-4,5 dibenzoyl 1,2,3 triazole	70
19 Initial AC impedance scan of the blank solution	71
20 Results of the continuous monitoring of the blank solution	73
21 Final AC impedance scan of the blank solution	74
22 Tafel polarization scan of the blank solution	75
23 Initial and final Nyquist plots of 1(benzyl) -1-H- 4,5 dibenzoyl 1,2,3 triazole	79
24 Initial and final Nyquist plots of 1(4- bromobenzyl) -1-H- 4,5 dibenzoyl 1,2,3 triazole	79

Figure		Page
25	Initial Nyquist plots of 1(benzyl)-1-H- 4,5 dibenzoyl 1,2,3 triazole	80
26	Final Nyquist plots of 1(benzyl)-1-H- 4,5 dibenzoyl 1,2,3 triazole	80
27	Initial Nyquist plots of 1(4- bromobenzyl) -1-H- 4,5 dibenzoyl 1,2,3 triazole	81
28	Final Nyquist plots of 1(4- methylbenzyl) -1-H- 4,5 dibenzoyl 1,2,3 triazole	81
29	Final Nyquist plots of 1(4- nitrobenzyl) -1-H- 4,5 dibenzoyl 1,2,3 triazole	82
30	Corrosion rate measurements of 1(benzyl) -1-H- 4,5 dibenzoyl 1,2,3 triazole	85
31	Corrosion rate measurements of 1(4-bromobenzyl) -1-H-4,5 dibenzoyl 1,2,3 triazole	86
32	Corrosion rate measurements of 1(4-methylbenzyl) -1-H-4,5 dibenzoyl 1,2,3 triazole	87
33	Corrosion rate measurements of 1(4-nitrobenzyl) -1-H-4,5 dibenzoyl 1,2,3 triazole	88
34	Potential Vs. time of 1(benzyl)-1-H-4,5 dibenzoyl 1,2,3 triazole	89

Figure	Page
35 Potential Vs. time of 1(4-bromobenzyl)-1-H-4,5 dibenzoyl 1,2,3 triazole	90
36 Potential Vs. time of 1(4-methylbenzyl)-1-H-4,5 dibenzoyl 1,2,3 triazole	91
37 Tafel scans of 1(benzyl)-1-H-4,5 dibenzoyl 1,2,3 triazole at 10,25, and 50 ppm	94
38 Tafel scans of 1(4-bromobenzyl)-1-H-4,5 dibenzoyl 1,2,3 triazole at 10,25, and 50 ppm	94
39 Tafel scans of 1(4-methylbenzyl)-1-H-4,5 dibenzoyl 1,2,3 triazole at 25 and 50 ppm	95
40 Corrosion rate Vs. time of dimethyl 1(benzyl)1-H-1,2,3 triazole 4,5 dicarboxylate at 10 and 25 ppm	101
41 Corrosion rate Vs. time of dimethyl 1(4-bromo-benzyl)1-H-1,2,3 triazole 4,5 dicarboxylate	102
42 Corrosion rate Vs. time of methyl 1(4-bromo-benzyl)1-H-1,2,3 triazole 4- carboxylate	103
43 Corrosion rate Vs. time of ethyl 1(4-bromobenzyl) 1-H-1,2,3 triazole 4- carboxylate	104
44 Potential Vs. time of dimethyl 1(benzyl)1-H-1,2,3 triazole 4,5 dicarboxylate at 10 and 25 ppm	105
45 Potential Vs. time of dimethyl 1(4-bromobenzyl)1-H-1,2,3 triazole 4,5 dicarboxylate at 10 and 25 ppm	106

Figure	Page
46 Potential Vs. time of methyl 1(4-bromobenzyl)1-H-1,2,3 triazole 4- dicarboxylate at 10 and 25 ppm	107
47 Potential Vs. time of ethyl 1(4-bromobenzyl)1-H-1,2,3 triazole 4- dicarboxylate at 10 and 25 ppm	108
48 Tafel plots of dimethyl 1(benzyl)1-H-1,2,3 triazole 4,5 dicarboxylate at 10 and 25 ppm	109
49 Tafel plots of dimethyl 1(4-bromobenzyl)1-H-1,2,3 triazole 4,5 dicarboxylate at 10 and 25 ppm	110
50 Tafel plots of methyl 1(4-bromobenzyl)1-H-1,2,3 triazole 4- carboxylate at 10 and 25 ppm	110
51 Tafel plots of ethyl 1(4-bromobenzyl)1-H-1,2,3 triazole 4- carboxylate at 10 and 25 ppm	111
52 Corrosion rates behavior of both methyl & ethyl of 1(4-bromobenzyl)1-H-1,2,3 triazole 4-carboxylate at 10 ppm	116
53 Corrosion rates behavior of both methyl & ethyl of 1(4-bromobenzyl)1-H-1,2,3 triazole 4-carboxylate at 25 ppm	117
54 Film persistency test of 1(benzyl)-1-H-4,5 dibenzoyl 1,2,3 triazole after 30 minutes filming in 10,000 ppm	119
55 Film persistency test of 1(benzyl)-1-H-4,5 dibenzoyl 1,2,3 triazole after 60 minutes filming in 10,000 ppm	120

THESIS ABSTRACT

ABDULLATIF IBRAHIM AL- ABDULHADI

PROTECTIVE EFFECTS OF SUBSTITUTED 1(BENZYL)1-H- 1,2,3 TRIAZOLE COMPOUNDS ON THE DISSOLUTION OF IRON IN HCl SOLUTION

CHEMISTRY

January 30, 1995

Understanding the structure of the organic compounds can provide a very useful tool in selecting the best inhibitors. To demonstrate that, the corrosion behavior of mild steel electrode in the presence of eight triazole compounds were studied in deaerated solution of 1% HCl. Three electrochemical techniques in conjunction with rotating cylinder electrode were employed at 1000 rpm.

The tested compounds exert interface inhibition with a cathodic behavior. 1 (benzyl)-1-H-4,5 dibenzoyl 1,2,3 triazole gave the best results and suppressed the corrosion rate to more than 95% at 50 ppm at room temperature. Also, its film persistence test indicated that the formed film is inert and long lasting.

MASTER OF SCIENCE DEGREE

KING FAHD UNIVERSITY OF PETROLEUM AND MINERALS
DHAHRAN 31261, SAUDI ARABIA

January 30, 1995

بسم الله الرحمن الرحيم

خلاصة الرسالة

عبد اللطيف إبراهيم العبد الهادي

دراسة تأثير وجود مركبات النيتروجين الثلاثية الحلقية في إذابة مادة الحديد في وجود حامض الهيدروكلوريك .

كيمياء :

٢ شعبان ١٤١٥ هـ

يمكن استخدام بنية المركبات العضوية كوسيلة لإختيار أفضل موانع الصدأ . ولتطبيق ذلك قمت بدراسة تأثير ثمانية مركبات تنتمي الى مجموعة ثلاثية النيتروجين الحلقية على قطب من الحديد غُمس في محلول الهيدروكلوريك في غياب عنصر الأوكسجين . حيث أستخدم ثلاث تقنيات كهروكيميائية وصلت بقطب دوار تحت سرعة ١٠٠٠ د/ن .

لوحظ أن هذه المركبات تسلك نموذج الإمتصاص الداخلي وسلوك تثبيطي سالب . كذلك فإن مركب ١ (بنزيل) - ١ - هـ - ٤ ، ٥ ثنائي البنزيل ١ ، ٢ ، ٣ ثلاثية النيتروجين الحلقية اعطى أفضل النتائج حيث قلل من معدل التآكل الى ٩٥ ٪ عند تركيز ٥٠ جزء من المليون .

CHAPTER 1

INTRODUCTION

Acid solutions have wide industrial applications for instance, they are commonly used in; industrial cleaning, in acid descaling, and in acid pickling of process equipment. Among the acids used, hydrochloric acid is considered the most frequently used commercially available acid. However, this acid is the most difficult to handle from the point of corrosion and materials of construction. Extreme care is required in the selection of materials to handle hydrochloric acid by itself, or in process solutions containing appreciable amounts of this acid. Moreover, hydrochloric acid is very corrosive to most of the common metals and alloys.

In oil and gas industries for example, hydrochloric acid is generally used in cleaning applications. These applications include:

- Oil well stimulation
- Boiler tube cleaning
- Oil transport pipelines and flowlines descaling, and
- Gas flowlines cleaning.

Because of the cost of the cleaning process and its potential for short term corrosion damage to the equipment, it has become necessary to determine what corrosion protection technique will be optimal during cleaning.

Corrosion inhibitors have been found to be the most effective and flexible means of corrosion mitigation. Selecting the effective inhibitor was based to a great extent on an empirical approach. However, the understanding of corrosion processes has increased significantly over the past thirty years, so that the subject is no longer an empirical one, but it has an extensive theoretical background. This has resulted in introducing new inhibitor products and a new treatment methodology for the oil and gas industries. However, it seems that the molecular structure of the inhibitor and the nature of bonding that occur at the surfaces to be protected are essential to any serious investigations especially if organic inhibitors are being considered.

OBJECTIVES

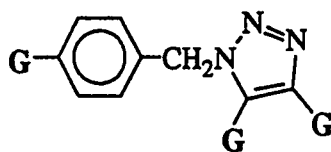
The general objective of this study was to investigate and/or correlate the effect of chemical structure of *triazole ring* and its inhibition action on mild steel in deaerated hydrochloric acid solution.

Specifically, the objectives consisted of the following:

- I- To investigate the theoretical aspects that explains the relations between the structure of the compound and its inhibition effect.
- II- To investigate the interaction between the acid and the inhibitors used.
- III- To understand the effect of certain functional groups on the inhibition performance .
- IV- To determine the substituent that has the major inhibition effect .
- V- To elucidate the substitution site which has the most effect in reducing corrosion rate, and
- VI- To find out the effectiveness of the substituent on batch treatment compared with continuous treatment.

METHODOLOGY

In order to fulfill the objectives of the study, different substituents of *1(Benzyl)-1-H- 1,2,3- triazole* compounds which can be classified into two groups as shown below were studied :



G represents substitution site

- 1- Substituents at *para*- position of the benzyl ring including H, CH₃, Br, or NO₂
- 2- Substituents at positions of 4 & 5 of the triazole ring such as H, CO₂CH₃, CO₂C₂H₅, or COC₆H₅

The evaluation of the inhibitors was carried out by using three electrochemical techniques namely; AC impedance, on-line linear polarization, and Tafel polarization.

The inhibition effects of the following triazole compounds were investigated in deaerated solution of 1% hydrochloric acid:

- 1- 1(Benzyl)1-H-4,5- Dibenzoyl-1,2,3- Triazole
- 2- 1-(4- Bromobenzyl) 1-H-4,5- Dibenzoyl-1,2,3- Triazole
- 3- 1-(4- Nitrobenzyl) 1-H-4,5- Dibenzoyl-1,2,3- Triazole
- 4- 1-(4- Methylbenzyl)-1-H-4,5- Dibenzoyl-1,2,3-Triazole
- 5- Dimethyl 1-(Benzyl)-1-H-1,2,3-Triazole 4,5- Dicarboxylate
- 6- Dimethyl 1-(4- Bromobenzyl)-1-H-1,2,3-Triazole 4,5- Dicarboxylate
- 7- Methyl 1-(4-Bromobenzyl)-1-H-1,2,3-Triazole 4- Carboxylate
- 8- Ethyl 1-(4-Bromobenzyl)-1-H-1,2,3-Triazole 4- Carboxylate

SUMMARY OF THE RESULTS

Among the compounds which were studied, 1-(benzyl)-1-H-4,5-dibenzoyl 1,2,3 triazole gave the best result and suppressed the corrosion rate to more than 95% at 50 ppm at room temperature. Substitution at the aromatic ring showed pronounced effect on the corrosion rate. It has been observed that electron withdrawing substituents had minimized the corrosion protection.

It was found also that an increase in the inhibitor concentration have decreased both the corrosion rate and the corrosion current. A shift in the corrosion potential, E_{Corr} , to more negative values has been observed. The inhibition efficiency of the 1-(*4-substituted* benzyl)-1-H-4,5-dibenzoyl 1,2,3 triazole derivatives follows the order: $\text{H} < \text{Br} < \text{CH}_3 < \text{NO}_2$. The performance ranking of the substituents at 4 and 5 positions of the triazole ring are as follow: $\text{I} > \text{III} > \text{II} > \text{IV}$.

The one hour film persistence of the 1(benzyl)-1-H-4,5-dibenzoyl 1,2,3 triazole compound test indicated that it can be safely used for batch treatment where the corrosion rate was maintained to 3 mpy up to 4000 minutes.

The E_{Corr} of the steel shifted to the more negative potentials in the presence of the compounds compare to the blank solution. These compounds can be classified as cathodic inhibitors depending on their effect on the corrosion potential. Moreover, it was noticed from Tafel plots that, the anodic scan of the 1(benzyl)-1- H- 4,5 - dibenzoyl 1,2,3 triazole compound has a potential independent region at current range from 4×10^{-5} to 1×10^{-3} A/ cm^2 .

Finally, the initial and final AC impedance scans suggested adsorption processes were taken place during the exposure and the adsorbed film is affected by both concentration and exposure period.

CHAPTER 2

BASICS OF ELECTROCHEMICAL CORROSION

2.1 ELECTROCHEMICAL REACTIONS

The electrochemical nature of corrosion can be illustrated by considering the dissolution of iron metal by hydrochloric acid. When iron metal is immersed in dilute hydrochloric acid, both reduction and oxidation processes occur on its surface. Typically, the metal oxidizes (corrodes) and some species in the solution is reduced, consequently hydrogen gas is liberated. The metal usually acts as both an anode and a cathode, and consequently anodic and cathodic currents occur on the metal surface. Corrosion processes that occur are usually a result of anodic currents. The reaction can be expressed as follow:

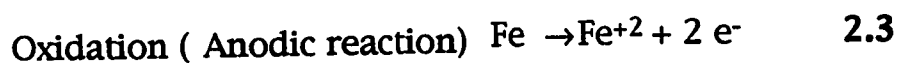


Equation 2.1 can be written in the simplified form:



Examining the above equation, it can be seen that during the reaction, Iron is oxidized to iron(II) ions and hydrogen ions are

reduced to hydrogen gas. Thus equation 2.2 can be conveniently divided into two reactions, the oxidation of iron and the reduction of hydrogen ions:



Equations 2.3 and 2.4 are partial reactions, both must occur simultaneously and at the same rate on the metal surface. The electrochemical circuit is completed by the electrolytic conductivity of the salt solution and the electronic conductivity of the metal. Each of the equal currents flowing both ways at equilibrium is called the exchange current . Also, as a result of the corrosion process, an electrochemical potential will be established which is usually called the corrosion potential or the open circuit potential, E_{corr} . This type of potential occurs at the metal-solution interface and can be measured indirectly. It can also be compared to the potential of a known reference system.

If the value of the exchange current is large, there will be a large change in current for a given change in potential. In practice, this means that the electrode for which the exchange current is high will exhibit a potential that is stable and difficult to disturb significantly as SHE [73]. On the other hand, if the exchange current is small, large differences in potential from equilibrium can lead only to small net restoring currents, and the electrode is said to be readily polarized [73].

At E_{corr} , the rate of oxidation process is exactly equal to and nonzero of the reduction process and is said to be at equilibrium. It is possible to impose potentials other than E_{corr} at the metal-solution interface by a potential source. Imposing potential or polarization stimulates the oxidation or reduction reactions on the specimen. If the polarization process is carried out in a systematic manner then, the value of oxidation or reduction currents, i_{ox} or i_{red} respectively, at E_{corr} can be easily determined. The resulting current is commonly called the corrosion current, I_{corr} , and is directly related to the corrosion rate. So the polarization process is associated with two processes: a net flow of current and a net shift of the electrode potential from equilibrium [54].

2.2 ELECTRODE THERMODYNAMICS AND KINETICS

The corrosion behavior of a certain metal can be described using different approaches such as[56]:

- Nernst equation
- Activation potential
- Concentration potential
- Mixed potential theory

2.2.1 Nernst Equation is a modification of the Gibb's Free Energy equation and it expresses the thermodynamic tendency of a corrosion reaction to proceed in terms of EMF based on the activities of the products and reactants of the half-cell reaction [56].

$$E = E_0 - 2.3 \frac{RT}{nF} \log \frac{a_{\text{product}}}{a_{\text{reactant}}} \quad 2.5$$

- E : half-cell potential
 E₀ : standard half-cell potential
 R : gas constant
 T : absolute temperature
 n : number of electrons transferred
 F : Faraday constant
 a : activities of the products or reactants

As indicated in the above equation, half-cell potential becomes more positive as the amount of products species increases. The over potential of the cell is the algebraic sum of both the oxidation potential and the reduction potential of each half-cell reaction.

2.2.2 Activation Polarization is used to indicate retarding factors that are inherent in the reaction itself [65]. It is caused by a slow electrode reaction. In the case of hydrogen reduction at a cathode:



where H_{ads} represents hydrogen atoms adsorbed on the metal surface. This relatively rapid reaction is followed by a combination of adsorbed hydrogen atoms to form hydrogen molecules and bubbles of gaseous hydrogen.



This reaction is relatively slow, and it is the rate determining step.

Activation polarization potential is characteristic of metal-ion deposition or dissolution. The value of this potential can be small for non-transition metals like silver and zinc, but for the transition metals like iron, the value of activation potential is high [57].

Activation polarization, η_a , of any kind, increases with current density i_o . The relationship between reaction rate and overvoltage for activation polarization, η_a , is given by the following relationships [56,58]:

$$i_{\text{anodic}} = i_o e^{\left(\frac{nF\alpha\eta_a}{RT}\right)} \quad 2.8$$

$$i_{\text{cathodic}} = i_o e^{\left(\frac{-nF(1-\alpha)\eta_a}{RT}\right)} \quad 2.9$$

where

i_{anodic} , i_{cathodic} are anodic and cathodic current respectively
 α symmetry coefficient which describes the shape of the rate-controlling of energy barrier

By rearranging the above equation, the activation polarization η_a can be written as:

$$\eta_a = \pm \beta \log \left(\frac{i}{i_o} \right) \quad \text{where } \beta = \frac{2.3RT}{\alpha nF} \quad 2.10$$

β is termed as Tafel constant

For small deviation from E_{corr} , the relationship between overvoltage and current density is a linear function.

2.2.3 Concentration Polarization, η_c , It refers to the retardation of an electrochemical reaction as a result of concentration changes in the solution adjacent to the metal surface [65]. Concentration polarization of an electrode in the absence of activation polarization, is expressed as :

$$\eta_c = \frac{2.3}{nF} RT \log \left(1 - \frac{i}{i_L} \right) \quad 2.11$$

$$i_L: \quad \text{limiting current density} = \frac{D n F C_B}{\delta} \quad 2.12$$

D diffusion coefficient of the reacting ions
 C_B concentration of the reacting ions in the bulk solution
 δ thickness of the diffusion layer

From equation 2.12, the limiting current is inversely proportional to the thickness of the diffusion layer. The effect of concentration polarization can be minimized by agitating or heating the solution [56,58].

2.2.4 Mixed Potential Theory : The concepts of this theory were well known before 1900, however, it was attributed to Wagner and Traud in 1938, and popularized by Stern and Geary [56,58,62]. It consists of two hypotheses:

- 1- Any electrochemical reaction can be divided into two or more partial oxidation and reduction reactions
- 2- There can be no net accumulation of electric charge during an electrochemical reaction. This is merely a restatement of the law of conservation of charge. It follows that during the corrosion of an electrically isolated metal sample, the total rate of oxidation must be equal the total rate of reduction.

2.3 CORROSION RATE EXPRESSIONS

Due to a considerable number of reasons, the rate of corrosion of any material must be expressed quantitatively. Some of these reasons can be summarized as follows [60]:

- comparison of corrosive properties of chemicals,
- evaluating the behavior of materials,
- estimating the life of the selected material,
- determining the aggressiveness of a process fluid [77]

There are several ways of expressing the corrosion rates. Examples are given in the following [57]:

percent weight loss	% wt loss
milligrams per square centimeter per day	mcd
milligrams per square decimeter per day	mdd
grams per square inch per hour	gih

inches per year	ipy
milliinches (miles) per year	mpy

The last expression is the most common unit for expressing the corrosion rates and it will be used in this work.

2.4 EQUILIBRIUM AND NON EQUILIBRIUM ASPECTS OF ELECTROCHEMISTRY

One of the most significant types of polarization is activation polarization. When the rate of an electrochemical reaction is controlled by the activation energy. A theoretical model of the current/ overvoltage reaction can be drawn up in the form of the *Butler- Volmer Equation 2.13* where the concentration polarization or mass transfer effects on the current is neglected [73,78]

$$I = i_o \left\{ e^{\left[\frac{(1-\alpha) F \eta}{RT} \right]} - e^{\left[\frac{-\alpha F \eta}{RT} \right]} \right\} \quad 2.13$$

where α is the symmetry factor and usually equals 0.5 for Fe, Ni, Cu, and several other metal [57,73].

There are two important limiting cases of the *Butler- Volmer Equation* .

I- When η is large (> 50 mV):

For large values of η (either negative or positive), one of the

bracketed terms in the *Butler- Volmer Equation* becomes small and may be neglected. For example, at large positive values of η , $e^{\left[\frac{(1-\alpha) F\eta}{RT}\right]} \gg e^{\left[\frac{-\alpha F\eta}{RT}\right]}$ and equation 2.13 becomes:

$$I = i_0 e^{\left[\frac{(1-\alpha) F\eta}{RT}\right]} \quad \text{for positive values of } \eta, \quad 2.14$$

or

$$I = i_0 e^{\left[\frac{-\alpha F\eta}{RT}\right]} \quad \text{for negative values of } \eta, \quad 2.15$$

Equation 2.14 may be rewritten as:

$$\ln I = \ln i_0 + \frac{(1-\alpha) F\eta}{RT} \quad 2.16$$

or as:

$$\eta = - \frac{RT}{(1-\alpha) F} \ln i_0 + \frac{RT}{(1-\alpha) F} \ln I \quad 2.17$$

Thus, we find that the kinetic treatment outlined above does yield a relation of the Tafel form for the appropriate conditions. Since only η and I are variables for a given electrode system, this reduces to:

$$\eta = a + b \ln I \quad 2.18$$

where a and b are constants and equal to $\frac{2.3 RT}{\alpha n F} \log i_0$ and $-\frac{2.3 RT}{\alpha n F}$ respectively.

This is the so called Tafel equation, in which the linear relationship between overvoltage and logarithm of current was established on an empirical basis. When electrode kinetics are sluggish and significant activation overpotentials are required, good Tafel relationships can be seen [78]. Also, it is a fact that Tafel

behavior is an indicator of totally irreversible kinetics where no significant current flow except at high overpotentials[78]. As a result the faradaic process is effectively unidirectional and, therefore, chemically irreversible.

II- When $|\eta|$ is small (< 20 mV):

In this case, the exponential terms in the equation may be replaced by the first two terms in the McLaurin series expansion of e^x and the *Butler-Volmer Equation* 2.13 becomes:

$$I = i_o \left[1 + \frac{(1-\alpha) F \eta}{RT} - 1 + \frac{\alpha F \eta}{RT} \right] \quad 2.19$$

where

$$I = \frac{i_o F \eta}{RT} \quad 2.20$$

and:

$$\eta = \frac{RT I}{i_o F} \quad 2.21$$

Equations 2.20 and 2.21 show that the net current is linearly related to overpotential at a narrow potential range near E_{Corr} . The significance of this approach is that low overvoltage laboratory studies of reactions under activation control can be made with adequate experimental control and can allow calculation of i_o or i_{corr} . Tafel constants derived from this serve as the basis for predicted behavior under the more practical condition of high overvoltage. This constitutes the so called linear polarization method for study of corrosion processes. Since the ratio $\frac{\eta}{I}$ has dimensions of

resistance and is often called either charge transfer resistance¹⁷ or polarization resistance.

2.5 CORROSION RATE MEASUREMENTS

Electrochemical techniques are now widely applied in corrosion field and in industrial problems. Also, they help in formulating criteria and establishing an objective classification in material selection and inhibitor testing [67]. Electrochemical corrosion results from the flow of current between the anodic and the cathodic areas on a metal surface. The effect of an inhibitor is to reduce this type of current which will in turn decrease the corrosion effect. The most common electrochemical techniques used to determine corrosion rate are Tafel extrapolation and linear polarization. The mixed-potential theory forms the basis for these tools [62].

Generally, all electrochemical methods are based on Faraday's Law relating the mass flux per unit area and time with the current flux [64]. The great advantages of electrochemical methods are:

- The relatively short time of measurement [67] and
- Possibility of on-line corrosion monitoring [62].

However, a main disadvantages of all electrochemical methods is the perturbation caused on the corroding system by an externally imposed polarization which will affect the electrode surface. Another limitation of electrochemical methods is the presumption that the

entire surface of the corroding sample is accessible to uniform corrosion [62]. For many inhibited and uninhibited systems this is not true.

In studying corrosion processes, it is advantageous to control the electrochemical reaction of the electrode separately by letting it to act as either an anode or a cathode. By separating the two processes, we can follow the behavior of the electrode in the medium. If the electrode is polarized anodically, then the anodic current predominates at the expense of the cathodic current. As the electrode potential is driven further positive, the cathodic current component becomes negligible with respect to the anodic components.

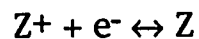
2.5.1 Tafel Plot Technique:

Most corrosion measurements involve a scan of the working electrode potential and measuring the resulting current. This is referred to as a potentiodynamic scan, since the applied potential continuously changes.

Tafel mode which is an example of potentiodynamic technique, is used to measure corrosion current. The Tafel plot yields corrosion current and Tafel constants β_c and β_A . These constants can then be used to calculate either I_{corr} or R_p .

Tafel plot can be generated by scanning the electrode potential to ± 250 mV vs. E_{Corr} . The resulting curve is a plot of applied potential Vs. logarithm of measured current. Under ideal conditions, the Tafel plot will be linear from -50 to -250 mV and from +50 to +250 mV vs. E_{Corr} . The slopes of these linear regions are called cathodic and anodic Tafel constants [74].

In a corroding system, two co- existing electrochemical reactions are present [47.48.57.69]



Where M is the corroding metal and Z^+ is usually a species in a solution. In the above system, oxidation of the metal and the reduction of certain species in solution usually takes place at the same rate, and the net measurable current will be zero:

$$I_{\text{MEAS}} = I_{\text{O,M}} - I_{\text{R,Z}} = 0 \quad 2.22 \quad \text{and}$$

$$I_{\text{Corr}} = I_{\text{O,M}} = I_{\text{R,Z}} \quad 2.23 \quad \text{at } E_{\text{Corr}}$$

Unfortunately, only the total current is measurable, and the net current is zero as shown by the preceding equation.

The mechanism of corrosion is extremely complex if it is compared with a homogeneous chemical system. This is because several different elements can exist in the tested specimen, also a great deal of different compounds of each element may be present or

may be formed during corrosion process. In addition, there are the surface effects that have to be considered. For these reasons, corrosion rate measurements must be made rather non-specific with regard to the element in the metal or alloy [69].

The electrochemical corrosion rate measurement is usually based on the determination of the oxidation current at the corrosion potential. This current is called the corrosion current I_{CORR} . Equation 2.22 defining I_{MEAS} may now be rewritten as:

$$I_{\text{MEAS}} = I_{\text{CORR}} - I_{\text{R,Z}} = 0 \quad 2.24 \text{ at } E_{\text{CORR}}$$

The corrosion current, I_{CORR} , is then related directly to corrosion rate.

The current can be deduced in many cases by displacing the open circuit potential of the metal by applying gradually increasing voltages from an external potential source to produce a linear plot of potential against log current density, i.e., the Tafel region. Extrapolation back to the open circuit potential value will then provide the corrosion current, I_{CORR} [39]. When a potential is applied, a current will pass according to the following equation:

$$I_{\text{MEAS}} = I_{\text{O,M}} - I_{\text{R,Z}} = I_{\text{CORR}} \quad 2.25$$

Since the reaction rate is controlled by a slow chemical step that requires an activation energy [47.57.69]

$$I_{\text{R,Z}} = I_{\text{CORR}} e^{-\eta/\beta} \quad 2.26$$

$$I_{O,Z} = I_{CORR} e^{\eta/\beta''} \quad 2.27$$

where

η : overvoltage, and equal to $E_{APP} - E_{CORR}$.

β', β'' constants

Taking the log of the above equations and solving for η yields

$$\eta = -\beta_c \log \frac{I_{R,Z}}{I_{CORR}} \quad 2.28$$

and

$$\eta = \beta_A \log \frac{I_{O,M}}{I_{CORR}} \quad 2.29 \text{ where}$$

$\beta_c = 2.3\beta'$ and $\beta_A = 2.3\beta''$ which vary from 0.03 to 0.30 V [47]

The above equations are called Tafel equations after J. Tafel, who proposed an equation of similar form in 1904 to express hydrogen overvoltage as a function of current density.

As the difference between E_{app} and E_{corr} becomes more negative, I_{MEAS} approaches $I_{R,Z}$. Solving equation 2.22 for $I_{R,Z}$ and substituting in equation 2.28 gives:

$$\eta = -\beta_c \log \frac{I_{MEAS} + I_{O,Z}}{I_{CORR}} \quad 2.30$$

A plot of η Vs $\log I_{MEAS}$ is shown in **Figure 1**. Deviation from linear Tafel behavior occurs at low current levels. A true Tafel relationship be obtained only when the oxidation current becomes insignificant with respect to the reduction current [47]. So the Tafel

behavior depends only on the activation overvoltage. The measurement may be complicated where there is concentration polarization and IR drop in the solution [47].

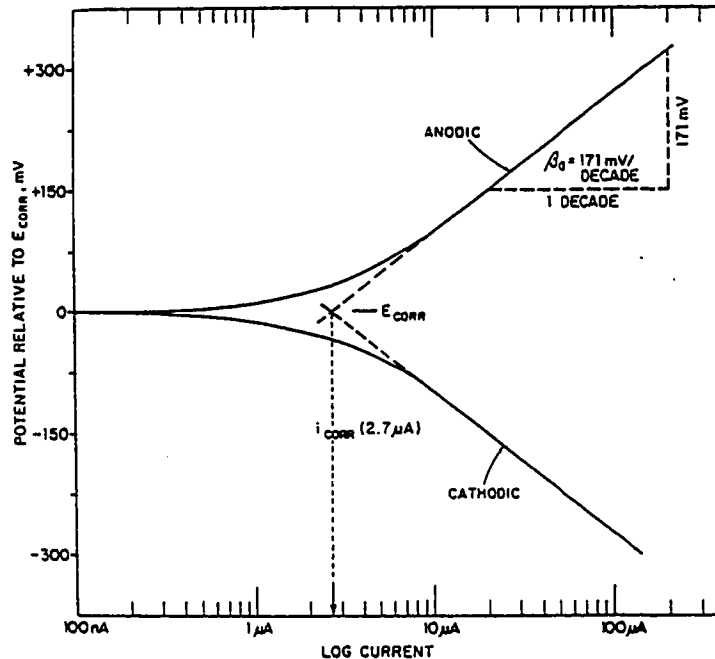


Figure 1: Schematic representation of Tafel plot

2.5.1.1 Effect of Concentration Polarization

Concentration polarization occurs when the reaction rate is so high that the electroactive species cannot reach or be removed from the electrode surface at a sufficiently rapid rate. The reaction rate becomes diffusion controlled. As η increases, the current becomes diffusion limited and the linear current range is truncated [47,69].

The effect of concentration polarization is minimized by stirring the solution. It may be represented in its simplest form as shown in equation 2.11.

2.5.1.2 Effect of Solution Resistance

Electrochemical cells are designed to allow current to flow between the working and counter electrodes. A reference electrode is inserted near the working electrode to sense the applied potential which is then fed back to the associated potentiostat to control its potential. However, no matter how closely the reference is positioned to the working electrode, there will always be some solution resistance between them [47,69]. Since a large current often flows through the solution, there can be a significant voltage (or IR) drop between the working and reference electrodes. Solution resistance drops can also cause non-linear Tafel behavior at high currents since:

$$E = I_{MEAS} * R_{SON} \quad 2.31$$

Moreover, the uncompensated resistance of the solution, R_{uncomp} is the resistance between the working electrode and the reference electrode bridge tube. It prevents the reference electrode from sensing the true potential at the specimen. Instead, it will sense the applied voltage minus the IR drop($E_{APP} - IR_{drop}$) and transmit a distorted reading of the effective potential to the controlling potentiostat [74]. Thus, an error will be introduced into the measurement.

The effects of concentration polarization and resistance drops are most serious when I_0 or I_{CORR} , is large and high currents are needed to verify Tafel behavior.

2.5.2 Linear Polarization Technique

The electrochemical technique of polarization resistance or linear polarization, is another method of measuring corrosion rates. This technique is widely used by both corrosion engineers and scientists [72]. Also, it has been used for many years to study electrochemical corrosion processes. A simple procedure for determining corrosion rate was developed in 1938 by Wagner and Traud on a small potential approximation which has become well established experimentally by Stern and Geary [57,62,64]. The concept depends on the fact that corrosion rate of an electrode is inversely proportional to its polarization resistance.

This technique is usually performed by applying a controlled potential scan over a very small range, typically ± 10 mV with respect to E_{corr} . The resulting current is linearly plotted versus potential. The slope of this potential - current function at E_{corr} is identically the polarization resistance, R_p , which, as will be shown, is used together with the Tafel constants to determine I_{corr} .

Linear polarization technique is a rapid procedure. The rapidity of the measurement makes it useful for less rigorous

experiments, such as qualitative evaluation of inhibitors. In addition, the applied potential in a polarization resistance measurement is very small, hence, the surface of the specimen will not be affected during the experiment. Therefore, the sample can often be used for other studies or for on-line corrosion monitoring [48,70,71].

The theoretical background of the linear polarization technique has been provided by Stern and Geary[47,57,58,68,69]. Using the previous corroding system, where the measured net current will be zero as shown in equations 2.22, 2.23, and 2.24. and the anodic and cathodic currents obey the Tafel equations 2.28 and 2.29 which may be rearranged to give

$$\frac{\eta}{\beta_A} = \log \frac{I_{O.M}}{I_{CORR}} \quad 2.32$$

$$\frac{\eta}{\beta_C} = \log \frac{I_{R.Z}}{I_{CORR}} \quad 2.33$$

or

$$10^{\eta/\beta_A} = \frac{I_{O.M}}{I_{CORR}} \quad 2.34$$

$$10^{-\eta/\beta_C} = \frac{I_{R.Z}}{I_{CORR}} \quad 2.35$$

Substitution of equations 2.34 and 2.35 into equation 2.22 gives

$$I_{MEAS} = I_{CORR} (10^{\eta/\beta_A} - 10^{-\eta/\beta_C}) \quad 2.36$$

If E_{APP} is sufficiently close to E_{CORR} , then it is possible to simplify this equation by making use of a power series expansion (McLaurin Series) of this form:

$$10^x = 1 + 2.3x + \frac{(2.3x)^2}{2!} + \dots + \frac{(2.3x)^n}{n!}$$

If x is small, the third and later terms of the series can be neglected without significant error. Substituting η/β_A and $-\eta/\beta_C$ for x gives:

$$10^{\eta/\beta_A} = 1 + 2.3\eta/\beta_A \quad 2.37$$

$$10^{-\eta/\beta_C} = 1 - 2.3\eta/\beta_C \quad 2.38$$

Substitute equations 2.37 and 2.38 in 2.36 and simplifying

$$I_{MEAS} = 2.3 I_{CORR} \eta \left(\frac{\beta_A + \beta_C}{\beta_A \beta_C} \right) \quad 2.39$$

and substitute for η to give

$$I_{MEAS} = 2.3 I_{CORR} (E_{APP} - E_{CORR.}) \left(\frac{\beta_A + \beta_C}{\beta_A \beta_C} \right) \quad 2.40$$

Solve for E_{APP}

$$E_{APP} = \frac{I_{MEAS} \beta_A \beta_C}{2.3 I_{CORR} (\beta_A + \beta_C)} + E_{CORR} \quad 2.41$$

OR

$$\frac{\eta}{I_{MEAS}} = \frac{\beta_A \beta_C}{2.3 I_{CORR} (\beta_A + \beta_C)} \quad 2.42$$

$$\frac{\Delta E}{\Delta I} = \frac{\beta_A \beta_C}{2.3 I_{CORR} (\beta_A + \beta_C)} = R_p \quad 2.43$$

The above equation was derived by Stern and Geary[58,68]. In the above equation, ΔE is the difference in potential of the corroding electrode produced by a polarizing current, ΔI . Stern showed that :

- 10 mV or less was the optimum value for ΔE [68]
- concentration polarization effects would not be expected to alter the results seriously [68], and
- the slope ($\Delta E / \Delta I$) is controlled mainly by I_{corr} and is relatively insensitive to changes in beta values[58]

Equation 2.41 predicts that I_{MEAS} and E_{APP} will be linearly related at potentials close to E_{CORR} . In a Linear polarization experiment the conditions are usually selected so that this correlation of I_{MEAS} and E_{CORR} can be observed.

Traditionally, corrosion data from a Linear Polarization experiment is plotted as E vs. I . It is easy to see from equation 2.41, that when I_{MEAS} is 0, the Y- intercept will be E_{CORR} . The slope from these plots is termed the polarization resistance. The ratio of $\frac{\Delta E}{\Delta I}$ has the units of resistance which commonly abbreviated as R_p and given in units of ohms as shown in equation 2.43. It is important to realize that this relation is valid only if $\frac{\eta}{\beta}$ is small.

In addition, if $E_{\text{app}} = E_{\text{CORR}}$, I_{MEAS} will be zero which means that the anodic current must balance the cathodic current at E_{CORR} as concluded from equation 2.40. Also, at potentials greater than E_{CORR} the anodic reaction predominates, while at potentials less than E_{CORR} the cathodic reaction predominates.

The polarization resistance plot has two advantages over a Tafel plot. These advantages include: the short time of measuring R_p and R_p technique exposes the specimen to smaller voltages which will not change the surface of the specimen.

Once the R_p is determined, the corrosion rate can be calculated in milli-inches per year(mpy) from the following equations:

$$I_{\text{corr}} = \frac{\beta_A \beta_c}{2.3 R_p (\beta_A + \beta_c)} \quad 2.44$$

$$\text{CORROSION RATE (mpy)} = \frac{0.13 I_{\text{corr}} E.W}{A d} \quad 2.45$$

where

I_{corr}	corrosion current in μA
2.3	the natural log of ten
β_A, β_c	Tafel constants in V/ decade of current
E.W	equivalent weight g/eq
A	area in cm^2
d	density g/cm^3
0.13	metric and time conversion factor

2.5.3 On-line Corrosion Monitoring Technique

Close attention has been directed at corrosion monitoring in an attempt to develop some measurement techniques and elaborate on some calculation methods for the interpretation of experimental results. This has led to computerization of experimental measurements and development of relevant software for on-line monitoring of the corrosion rate. The developed on-line software is based on linear polarization technique.

The program has been developed in The Laboratories Research and Development Center of the Saudi ARAMCO Oil Company. This program provides the software necessary to control the potentiostat model 273A from a host computer via the GPIB interface card. Actual measurements which are done by this program are entirely controlled by complex subroutines run on the host computer.

After opening data file, The subroutine initially clears the video screen of the potentiostat, checks the system, searches for the instrument's GBIP address, and then executes the scanning commands. If the potentiostat generates an output, it will be sent to an opened file for saving after performing the necessary calculations. In addition, once the measurements are performed, potential versus current is plotted and the corrosion rate is calculated after finding R_p from the slope of the line as illustrated in FIGURE 2. The linear regression of the potential-current relationship is determined and saved. E_{CORR} is also measured and recorded before each scan.

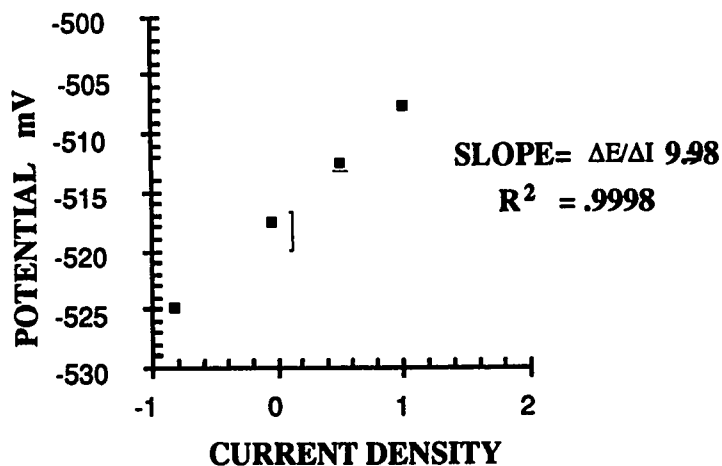


Figure 2: Current- potential scan for calculating corrosion rate

The program requires windows software installation, GPIB interface, and a potentiostat. It performs the following operations:

- 1- All of the data concerning the corrosion rate calculation are read from an open file including the surface area of the sample, density, equivalent weight of the electrode, as well as the Tafel constants as shown in Appendix 1.
- 2- Correction of the ohmic drop is made. Where current-interrupt mode is used. The test is interrupted at many points for very short period of times (< 0.0002 seconds). Each time, a new value of E_{Corr} is determined and the value of E_{App} is appropriately corrected.
- 3- Saving the data in the opened file. Also, the user can change the range of the data, merge two files, or perform data analysis.

2.5.4 AC Impedance Technique:

Both DC and AC techniques have been used in the evaluation of the organic inhibitor. DC techniques some time tend to introduce measurement errors due to the ohmic potential drop across the high resistance of the adsorbed organic film. Moreover, DC techniques may lead to irreversible changes of the substrate/ adsorbed film interface

as a result of the large signal perturbations employed. AC techniques on the other hand, employ small perturbations of the order of ± 5 mV. Consequently, the AC technique leaves the testing system unchanged.

Electrochemical impedance spectroscopy (EIS), or AC impedance spectroscopy (ACIS), as it is popularly called, has gained an acceptance in recent years [80-83] as a laboratory tool for evaluating and selecting organic inhibitors and coatings. The technique is also able to:

- 1- Supply valuable mechanistic information on the stages involved in inhibitor filming,
- 2- Provide quantitative means of comparing the performance of different inhibitors,
- 3- Use very small signals which do not disturb the electrode properties to be measured, and
- 4- Provide valuable information on the kinetics and associated interfacial phenomena during film degradation

In the ACIS technique, a small sinusoidal voltage is applied across the specimen. The current response of the specimen to the applied voltage is then measured using a transfer function analyzer. The output data is analyzed by computer to produce plots of impedance response over a very wide frequency range. This enables one to separate the various processes participating in the corrosion

phenomena, and to determine their relative contribution. Also, the automated data collection employed optimizes the impedance measurements with respect to both speed and accuracy. In this way, mechanistic information and patterns of performance and behavior can be built up long before visible signs of failure occur or retreatment schedule.

2.5.4.1 Analysis of ACIS data: The response of any linear system to a perturbation of arbitrary form may be described by an impedance Z [80-84]

$$Z(j\omega) = Z' + jZ'' \quad 2.46$$

$$Z(j\omega) = [(Z')^2 + (Z'')^2]^{1/2} \quad 2.47$$

$$\tan\theta = \frac{|Z''|}{|Z'|} \quad 2.48$$

where

Z' and Z'' are the real and imaginary components of impedance



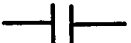
$$j = \sqrt{-1}$$

ω angular frequency and equal to $2\pi f$

θ phase shift in degrees

In AC impedance, the electrode response can be modeled in terms of resistors, inductors, and capacitors. The three basic circuit elements can be written as shown in Table 1.

Table 1
AC impedance equivalent circuit elements representation

CIRCUIT ELEMENT	IMPEDANCE EQUATION
	$Z = R + 0j$
	$Z = 0 + j\omega L$
	$Z = 0 + j/\omega C$

The reactions which occur in an electrochemical system may be represented by a number of equivalent electrical circuits. **Figure 3** may be used to represent the equivalent electrical circuit of uninhibited metal; R_s is the uncompensated electrolyte or solution resistance, C_{dl} is the double layer capacitance (solution /metal interface), and R_p is the polarization resistance.

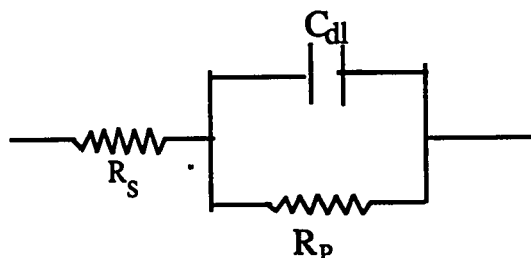


Figure 3: Equivalent electrical circuit for a simple electrochemical cell with bare metal specimen

Once a corrosion film has built up or an adsorption process took place, the electrochemical reaction may be influenced by diffusional processes. In this case the *Warburg impedance*, Z_ω , is

introduced to account for mass transfer caused by the diffusion of one or more of the reactants or products to or from the surface of the metal. This process may result in the surface being covered with reaction products or adsorbed solution components. The equivalent circuit representing a bare metal with a diffusion process at the solution/ metal interface is shown in Figure 4.

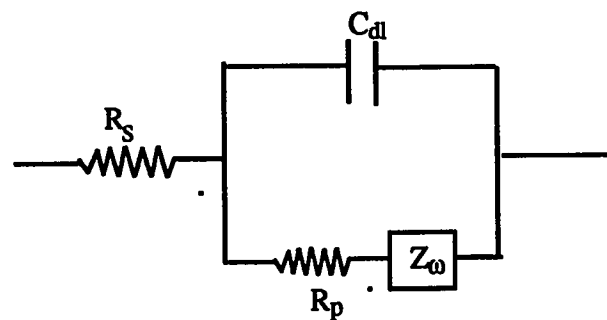


Figure 4: Circuit that models impedance under diffusion processes

The equivalent mathematical forms of the complex impedance for circuit in Figure 3 is given by the following equations:

$$Z(j\omega) = R_s + \frac{R_p}{j\omega R_p C_{dl}} \quad 2.49$$

or

$$Z(j\omega) = R_s + \frac{R_p}{1+(\omega R_p C_{dl})^2} - j \frac{R_p^2 \omega C_{dl}}{1+(\omega R_p C_{dl})^2} \quad 2.50$$

Rearranging equation 2.50 leads to the expression:

$$\left[Z' - \left(R_s + \frac{R_p}{2} \right) \right]^2 + (Z'')^2 = \left(\frac{R_p}{2} \right)^2 \quad 2.51$$

This is an equation of a circle with a radius of $\frac{1}{2} R_p$ and the center of which lies on the Z' -axis at $Z' = (R_s + \frac{R_p}{2})$. The term of this equation lead directly to the two common methods for displaying impedance data: Nyquist or Bode plots.

The Nyquist or cole- cole plot, such that shown schematically in **Figure 5**, is usually used in evaluating AC impedance data [80- 84]. The circuit elements (R_s , R_p , and C_{dl}) can be obtained from the Nyquist plot as illustrated in **Figure 5**.

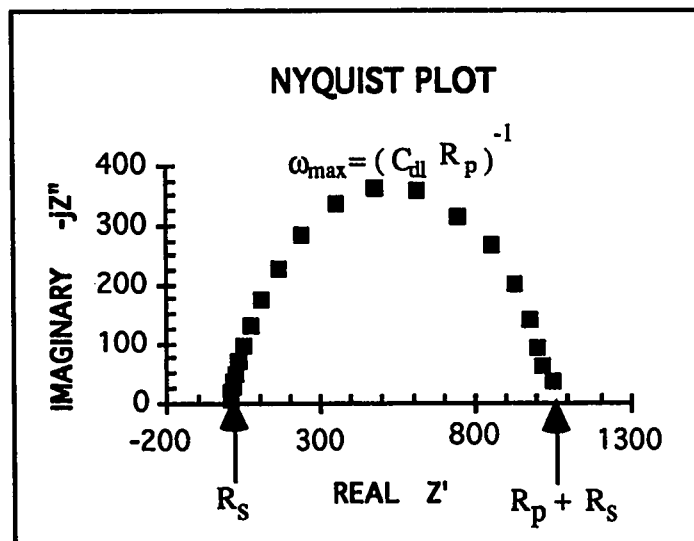


Figure 5: Nyquist or cole- cole plot

A Bode plot, such as that shown in **Figure 6**, is used in conjunction with the Nyquist plot and provides a clear description of the frequency dependent behavior of the corroding cell. The $\log |Z|$ is plotted versus $\log \omega$ where the values of R_s , and R_p can be obtained.

At intermediate frequencies, it should lie on a straight line with a slope of -1. Extrapolating this line to the $\log |Z|$ axis at $\log \omega = 0$, yields the value of C_{dl} from the relationship:

$$|Z| = \frac{1}{C_{dl}} \quad 2.52$$

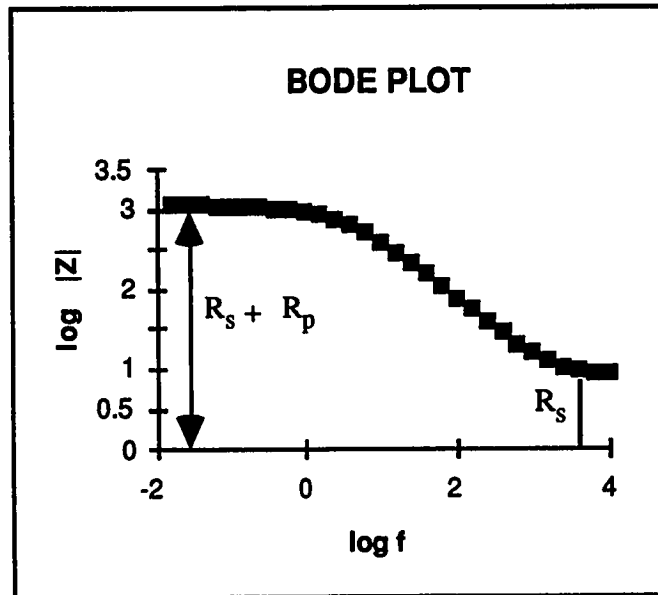


Figure 6: Bode plot representation

CHAPTER 3

CORROSION INHIBITORS

3.1 DEFINITION AND INTRODUCTION

Corrosion inhibitors have been known and used for many years. Many investigators have studied and reported the results of their efforts to elucidate the mechanisms of the inhibitors [45]. These inhibitors still represent the most cost effective and flexible means of corrosion control. They continue to play a key role in controlling internal corrosion associated with oil, water, and gas production and transportation. They can not stop corrosion but slow it to economically acceptable levels.

The shortages of inorganic corrosion inhibitors has increased the demands and interest in organic compounds [63]. Many organic compounds have been reported as effective corrosion inhibitors in the literature, but not a great many are ever used in practical systems[45]. Any practical inhibitor must possess properties beyond its ability to control corrosion including cost, toxicity, and compatibility with the expected environment [45].

The term "*Corrosion Inhibitor* " by common usage is taken to mean addition of a chemical or chemicals to the fluid phase for its effect on the metal [2]. Available references to corrosion phenomena in the technical literature appeared by the end of the 18th century. The first patent in corrosion inhibition was given to Baldwin, British Patent 2327. Robinson and Sutherland in 1900 , US Patent 640491, used starch [2]. Since 1950, the scientific tone on studying corrosion inhibition mechanism increased and the conversion of the field from art to science have started with the recognition of adsorption phenomena [2]. Good inhibition in any system requires an understanding of the chemistry of the system with the inhibitor plus the knowledge of the parameters involved.

3.2 TYPES OF INHIBITORS

There are various inhibitors classifications listed in the literature and books. However, there is no completely satisfactory way to categorize inhibitors. They fall into several classes, for example, some authors classify them according to their interaction with the metal to[54] :

- 1- adsorptive
- 2- bulk film former

Other classify them corresponding to their mechanism into[43]:

- 1- interface
- 2- interphase

Also, they can be categorized in term of their reaction at the metal surface and how the potential on the substrate is affected into [54] :

- 1- anodic
- 2- cathodic
- 3- mixed

Moreover, they can be subdivided depending on their reaction with the substrate and medium into [54]:

- 1- passivator
- 2- precipitator
- 3- neutralizer

Another systematic approach has classified them into [44]:

- 1- barrier layer former
- 2- neutralizer
- 3- scavenger
- 4- miscellaneous

3.3 INHIBITION MECHANISMS

In general, organic corrosion inhibitors contain functional groups which can be adsorbed and then complexed onto the metal substrate. As a result, an insoluble protecting film will be formed. This protecting film will retard the anodic and/or cathodic electrochemical corrosion reactions. An understanding of the surface

chemistry of adsorbed corrosion inhibitors would aid in the elucidation of the mechanism of corrosion inhibition. There are three types of adsorption associated with organic inhibitors[54]:

- 1- π - bond orbital adsorption
- 2- electrostatic adsorption
- 3- chemisorption

Also, the mode of adsorption depends on the following factors [54]:

- 1- the chemical structure of the molecule
- 2- the chemical composition of the solution
- 3- the nature of the metal surface
- 4- the electrochemical potential at the metal-solution interface

Lorenz and Mansfeld [43] have classified the modes of inhibition into two classes: interface and interphase retardation.

1- Interface inhibition is caused by specific adsorption forming two-dimensional layers on the corroding surface. It presumes a strong interaction between the corroding substrate and the inhibitor [43]. The inhibition efficiency decreases with increasing electrode potential because the surface charge becomes more positive and an electrostatic repulsion will weaken the sorption bond. Interface inhibition also can be further subdivided in term of the adsorbed film effect on the electrode surface to:

- geometrical blocking of the electrode by an inert adsorbate film
- deactivating the active sites on the electrode surface
- reactive film where the adsorbate itself undergoes an electrochemical redox process

41

2- Interphase inhibition is caused by a three-dimensional protective layers in which the inhibitor is incorporated. This type is represented by porous or non-porous three-dimensional layers or coatings. The inhibition efficiency depends strongly on the porosity and stability of the formed layer.

In most cases, corrosion inhibition is achieved through interaction or reaction between the corrosion inhibitor and the metal surface, resulting in the formation of an inhibitive surface film. The effect of organic compounds, like *triazole*, on corrosion inhibition depends on their [5,42,63]:

- chemical properties
- structure
- nature and types of the substituents
- metal and corrosion media

The inhibition mechanism of organic compounds is often associated with chemical adsorption, which usually involve a

variation in the charge of the adsorbed substance and also on a charge transfer from one phase to the other[4,63]. Therefore, the molecular structure of the inhibitor assumes special significance. The strength of the adsorption bond depends on the electron density of the atoms within the functional groups and on the properties of the metal as well as on the polarizability of the functional group [4]. There are also other factors that influence the inhibition performance . Amongst these are the nature of the corroding metal, the composition of the corrosive medium, temperature, and the conditions under which the corrosion process occurs[5]. Organic substances which effectively protects a given metal under certain conditions could lose this ability entirely under other conditions, or with other metal surfaces [5] .

3.4 STRUCTURE / INHIBITION RELATIONSHIP

The study of the structure / inhibition relationship of organic compounds has been considered since 1961 when Hackerman and Hurd plotted the degree of inhibition for ring substituted N- methyl amines Vs. the Hammett substituent constant [6]. In 1977, Thibault S., compared the inhibition properties of benzotriazole, benzimidazole, indazole, and indole [7]. Subsequently, many studies have been carried out to correlate the effects of a series of substituents related molecules such as pyridines, benzimidazole, benzotriazole, aliphatic amines, and etc. These studies have shown

that , the inhibitive efficiency would increase as the electron density at the functional group is increased due to easier electron transfer from the functional group of the inhibitor to the metal producing stronger coordinate bonding and hence greater adsorption[6]. For example aniline is an inhibitor for acid media which assumes a small positive charge in acid. It follows that if the acceptor characteristics of aniline could be increased, the inhibitory character of the structure could be made more effective at the same time. Some of the ways this can be accomplished are[54]:

- 1- Use of di- or tri- amino groups, since an electron acceptor is probably not strictly limited to a single position
- 2- Addition of a constituent to the ring to stabilize the electron acceptor characteristics of the amino group(s).
- 3- Addition of a constituent to the ring to give a permanent electron inductive effect or to cause inductomeric effect away from the benzene ring and/ or amino group(s).
- 4- Addition of a constituent to the amino group(s) to accomplish any or all of the above objectives.

Also, the principle of Hard and Soft Acids and Bases (HSAB), has been applied to correlate between the physical properties of

inhibitors and their inhibition efficiency [6,8,42]. For organic inhibitors of similar structure with oxygen, nitrogen, and sulphur as a functional groups; the inhibitor efficiency should follow the sequence $O < N < S$ [6]. Also according to Pearson's concept of the HSAB principle, the polar atoms or ions of "*hard*" acids and bases hold valence electrons tightly and those of "*soft*" acids and bases hold electrons with looseness [42]. The donor atoms of the *hard bases* are of high electronegativity, of low polarizability, and hard to oxidize. The atoms of *soft bases* are in reverse. The acceptor atoms or ions of *hard acids* are small in size, of high positive charge, of high electronegativity, and of low polarizability. The reverse are called acceptors of the soft acids [42]. The hard acids prefer to bind to the hard bases, forming a stable complex bond under the influence of electric interaction, and the soft acids prefer to bind to the soft bases, forming a covalent donor- acceptor bond [42].

3.5 TRIAZOLE AS ORGANIC INHIBITORS

Certain 1,2,4- and 1,2,3 triazole derivatives have been reported to possess useful industrial, as well as biological applications [9,75,76]. They have also been used as chelating ligand with transition metals giving several possible coordination modes due to strong nitrogen donor capacity[10]. C. O' Neal, Jr. ; U.S. Patent 3,985,503; Oct. 12, 1976; assigned to the Sherwin. Williams Company has found, however, that effective amounts of the carboxylated

benzotriazoles including their alkali metal salts and aliphatic esters have improved corrosion inhibiting characteristics and are superior to many of the other triazoles. Generally, this would not be expected since the introduction of a substituent (-COOH) to the benzene ring of benzotriazole increases its molecular weight and thereby lowers the relative proportion of the corrosion inhibiting center [45].

Among the triazole compounds is Benzotriazole which has been reported by many authors to be the most effective inhibitor for the corrosion of copper and its alloys in a large number of aggressive environments [3,7,11-22,41]. It also inhibits the stress corrosion cracking and dezincification of α - Brass under applied anodic potential [41]. In addition to copper inhibition, it has also been used for protection Aluminum and Zinc in acid and alkaline media [6,23] . The inhibition efficiency of some studied triazole derivatives, such as benzotriazole, 3-amino -5- heptyl -1,2,4 triazole and bisaminotriazole, on zinc metal surface depends on the following factors[23]:

- Stability of insoluble zinc triazole complexes formed on the zinc surface
- Solubility and adsorbability of the triazole molecules
- Hydrophobicity of the triazole molecules and triazole layer respectively

The inhibitive properties of benzyltriazole compounds are attributed to the formation of an adherent protective film on the metal surface. The protective films formed by these compounds are inert and long lasting on the metal surface [3,11-21]. The nature of the surface complex in this system have been widely studied using anodic and cathodic polarization, AC impedance, Electron spectroscopy, UV visible reflection spectra, Infra-red reflectance spectra, XPS, SERS ,Spectro electrochemical, Cyclic voltammetry, and weight loss techniques[3,9,11-21,24-27].

Substituted benzyltriazoles have also been extensively studied [12,15,18,21,26] . The inhibition action of other triazole compounds such as 3-amino, 5-heptyl-1,2,4- triazole, naphtha triazole, 3-phenyl 1,2,4-triazol-5-one, 2-amino-thiazole, mercaptobenzothiazole, benzimidazole, 3-amino, 1,2,4 triazole ,1-(3- chloro, 3- nitro, or 3-methoxyl - benzyl)-4, propanone- 1,2,3- triazole, and 4- arylazo pyrazolo -3-5, diamine [13,16,20,25,26,30,27,35,36] have also been investigated.

3.6 MILD STEEL INHIBITION BY TRIAZOLE COMPOUNDS

Despite the extensive studies, very few studies have been conducted on the mechanism of inhibition on steel surfaces using benzyltriazole or other triazole compounds [24,35-37,39] . Generally, when an organic compound is added in hydrochloric acid,

complexes with the steel surface and forms a combination chemical-metal layer which provides both physical and chemical protection [54]. In the case of inhibited iron by benzyltriazole, Robert Chin and co-worker found that the addition of chloride ions did not appreciably affect the rate of hydrogen evolution, but the corrosion potential increased about 25 mv. Also, it has been noticed that, the capacitance of iron in the presence of either chloride ions or *benzotriazole* did not increase with immersion time [24]. Other study showed that, the inhibition of iron using ethyl-1(meta substitutedbenzyl)-1H-1,2,3-triazole-4-carboxylate compounds in deaerated 3M HCl depends on the type of substituent on the benzyl ring [35]. Electron withdrawing groups enhance the desorption while electron releasing groups retard it [35]. Also, it has been noticed that if another triazole group is introduced on the benzyl ring, a remarkable inhibition is observed [35]. Gadallah and coworker found that the retardation efficiency of the different substituted *pyrazole* derivatives follows the order: *methyl* < *methoxyl* < *chloro*. On the other hand, the position of the substituent group with respect to the azo group affected the inhibition efficiency as follows: *ortho* < *para* < *meta* [36]. However, in case of substituted *N- arylpyrroles* the situation is different. The inhibition efficiency of the substituted *N- arylpyrroles* containing halide ions follows the order: *F* > *Br* > *Cl* [4]. The position of the substituent with respect to the benzene ring of the *N- arylpyrrole* affected the inhibition efficiency as follows: *ortho* > *meta* > *para* [4]. The efficiency of

inhibition of benzotriazole and amine mixtures in the corrosion of grey cast iron in chloride solutions has been investigated by Barbusa [37]. He showed that the inhibition is associated with formation of a passive film resulting in an increase in the break down potential of the iron metal. Benzotriazole film stability increases by adsorbing on the surface by a process of electron donation involving the pairs of lone electrons situated at the nitrogen atoms [37].

Comprehensive tests were carried out in Benzimidazole with 2-alkyl side chain on mild steel[38]. About 90 organic compounds were investigated at both heterocycle and side chain in an attempt to demonstrate the effect of structure in the inhibition action. The results of the study have shown that:

- Substitutions at the benzene nucleus influence the electron density, and provide some evidence that an increase in the electron density positively influences the inhibition effect
- Variation of type and length of the side chain bridging link is accompanied by pronounced differentiations in efficiency [38].

It was also found that, the efficiency of 3-(Alditol-1-yl)-1,2,4-triazolo [3,4-a] Phthalazine inhibitor decreases with the increase of the side chain length due to the following factors [6]:

- A decrease in the adsorbability of the molecules were observed as the chain gets longer due to an increase in the hydrophilic character of the molecule causing a higher interaction between the adsorbed molecules at the metal-solution interface and the bulk solution .
- The lesser contribution of the heterocyclic part of the compound as the chain side elongated.

The inhibition actions of other organic compounds such as amines, nitrogen-containing heterocyclic compounds, and sulfur containing compounds [28-34] has also been reported . For example, the interactions and interfacial bonding of pyridine, quinoline, and acridine derivative compounds with metal surfaces of steel in hydrochloric acid solution have been investigated [28]. It has been reported that the adsorption of heterocyclic compounds occurs with the aromatic rings parallel to the metal surface and depends mainly on the electronic structure of the molecules [28-32]. In addition , the inhibition efficiency of these organic compounds increases with the length of the hydrocarbon chain of the n-derivatives and the number of aromatic systems [28].

For example, the mode and strength of bonding to the surface, and the structure of the metal adsorbate complex are important factors that are not clearly understood for the majority of corrosion

inhibitors [3]. Some inhibitors are regarded as being element specific and thus would be expected to exhibit preferential adsorption onto one component of an alloy [3,42].

CHAPTER 4

MATERIALS AND EXPERIMENTAL APPROACHES

4.1 MATERIALS

The chemicals were used as they have been received without any further purification. They were dissolved in ethanol and some of them in toluene . Hydrochloric acid solution of 1% was prepared by diluting the reagent grade hydrochloric acid with distilled water using Baker Analyzed Reagent of 36.5-38% composition.

The electrode was fabricated from mild steel rod. The electrode's dimension were 1.20 cm in length, and 1.20 cm outside diameter with 0.38 cm bore diameter. The surface of the electrodes were prepared to 600 grit, cleaned ultrasonically in acetone, and then rinsed with distilled water.

EG&G Princeton Applied Research (PARC) model 616 rotating cylinder electrode apparatus was used in this study. The rotation can be set up to 9000 rpm, however, above 6000 rpm electrochemical measurements are unreliable[79].

Three electrochemical techniques were used in this study. On-line linear polarization and Tafel techniques as direct current methods. The third method is based on alternating current which is AC impedance. The data obtained by Tafel and AC impedance methods are operated and analyzed using EG&G softwares. The software for on-line linear polarization is written by the Laboratories Research & Development Center.

4.2 STRUCTURAL BACKGROUND OF THE STUDIED CHEMICALS:

The general principle for the synthesis of five membered rings was introduced in 1960 as 1,3-dipolar cycloaddition by Huisgen and co-workers [1]. The 1,3-dipolar is defined as species that is represented by zwitterionic octet structures and undergoes 1,3 cycloadditions to a multiple bond system. These compounds have a sequence of three atoms **a**, **b**, **c**, of which **a** has a sextet of electrons in the outer shell **a**, and **c** an octet with at least one unshared pair. A feature shared by all 1,3 dipoles is an allyl anion type π system, that is, four electrons in three parallel atomic π orbitals. Also, they contain an onium center **b** whose charge compensates the negative charge distributed in the two all octet structures over the two termini **a** and **c** as shown in **Figure 7**.

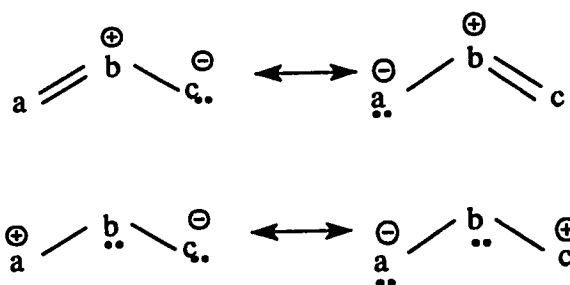


FIGURE 7: The Octet & Sextet Resonance Structures

If we limit ourselves to the first row of the periodic table, **b** can only be **Nitrogen**, **a** can be **Carbon** or **Nitrogen**, and **c** can be **Carbon**, **Oxygen**, or **Nitrogen**. So, there are six types which fit this description among these are **azides** [1] that may be donated as $a=b=c= N$.

Examples of **triazoles** or sometimes referred as **azimines** compared with some of the more familiar dipolar systems are limited for two main reasons:

- 1- Systematic studies of the preparation and properties of triazole compounds not well known until 1970.
- 2- The initial 1,3 dipolar adducts of azimines possess three continuous saturated nitrogen atoms, and the anticipated instability of such species is therefore likely to lead to complicating secondary reactions.

It is convenient to classify the known triazoles as follows:

- All three nitrogen atoms are part of the same cyclic system

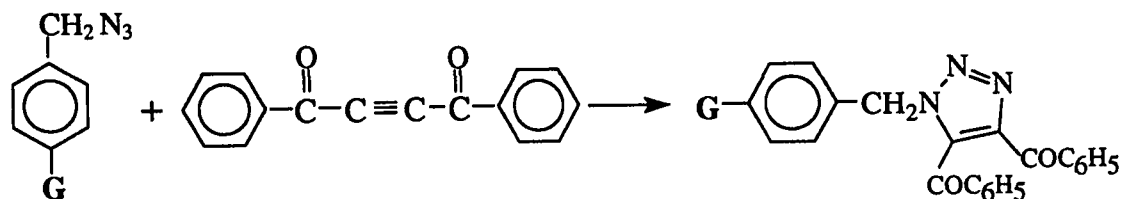
- Two of the nitrogen atoms are part of the same cyclic system (semicyclic).
- Open chain triazoles

4.3 SYNTHESIS OF THE STUDIED CHEMICALS

The use of 1,3-dipolar cycloaddition reaction in organic synthesis has been developed quite recently. Among a plethora of functional groups, azide functionality has etched an important place in organic chemistry.

4.3.1 Substituted 1(Benzyl) -1-H- 4,5 Dibenzoyl 1,2,3 Triazole Compounds:

The 1,3 dipolar cycloaddition reaction of benzylazide or several substituted benzylazides with dibenzoylacetylene afforded the corresponding triazoles in good yields. The reaction can be formulated as follows:

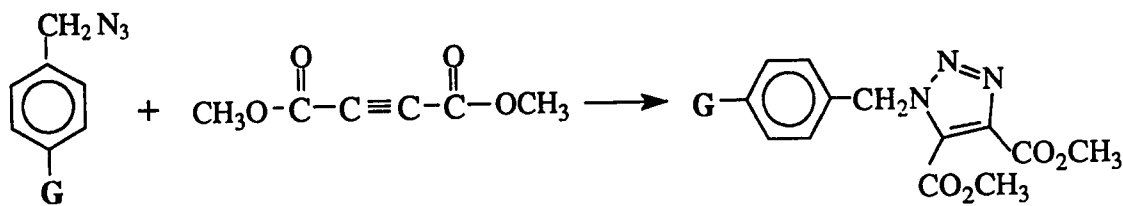


G here represents H, CH₃, Br, or NO₂

The reaction is a thermal concerted process with superficial addition. The heteroatomic triazole ring system is composed of five atoms; two carbons and three nitrogens, which can be arranged in two combinations to give either 1,2,3- or 1,2,4- triazoles.

4.3.2 Dimethyl 1-(Benzyl Or 4- Bromobenzyl)-1-H-1,2,3- Triazole 4,5- Dicarboxylate :

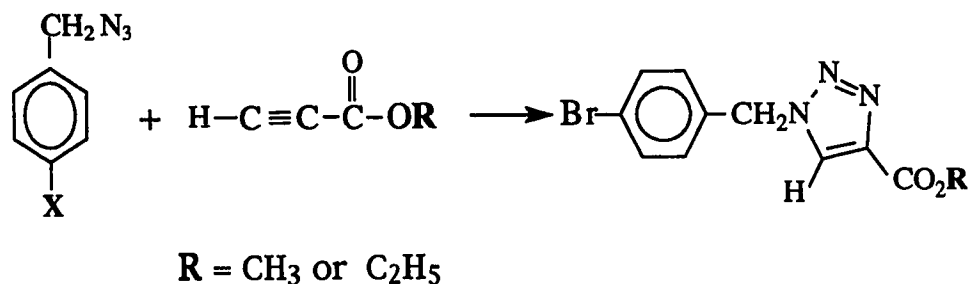
Benzyl azide or 4-bromobenzyl azide is reacted with dimethyl acetylene dicarboxylate in boiling ethanol to give the corresponding triazoles in more than 80% yield. The reaction scheme is shown below [75]:



G : is H or Br

4.3.3 Methyl & Ethyl 1-(4- Bromobenzyl)1-H-1,2,3- Triazole 4- Carboxylate :

The triazoles compounds are formed by the reaction of 4-bromobenzyl azide with methyl or ethyl propiolate in refluxed protic solvent such as methanol or ethanol resulting in forming mono esters as shown bellow [75]:



4.4 EXPERIMENTAL PROCEDURE:

4.4.1 Instrumentation

A schematic representation of the rotating electrode is shown in **Figure 8**. A standard PARC electrochemical cell as shown in **Figure 9**, was used and consisted of a reference electrode, two high density graphite electrodes, and the rotating cylinder as the working electrode. The rotating cylinder apparatus was coupled to a PARC model 273A Potentiostat and a Schlumberger model 1255 Frequency Response Analyzer. An IBM PS/2 model 70 was used for data acquisition and control via a National Instruments IEEE-488 (GPIB card) interface bus. A schematic representation of the whole setup is shown in **Figure 10**. All potentials were measured with respect to a saturated calomel reference electrode (SCE).

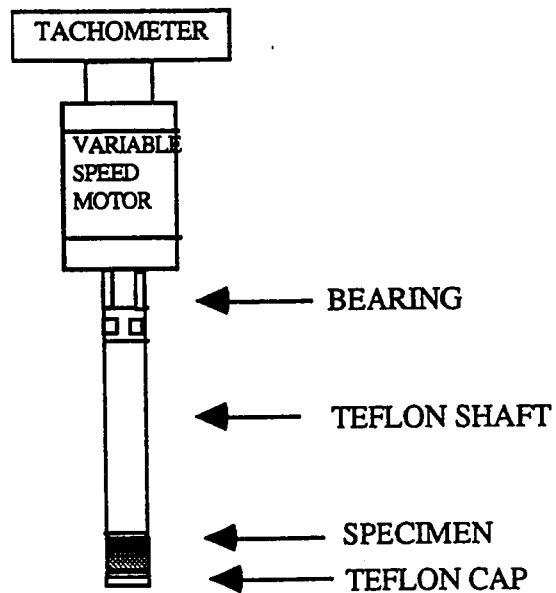


Figure 8: Schematic representation of a rotating electrode

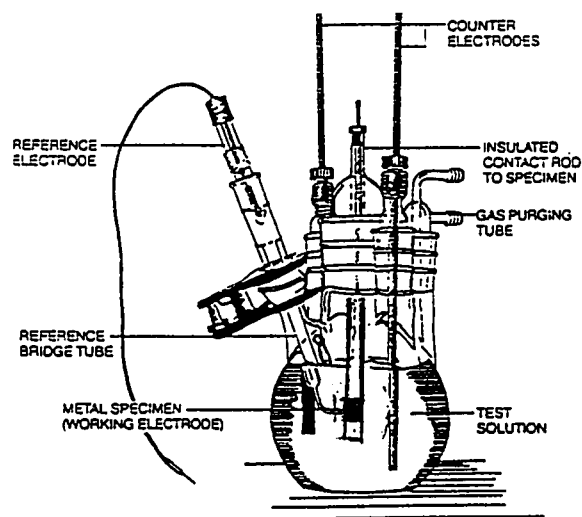


Figure 9: A typical electrochemical corrosion test cell

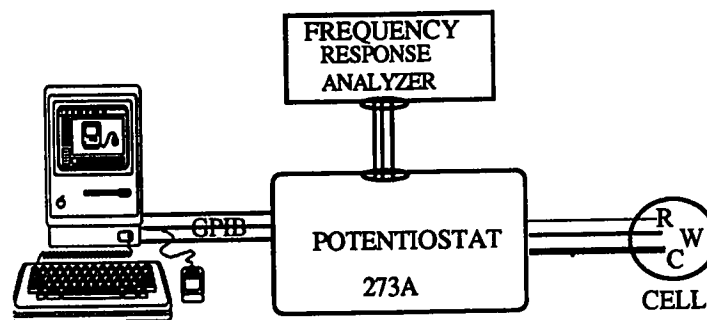


Figure 10: Block diagram of the testing instrument

4.4.2 Solution Preparation

The test solution was 1% HCl prepared by diluting a reagent grade of hydrochloric acid with distilled water. The PARC electrochemical cell, as described above, was filled with 900 ml of the solution which purged with nitrogen gas for 1.5 hours at 80 ml/min and then blanket at 150 ml/min during the experiment. The rotation of the electrode was set at 1000 rpm. The corrosion rate of mild steel in 1% HCl solution with and without the presence of the chemicals at 25°C were determined as a function of time using on-line direct current linear polarization program for 15 hours. Prior to each run and also after 15 hours exposure, AC impedance data were obtained over the range of 0.01 Hz to 1000 Hz. A 10 mV amplitude perturbation were used in these experiments. Finally, Tafel plot was performed and analyzed by corrosion software model 352 and

version 2.01. Where the cell was polarized to ± 250 mV from E_{Corr} . The scanning rate was 0.25 mV/s with scanning increments of 0.5 mV.

4.5 SYSTEM REPRODUCIBILITY :

Dummy cell is frequently employed for checking the performance of the potentiostat and the software. The dummy cell is equivalent to 10 mpy and is provided by PETROLITE Instruments. **Figure 11** represents some experimental data obtained where the corrosion rate is plotted against the time in minutes. The measured corrosion rates are ranged between 10.24 and 10.29 mpy with a percentage error of 2.4% as a minimum and 2.9% as a maximum. The statistical fit of each reading is illustrated in **Figure 12** where all the data are ranged between 0.99999 - 1.00000. This gives a strong evidence of the linearity of the applied potential.

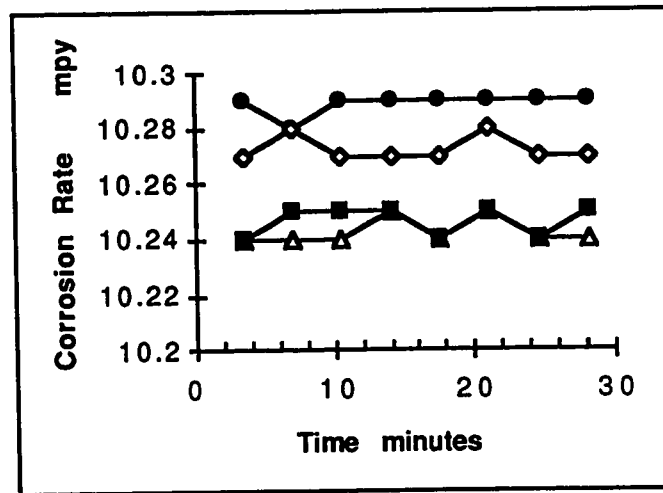


Figure 11: Corrosion rate Vs. time of 10 mpy prover

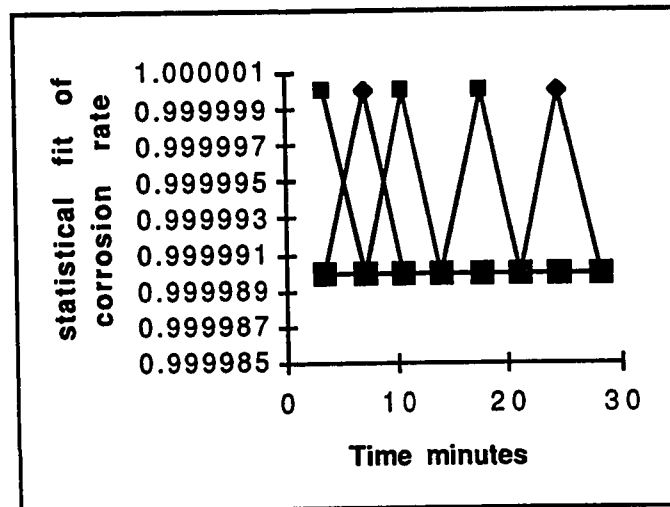


Figure 12: Corrosion rate Vs. statistical fit of 10 mpy prover

4.6 CLEANING PROCEDURE

After each experiment, the cell used to be washed with water and any dissolved Iron was removed by using 1:1 diluted hydrochloric acid. The cell then was rinsed with acetone to dissolve the adsorbed chemicals and remove any organic material. Finally, the cell was rewashed with distilled water to get rid of the acetone.

4.7 CHEMICAL APPLICATIONS

The corrosion inhibitor must reach the surface to be protected by transportation in the system fluids. The method of treatment is often dictated by the system design. Two basic methods of treatments are commonly used in the field; continuous and batch-wise feedings.

In this work, the chemical is added directly to the cell before starting the monitoring, simulating the continuous feeding. Another approach of treatment, the mild steel rotating cylinder is exposed to 10,000 ppm of inhibited solution for different periods of time then the electrode is switched to uninhibited solution. The adsorbed film formed during the chemical immersion is monitored. This approach has a relatively short period of inhibitor feeding, followed by a long period of protection.

4.8 OPTIMIZATION OF SOME EXPERIMENTAL CONDITIONS

The conditions were optimized by considering the purging time, the solvent effect, and the chemical concentration.

4.8.1- Purging Time

The role of oxygen in enabling a corrosion reaction to occur forms the basis for the fact that oxygen cannot only maintain a cathodic reaction but can also promote another one:

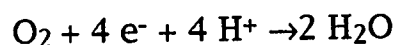


Figure 13 is demonstrating the effect of the purging time as well as the purging rate on corrosion reactions. Three experiments were conducted. In the first experiment, the cell was purged with nitrogen gas for 30 minutes at a rate of 45 ml/min before and during the experiment. The corrosion rate increased rapidly with time as shown in **FIGURE 3**. When the initial purging time increased to 60 minutes at a rate of 80 ml/min and then reduced to 45 ml/min during the measurements. The corrosion rate was reduced to about 50%. In the last experiment, the corrosion rate was maintained on 88 mpy after purging the cell for 90 minutes at a rate of 80 ml/min and then followed by flushing the cell with nitrogen gas at a rate of 150 ml/min. At the same time, the nitrogen gas was bubbled into the cell at a very low rate.

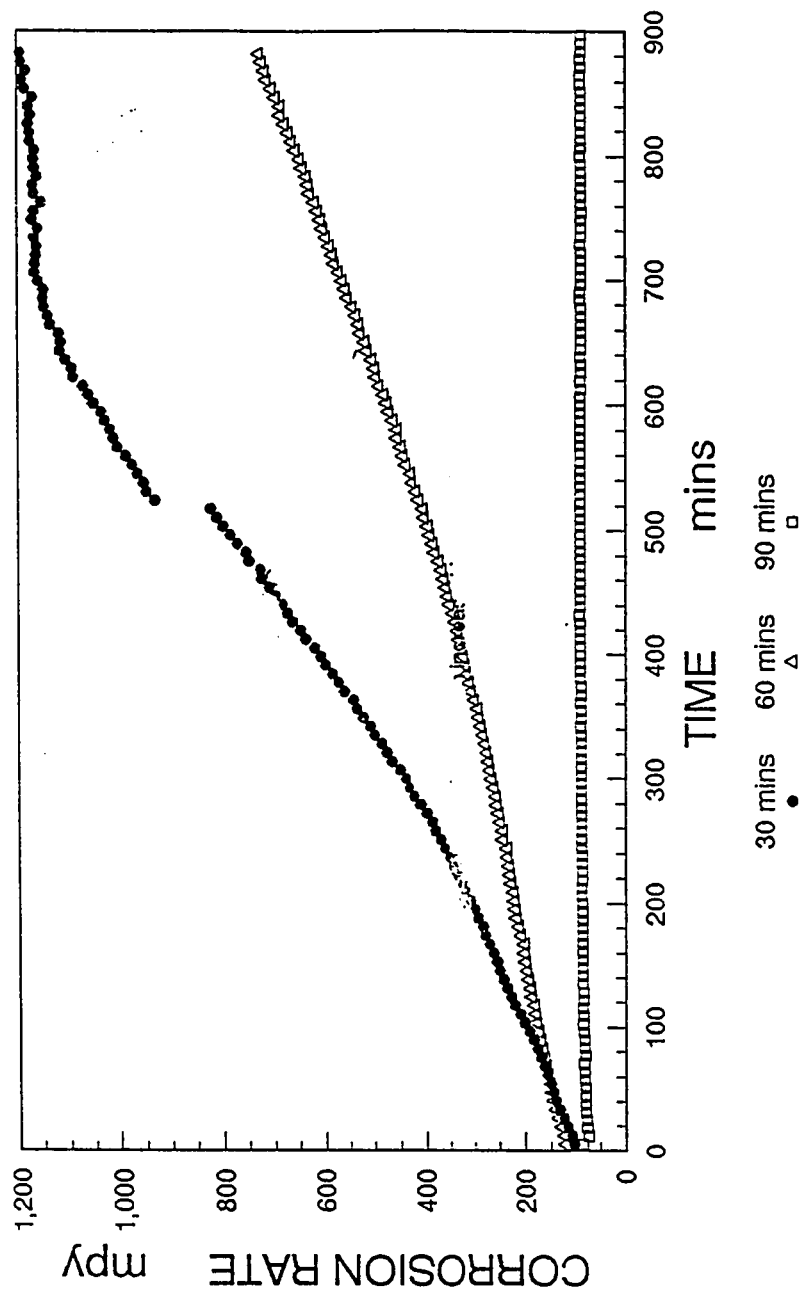


Figure 13: Effect of purging rate and purging time on the corrosion rate. Where mild steel rotating cylinder electrode was used as a working electrode in 1% HCl solution at 1000 rpm.

Flushing versus purging was selected after the chemical addition, to avoid the foaming problems. Since the cell cannot be sealed from the top, high blanketing flow rate was performed. The last experimental conditions have been selected and applied for the all conducted experiments.

4.8.2- Solvent Effects

The objective of this test is to study the inhibition efficiency of the tested solvents and to investigate their contribution when the studied compounds are added. Ethanol and toluene have been selected and tested in 1% HCl solution . These solvents were used for dissolving the studied compounds whereas concentrated stock solutions were prepared (25,000 ppm) to minimize the solvent effect in this work. 1-(4- Methylbenzyl and 4-Bromobenzyl) 1-H-4,5-Dibenzoyl-1,2,3- Triazole showed better dissolubility in toluene. Also, it has been noticed that the stock solution of 1-(4- Methylbenzyl) 1-H-4,5- Dibenzoyl-1,2,3- Triazole, in both solvents, caused cloudiness in 1% HCl solution. The time dependent of corrosion rate and corrosion potential of these solvents versus the blank is illustrated in **Figures 14 and 15** respectively. Toluene did not effectively suppressed the corrosion process compared with the blank or ethanol. This can be attributed to the nature of the solvents. Since toluene is a water immiscible, toluene/metal interface will be minimum. Also, the blank shifted the potential in the anodic direction

during the experiment compared with the solvents which shifted the potential in the cathodic side. Results of on-line linear polarization are summarized in Table 2.

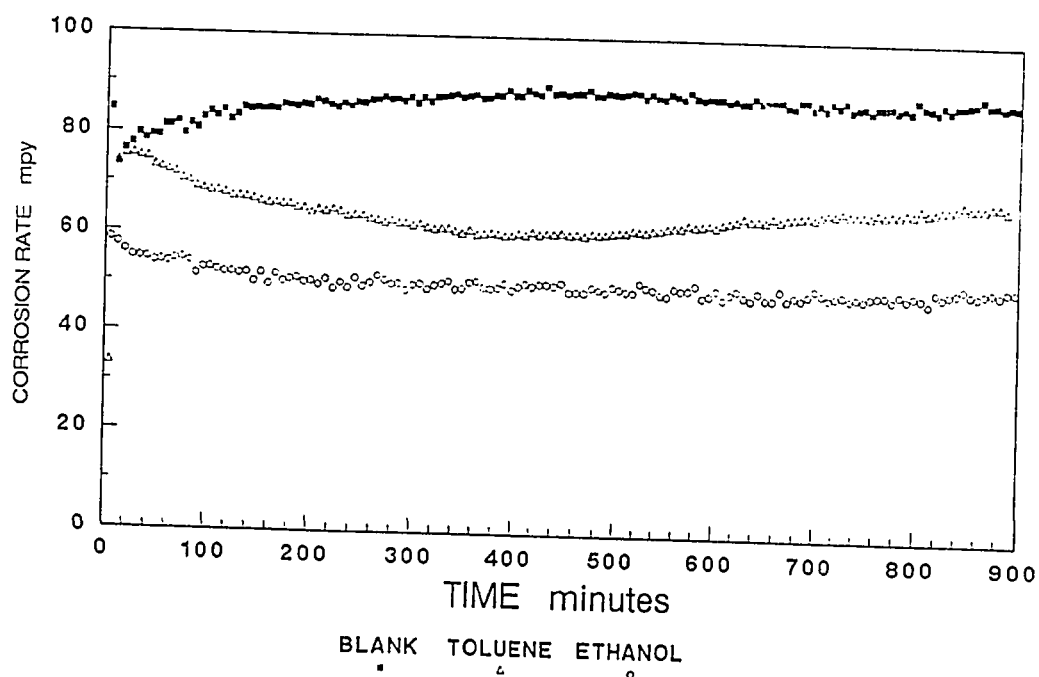


Figure 14: Corrosion behavior of the blank in the presence of toluene and ethanol. Mild steel rotating electrode was used at a speed of 1000 rpm.

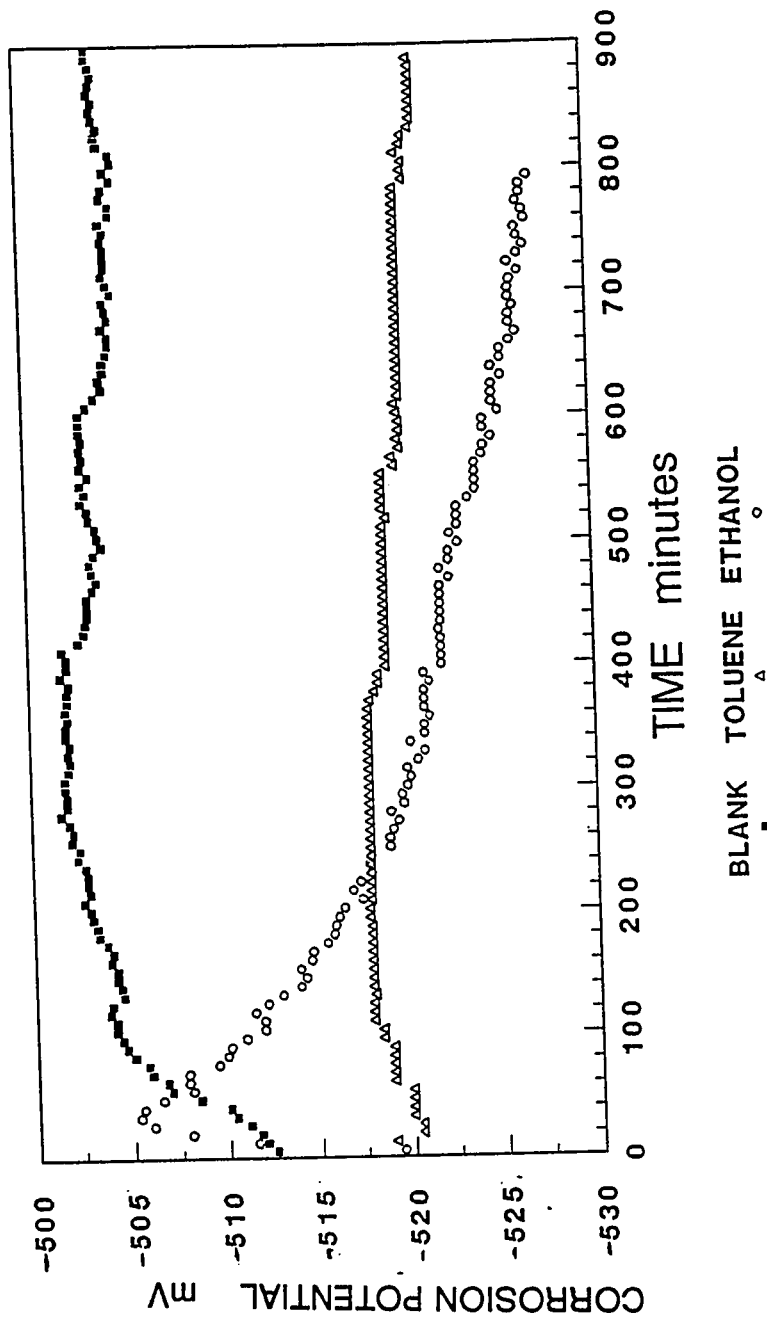


Figure 15: Corrosion potential behavior of the blank in the presence of toluene and ethanol as a solvent. Mild steel rotating electrode was used at a speed of 1000 rpm.

Table 2

Linear polarization results of the on-line monitoring

	CORROSION RATE MPY		CORROSION POTENTIAL mV	
	INITIAL	FINAL	INITIAL	FINAL
BLANK	79.2	88.0	- 510	- 504
TOLUENE	73.4	67.2	- 520	- 521
ETHANOL	55.4	50.4	- 509	- 527

The anodic and cathodic polarization scans of 1% HCl solution, toluene, and ethanol are illustrated in **Figure 16**. The solvents in 1% HCl solution exhibited two distinct behaviors; E_{corr} shifted to more negative potential compared to blank and a potential independent region was observed in the anodic scan of ethanol. Some calculated values from Tafel plots are presented in Table 3.

Table 3

Some calculated parameters from Tafel plots

		TOLUENE	ETHANOL	1% HCl
β_a *	mV/decade	153	162	290
β_c *	mV/decade	140	120	108
E	at (I=0) mV	- 508	- 492	-469
I_{corr}	$\mu\text{A}/\text{cm}^2$	152	86.8	180
Corrosion Rate mpy		70	40.0	90

* calculated at the end of the experiment

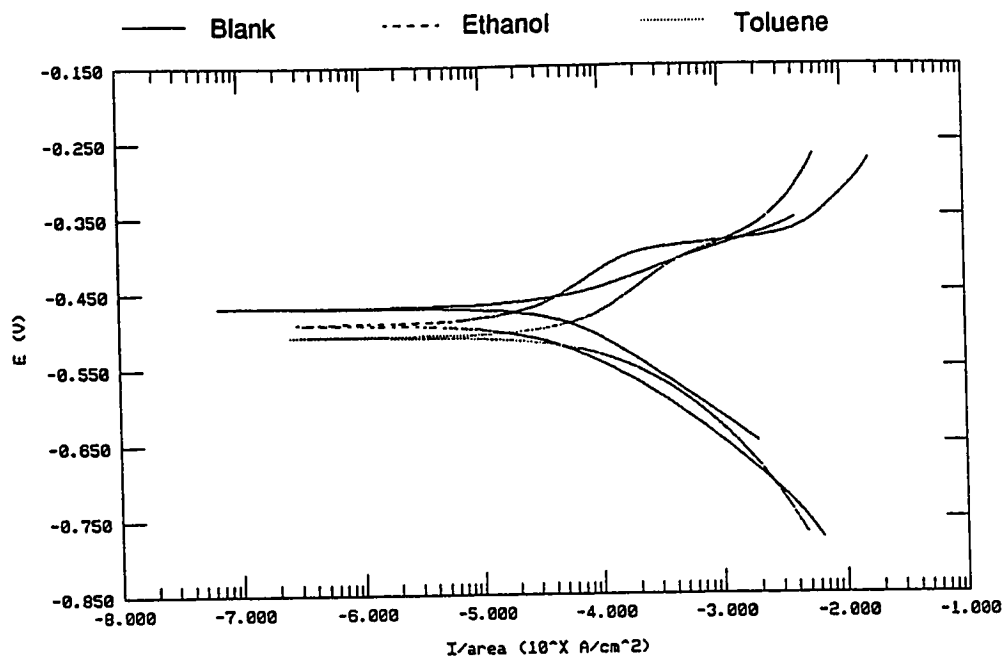


Figure 16; Tafel plots of the blank solution in the absence and present of toluene and ethanol. Rotating mild electrode at 1000 rpm was used. The scanning rate was 0.25 mV/s with scanning increments of 0.5 mV

4.8.3- Dosage Optimization

Corrosion inhibitor usually is added to a system of interest at a very low concentration. The added concentration must have a significant effect in slowing the process of corrosion. 1(Benzyl)1-H-4,5- Dibenzoyl-1,2,3- Triazole compound was selected for testing the effect of increasing concentration on the ability of the measurement techniques on monitoring the system without errors. Four concentrations of the selected compound were tested. These concentrations were 10, 25, 50, and 100 ppm. Among the studied concentrations only the first three were chosen. At 100 ppm, the

adsorbed film formed is responsible in introducing a measurement errors as a result of the ohmic potential drop across the high resistance of the adsorbed organic film. This conclusion is based on the result of unstable reading of the corrosion rate as shown in Figure 17 and its Tafel plot which illustrated in Figure 18.

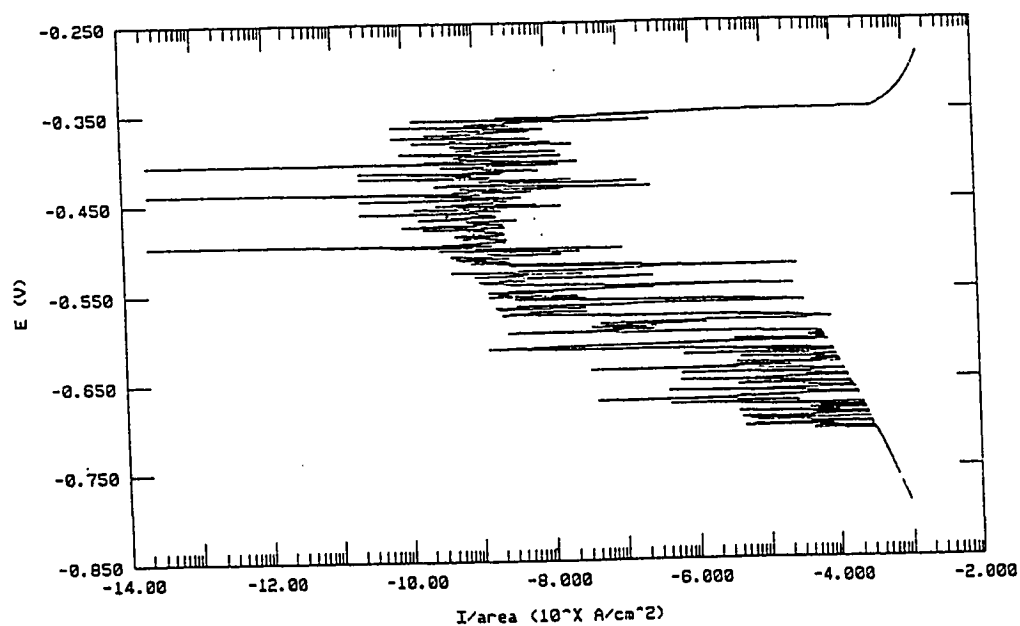


Figure 17: Tafel plot of 1(benzyl)1-H-4,5- dibenzoyl-1,2,3- triazole at 100 ppm in 1% deaerated HCl solution. Scanning rate was 0.25 mV/s with scanning increments of 0.5 mV

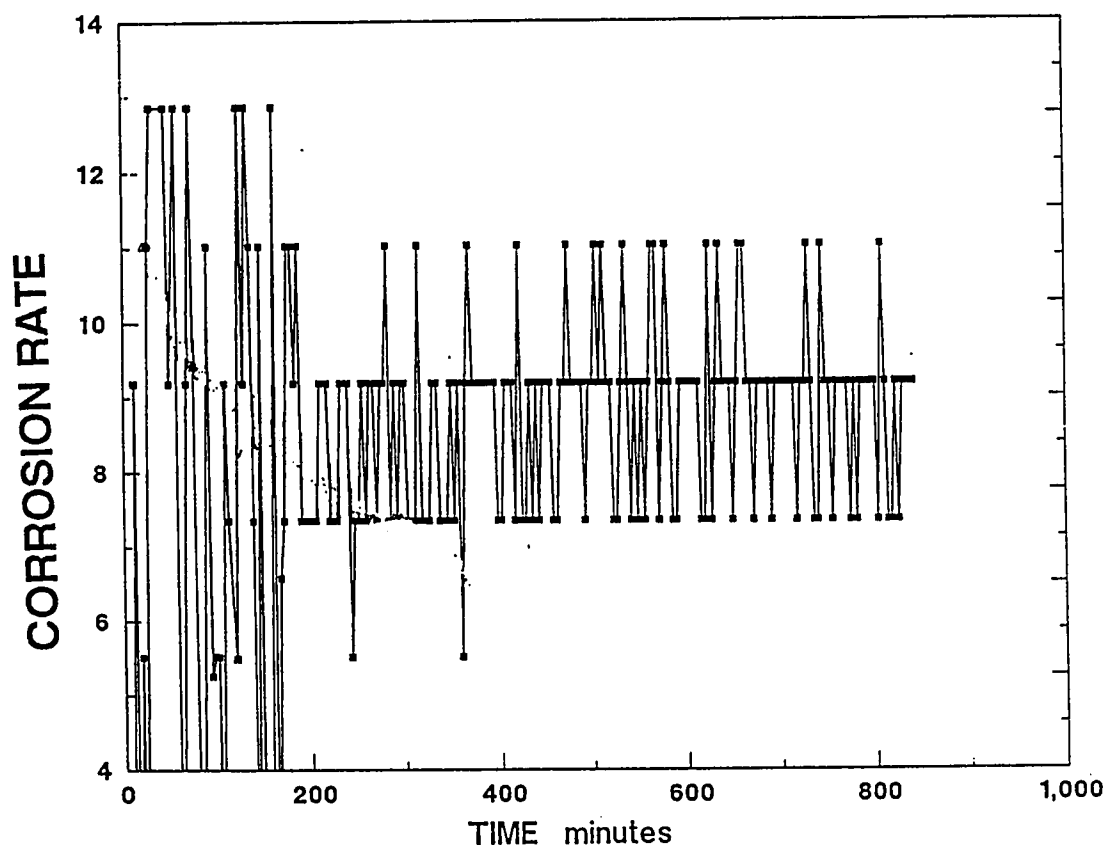


Figure 18: Corrosion rate profile of 1(benzyl)1-H-4,5-dibenzoyl-1,2,3-triazole at 100 ppm. Using continuous linear polarization program.

CHAPTER 5

RESULTS AND DISCUSSION

5.1 UNINHIBITED SOLUTION

The corrosivity of 1% deaerated hydrochloric acid solution was measured electrochemically using mild steel rotating electrode at 1000 rpm. Where 900 ml of the acid solution was purged vigorously with nitrogen gas at a rate of 80 ml/min for 90 minutes and then the cell was flushed with nitrogen gas at a rate of 150 ml/min during the measurement. Nitrogen gas also was bubbled into the cell at a very low rate to minimize oxygen ingress during the experiment. Initial AC impedance performed over the range of 0.01 Hz to 1000 Hz and the obtained data is represented by nyquist plot as shown in Figure 19.

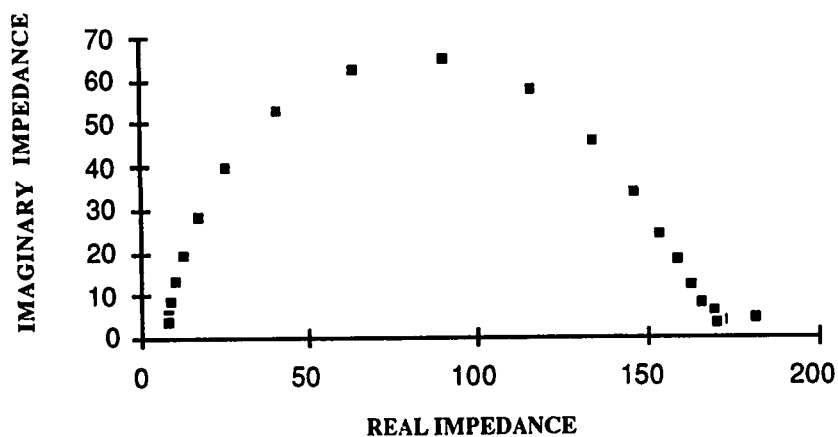


FIGURE 19: Nyquist plot of the initial scan of 1% deaerated solution

The corrosion rate and the corrosion potential of the system were then monitored continuously using linear polarization technique for 900 minutes. The measured data is shown graphically in **Figure 20**. A steady corrosion rate was recorded during the experiment with an average corrosion rate of 88 mpy. At the beginning, the potential had shifted to more positive direction until it reached a steady condition followed by a drop of the potential at the end of the experiment. Some readings during the course of the test are tabulated as **Table 4**.

Table 4
Some corrosion rate data obtained from the continuous linear polarization monitoring of the blank solution

TIME mins	CORROSION RATE mpy	CORROSION POTENTIAL mV
5.1	84.5	-513
200	85.8	-503
400	88.3	-502
600	88.3	-505
900	87.8	-504

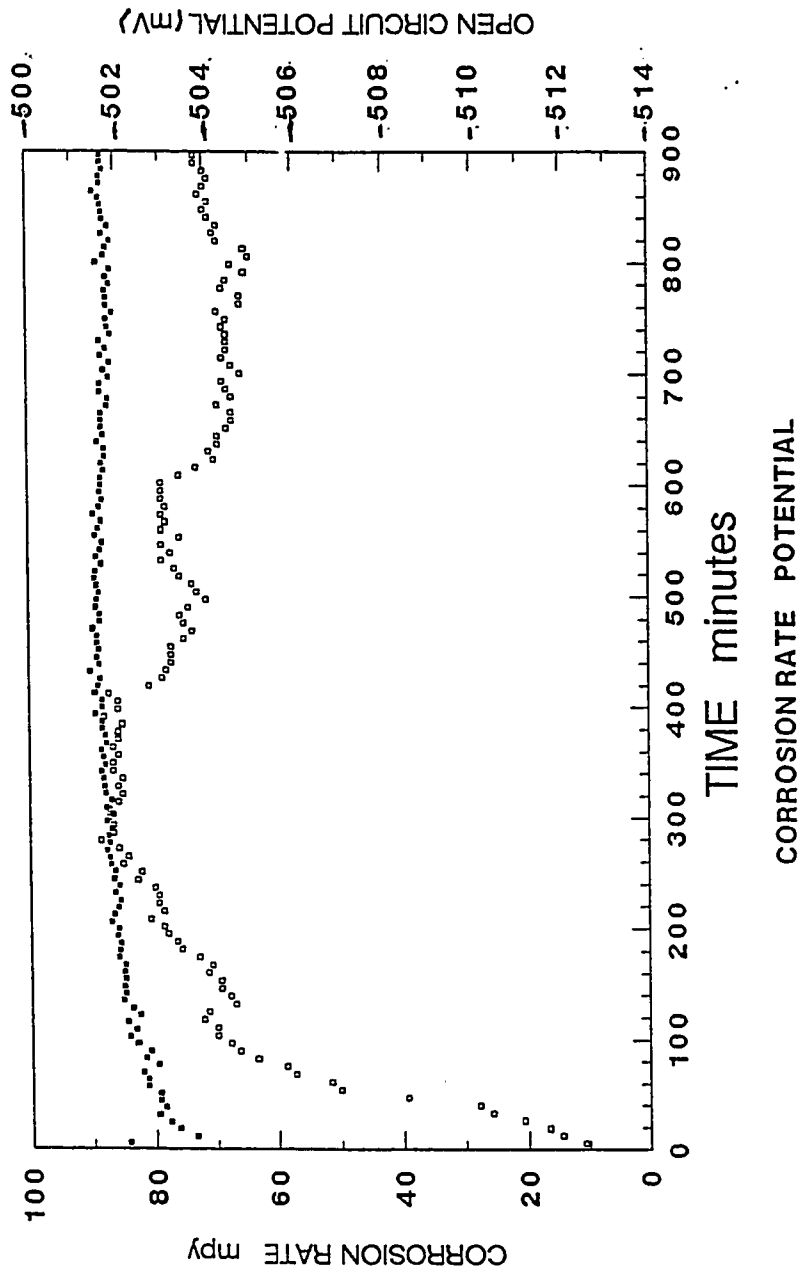


FIGURE 20: Corrosion rate and potential measurements during the exposure of the electrode in deaerated 1% HCl solution. The electrode set at 1000 rpm. The initial deaeration rate was 80 ml/min and then the cell was blanket at a rate of 150 ml/min.

AC impedance is performed again and nyquist plot of FIGURE 21 shows that the change in the polarization resistance of the electrode after 15 hours exposure in deaerated 1% HCl solution. R_p is increased by a factor of two.

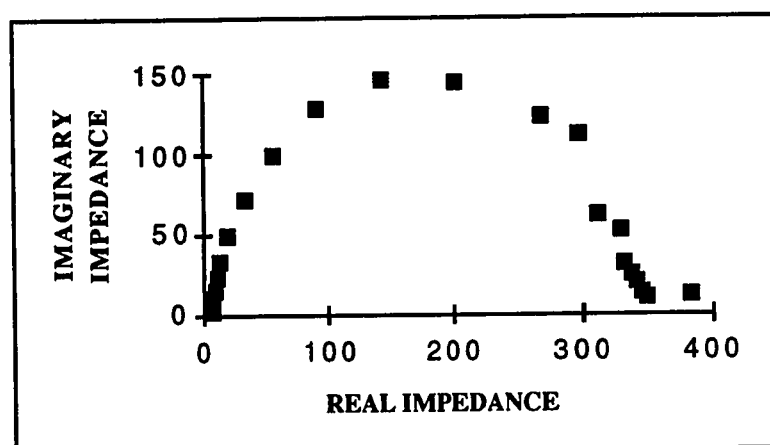


FIGURE 21: Nyquist plot of the final scan of the blank solution

At the end of the experiment cathodic and anodic scans were done and illustrated as Figure 22. In general, the slope of the anodic scan is $\frac{(1-\alpha)nF}{2.3 RT}$ and that of the cathodic scan is $\frac{-\alpha n F}{2.3 RT}$. At $\eta > 100$ mV, the reverse or back reaction becomes negligible and depends on the direction of the applied potential, the metal surface acts either as all anode or all cathode. As shown in Figure 10, both linear segments extrapolate to an intercept of $\log i_0$ which is equal to $\log i_{corr}$. It deviates sharply from linear behavior as η approaches zero, because the reverse reactions can no longer be regarded as negligible. Also, the deviations from linearity at very large overpotential, come from limitations imposed by mass transfer.

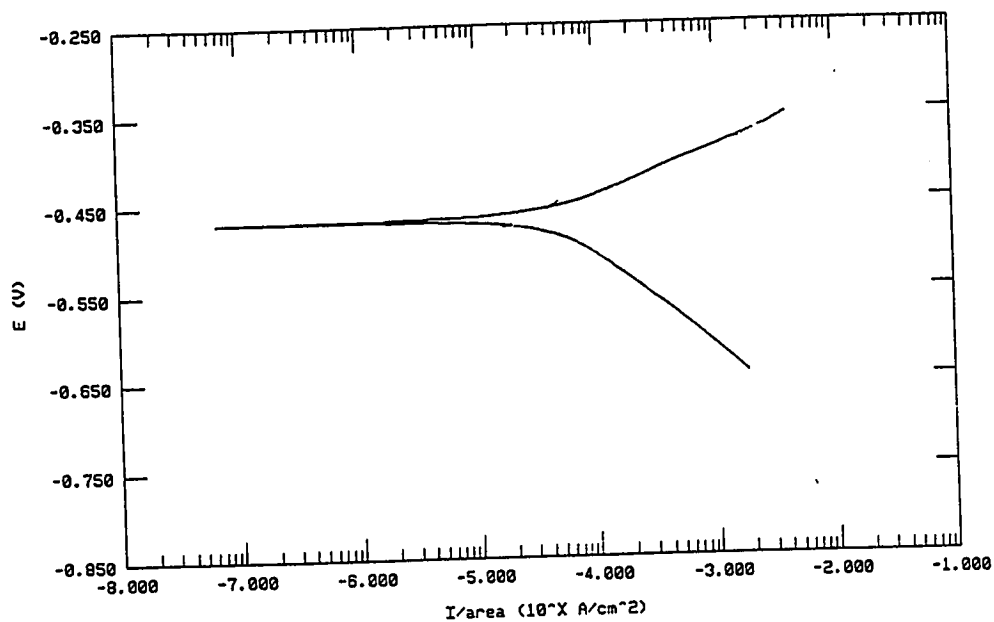
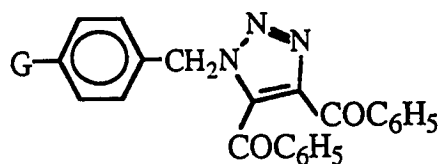


FIGURE 22: Tafel plot of rotating mild steel electrode immersed in 1% HCl solution after 15 hours exposure at 1000 rpm. The scanning rate was 0.25 mV/s with scanning increments of 0.5 mV.

5.2 INHIBITED SOLUTION

5.2.1- Substituents at the para- Position of 1-(Benzyl)- 1-H- 4,5 Dibenzoyl 1,2,3 Triazole:



G can be either H, CH₃, Br, or NO₂

This test was ultimately intended to provide information and to demonstrate structure/ effect relationships and particularly the field effect. The three substituent groups studied were bromo, nitro as electron withdrawing groups and methyl as electron donating located at the para position. The inhibition of such derivatives were compared with the parent 1-(benzyl)-1-H-4,5 dibenzoyl- 1,2,3 triazole. The effect of increasing the concentrations of these compounds on the corrosion rate was also investigated.

The on-line corrosion monitoring program, Tafel polarization plots, and AC impedance techniques were used in screening of these compounds and studying the field effect on their performance under the formerly mentioned conditions. The sequence of applying the instrumental techniques was as follow:

- 1- Initial AC impedance scan,
- 2- Continuous linear polarization,
- 3- Final AC impedance measurements, and
- 4- Tafel polarization scan.

5.2.1.1 Results of Initial and Final Scans of the AC Impedance

Figures 23 to 29 shows examples of the frequency response diagrams of mild steel electrode at zero hour and/or after 15 hours immersion. Various triazole compounds and concentrations were tested in deaerated 1% HCl solution. At low frequencies, the real

impedance corresponds to the polarization resistance plus the solution resistance ($R_p + R_s$), however at high frequencies, it corresponds to the solution resistance only (R_s). The value of R_s is negligible compared with the R_p which is inversely proportional to the corrosion rate. As the R_p increases, the corrosion rate decreases.

The initial and final AC impedance measurements at 10 ppm of 1-(benzyl) and 1-(4-bromobenzyl)-1-H-4,5 dibenzoyl- 1,2,3 triazole which shown in **Figures 23 and 24** respectively. These figures suggest that the change in the R_p from 400 to 1100 $\Omega \cdot \text{cm}^2$, as observed in **Figure 23**, might have been caused by adsorption processes developed during the immersion. The nyquist plots of 1-(benzyl)-1-H-4,5 dibenzoyl- 1,2,3 triazole at various concentrations and exposure periods as shown in **Figures 25 and 26** illustrate two important phenomena. The impedance of the substrate is increased as the concentration or the exposure time is increased. These observations provide further evidence that the physical adsorbed film is a function of time and concentration. As the concentration of the chemical or the immersion time increased, the percentage coverage will be increased and the corrosion rate will be decreased.

Figure 27 represents the initial impedance, which performed after chemical addition, of 1-(4-methylbenzyl)-1-H-4,5 dibenzoyl-1,2,3 triazole at 25 and 50 ppm. Similar behavior was observed at

both concentrations. This is attributed to similar coverage of the electrode surface. The nyquist plots of 1-(4- methylbenzyl) and 1-(4-nitrobenzyl)-1-H-4,5 dibenzoyl- 1,2,3 triazole exhibited two time constants as shown in Figures 28 and 29. This process might have resulted of the precipitated inhibitor on the electrode surface. Also, as noticed in Figure 29, the corrosion rate was increased at 50 ppm due to, most probably, the precipitation of the inhibitor.

From AC impedance measurements the inhibitory efficiency of the substituents at the para- position of 1-(benzyl)-1-H- 4,5 dibenzoyl-1,2,3 triazole compounds show the following sequence:



The impedance response diagram of mild steel in uninhibited HCl solutions significantly changed after addition of the triazole compounds. The greatest effect was observed with 1(benzyl)-1-H-4,5 dibenzoyl-1,2,3 triazole at 50 ppm which produced an R_p of 4900 $\Omega\cdot\text{cm}^2$ after 15 hours exposure, 12 times higher than that measured without chemical addition under the same experimental conditions.

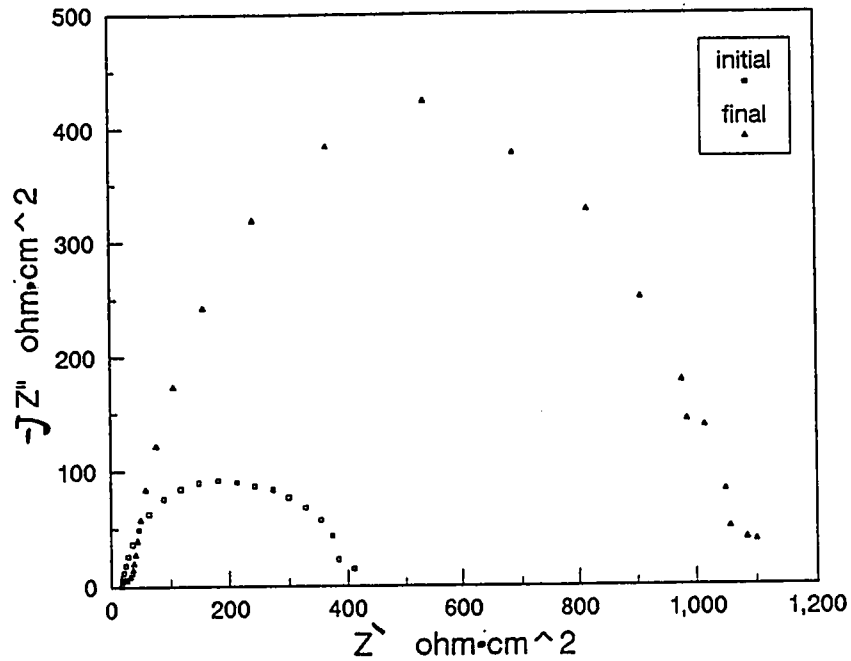


FIGURE 23: Initial and final impedance response at 10 ppm of 1(benzyl)-1-H-4,5 dibenzoyl-1,2,3 triazole

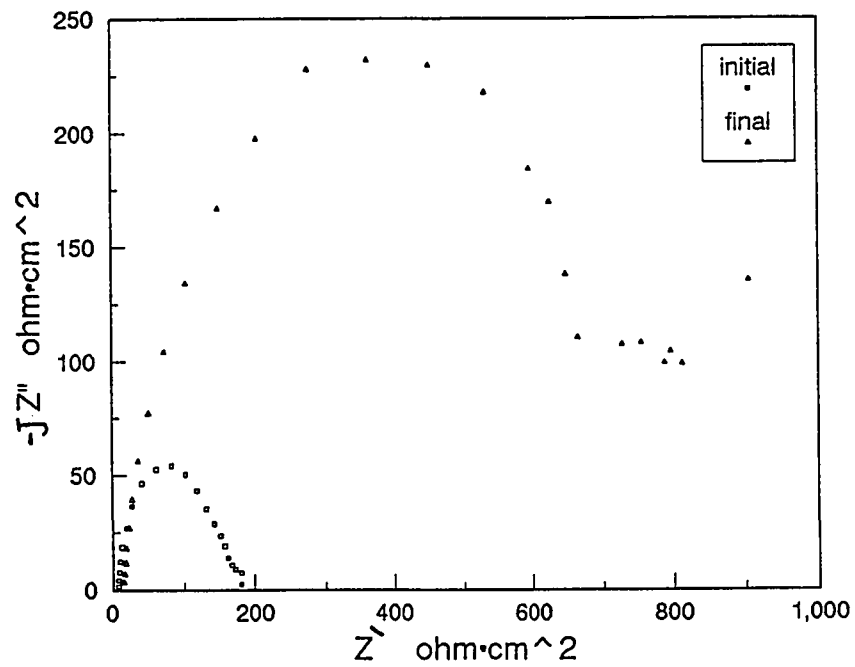


Figure 24 : Initial and final impedance response at 10 ppm of 1(4-bromobenzyl)-1-H-4,5 dibenzoyl-1,2,3 triazole

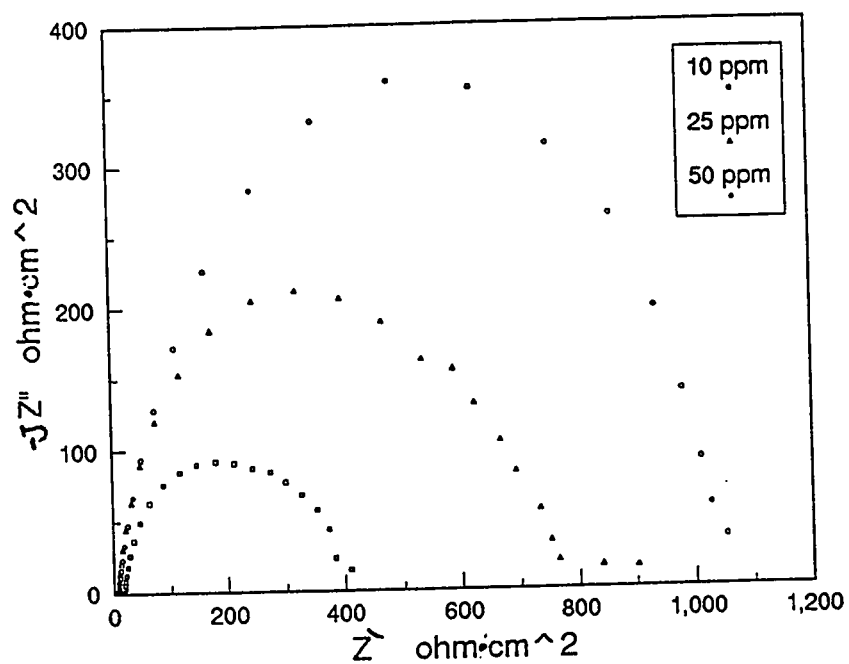


FIGURE 25: Initial impedance response of 1(benzyl)-1-H- 4,5 dibenzoyl-1,2,3 triazole at 10, 25, and 50 ppm

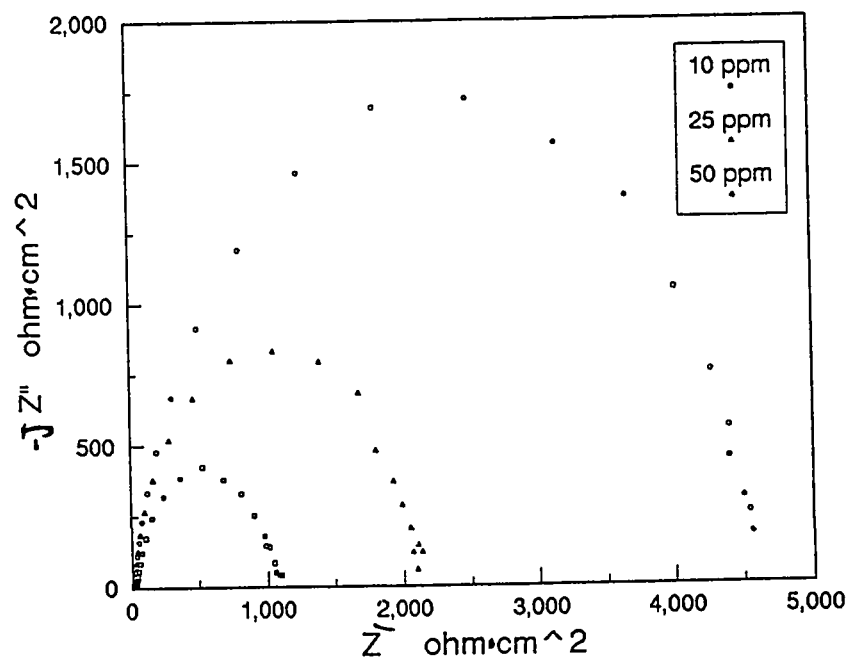


Figure 26 : Final impedance response of 1(benzyl)-1-H- 4,5 dibenzoyl-1,2,3 triazole at 10, 25, and 50 ppm

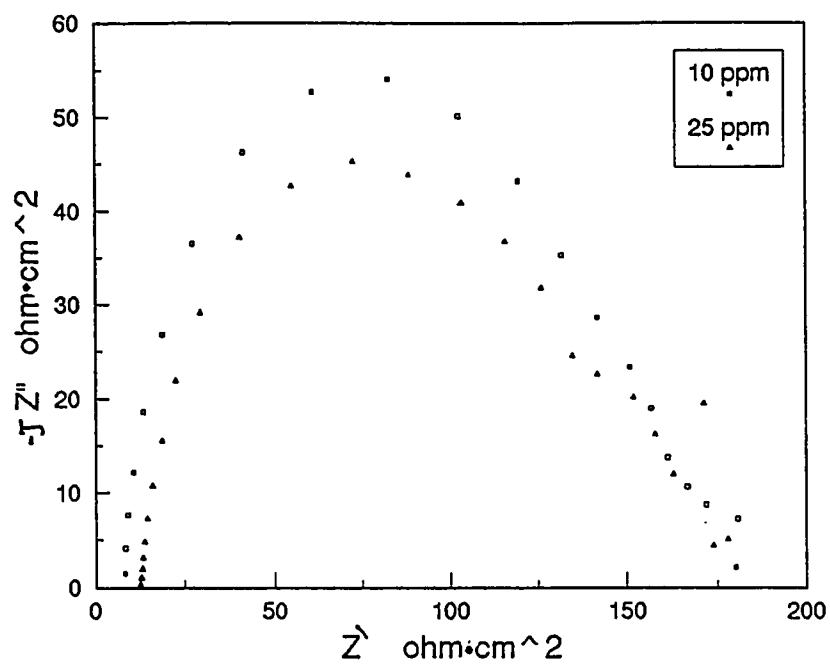


FIGURE 27: Initial impedance response of 1(4- bromobenzyl)-1-H-4,5 dibenzoyl-1,2,3 triazole at 10 and 25 ppm

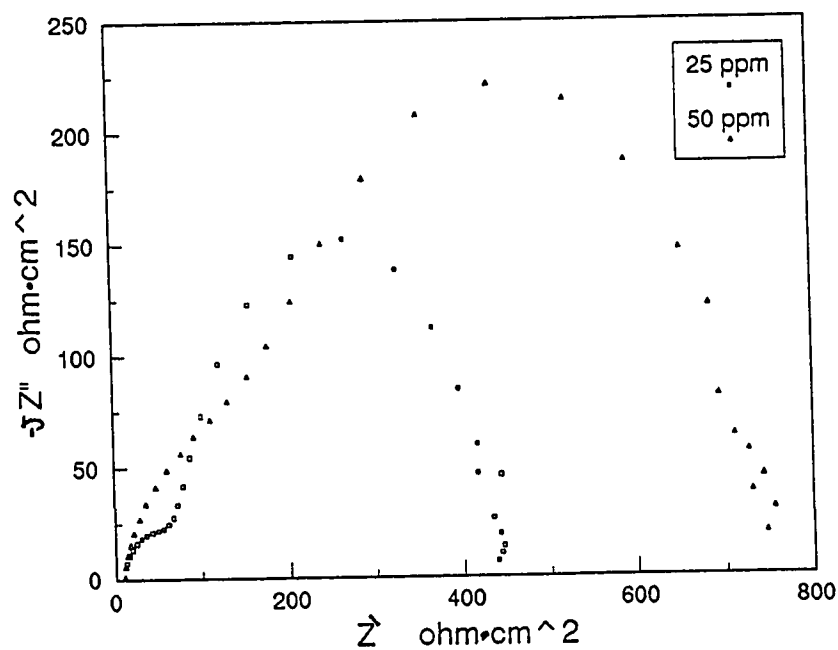


Figure 28 : Final impedance response of 1(4- methylbenzyl)-1-H-4,5 dibenzoyl-1,2,3 triazole at 25 and 50 ppm

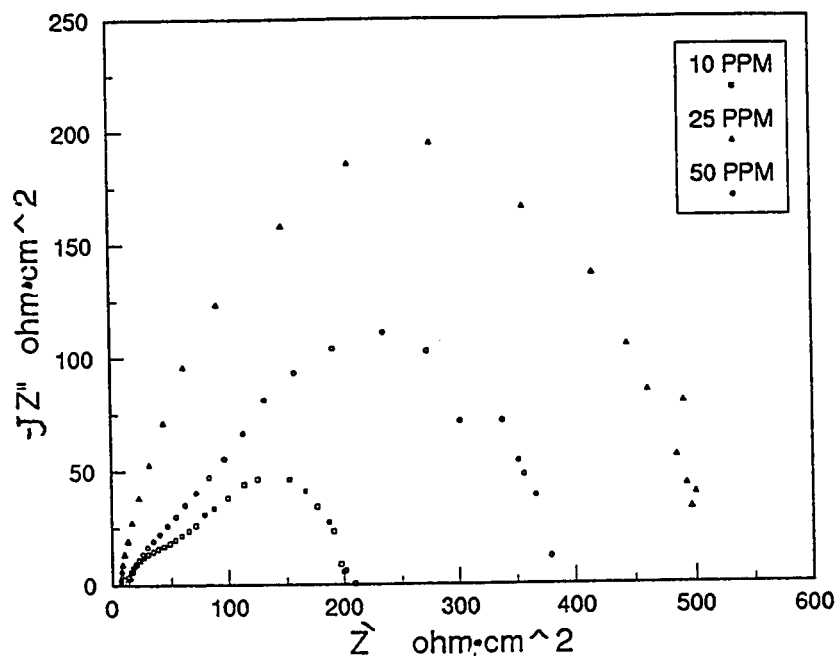


Figure 29 : Final impedance response of 1(4- nitrobenzyl)-1-H-4,5 dibenzoyl-1,2,3 triazole at 10, 25, and 50 ppm

5.2.1.2 Results of continuous Linear Polarization Resistance

The corrosion rate profiles of the parent compound and bromo, methyl, and nitro substituents at 10, 25, and 50 ppm are shown in Figures 30, 31, 32, and 33 respectively versus the corrosion rate of the uninhibited solution. Also, the behavior of the open circuit potential which was measured versus SCE during the experimental period for the previous sequence are illustrated as Figures 34, 35, and 36. As noticed from most of these figures, the corrosion rate

was decreased with increasing the exposure time while the open circuit potential is shifted to the more negative direction. The studied compounds were compared on the basis of their inhibition efficiency. It is the ratio of corrosion lowering in the presence of inhibitors to the corrosion in their absence expressed as percentage. The inhibition efficiency is calculated from the following formula:

$$\text{Inhibition Efficiency} = \frac{C_0 - C_i}{C_0} \times 100 \quad 5.1$$

where

C_0 : corrosion rate in the absence of inhibitor

C_i : corrosion rate in the presence of inhibitor

The corrosion rates obtained from on-line corrosion monitoring and the calculated inhibition efficiency are summarized in the following Tables 5, 6, 7, and 8.

Table 5

1-(benzyl)-1-H-4,5 dibenzoyl- 1,2,3 triazole

Conc.	Corrosion Rate *	Inhibition Efficiency
10 ppm	16.9 mpy	81 %
25 ppm	8.5 mpy	90.3 %
50 ppm	4.2 mpy	95.2 %

* represent the average of the last hour readings

Table 6

1-(4- bromobenzyl)-1-H-4,5 dibenzoyl- 1,2,3 triazole

Conc.	Corrosion Rate *	Inhibition Efficiency
10 ppm	23.6 mpy	73.2 %
25 ppm	19.9 mpy	77.4 %
50 ppm	38.4 mpy	56.8 %

* represent the average of the last hour readings

Table 7

1-(4- methylbenzyl)-1-H-4,5 dibenzoyl- 1,2,3 triazole

Conc.	Corrosion Rate *	Inhibition Efficiency
25 ppm	41.5 mpy	52.8 %
50 ppm	42 mpy	72.7 %

* represent the average of the last hour readings

Table 8

1-(4- nitrobenzyl)-1-H-4,5 dibenzoyl- 1,2,3 triazole

Conc.	Corrosion Rate *	Inhibition Efficiency
10 ppm	23.6 mpy	50.2 %
25 ppm	19.9 mpy	56.1 %
50 ppm	38.4 mpy	45.5 %

* represent the average of the last hour readings

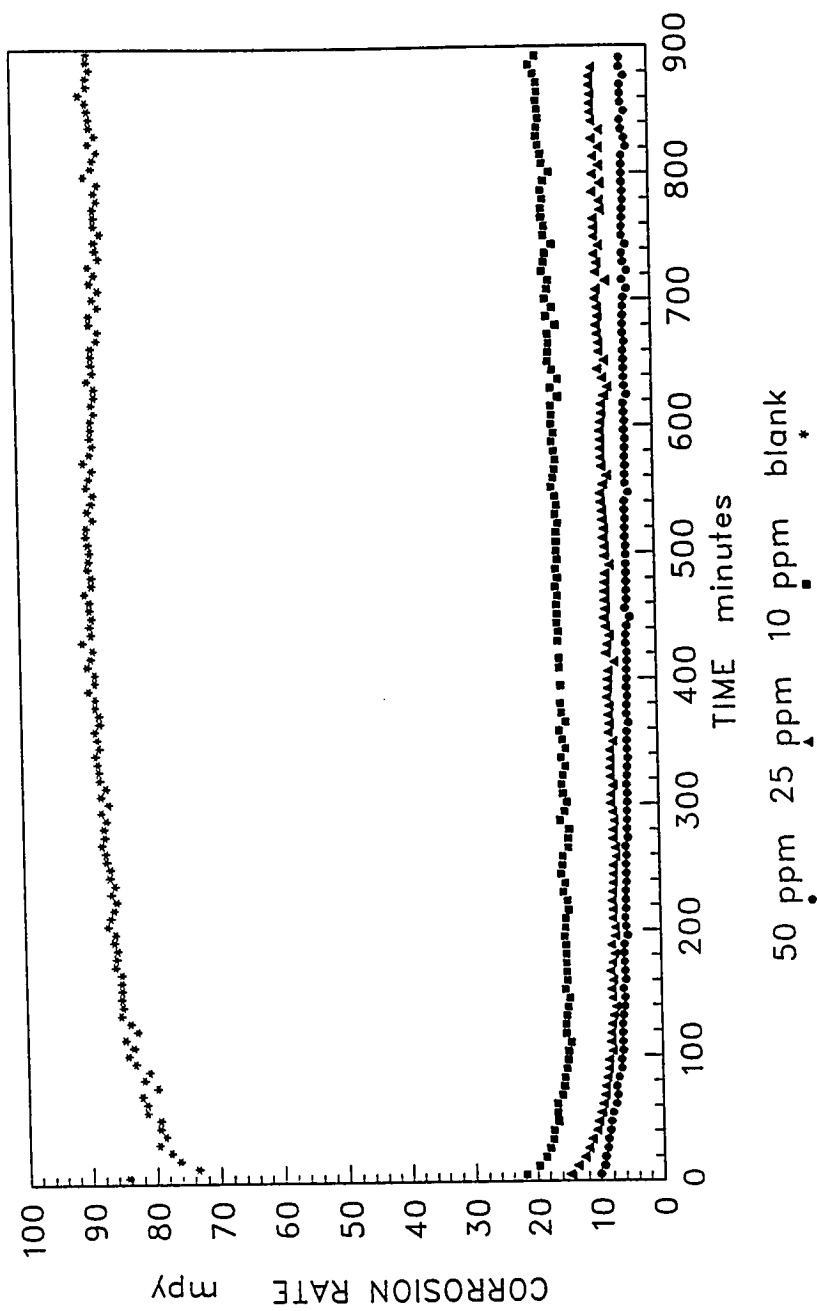


FIGURE 30; 0, 10, 25, and 50 ppm of 1 (benzyl)-1-H-4,5 dibenzoyl-1,2,3 triazole in deaerated 1% HCl solution using mild steel rotating electrode at 1000 rpm.

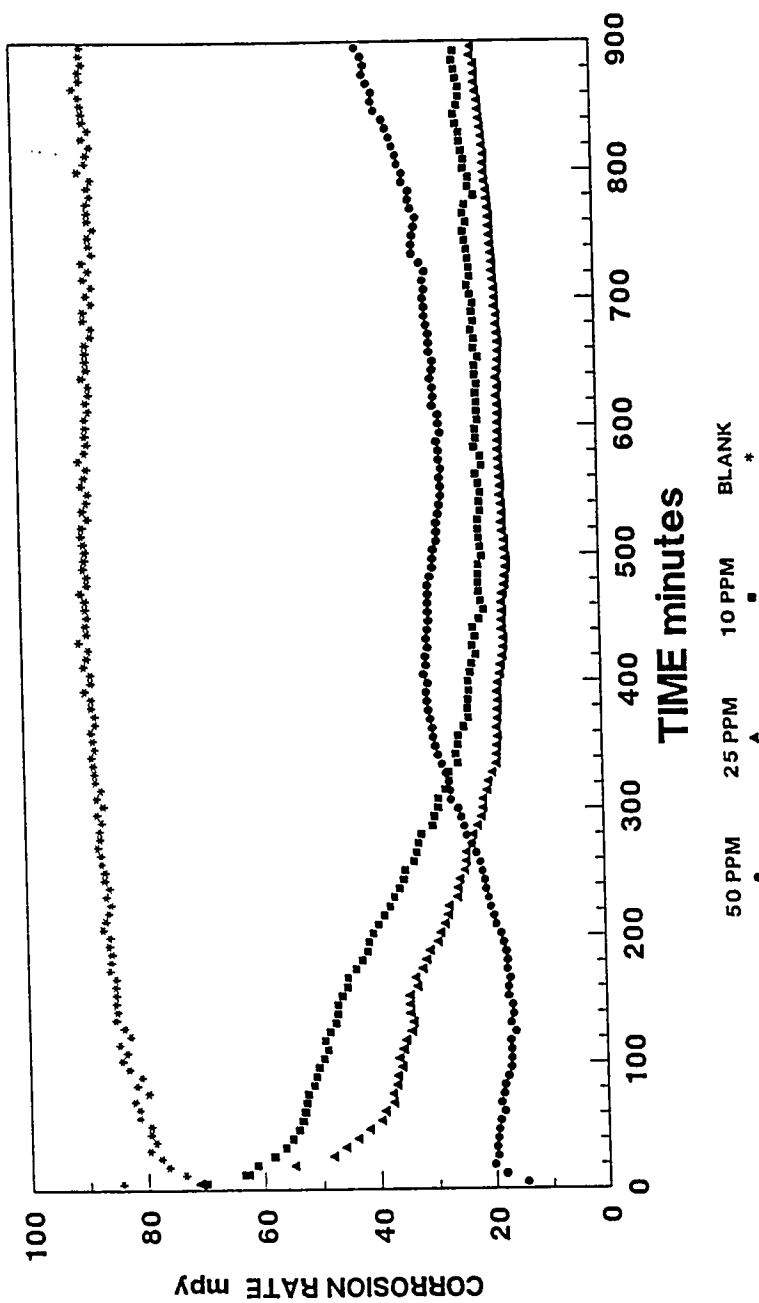


FIGURE 31; 0, 10, 25, and 50 ppm of 1-(4-bromobenzyl)-1H-4,5-dibenzoyl-1,2,3-triazole in deaerated 1% HCl solution using mild steel rotating electrode at 1000 rpm.

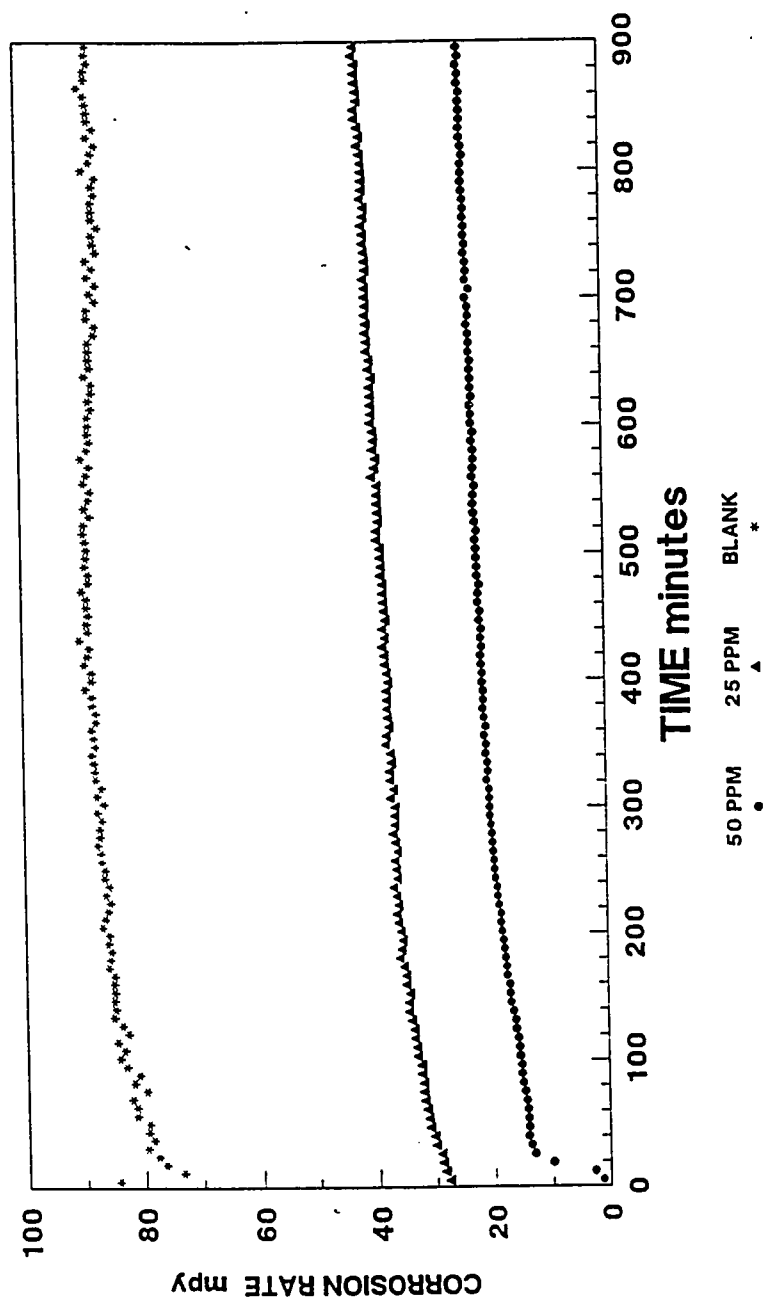


FIGURE 32; 0, 25, and 50 ppm of 1 (4-methylbenzyl)-1H-4,5-dibenzoyl-1,2,3-triazole in deaerated 1% HCl solution using mild steel rotating electrode at 1000 rpm.

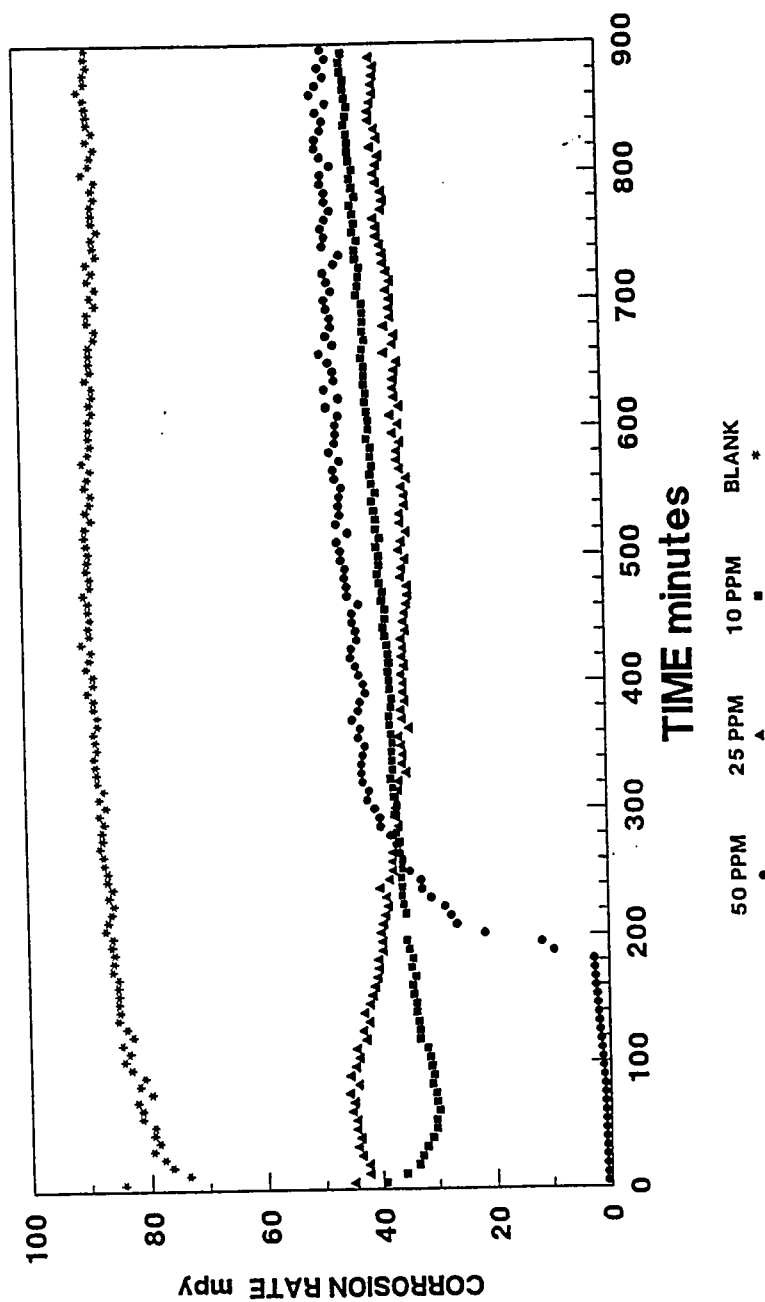


FIGURE 33; 0, 10, 25, and 50 ppm of 1-(4-nitrobenzyl)-1H-4,5-dibenzoyl-1,2,3-triazole in deaerated 1% HCl solution using mild steel rotating electrode at 1000 rpm.

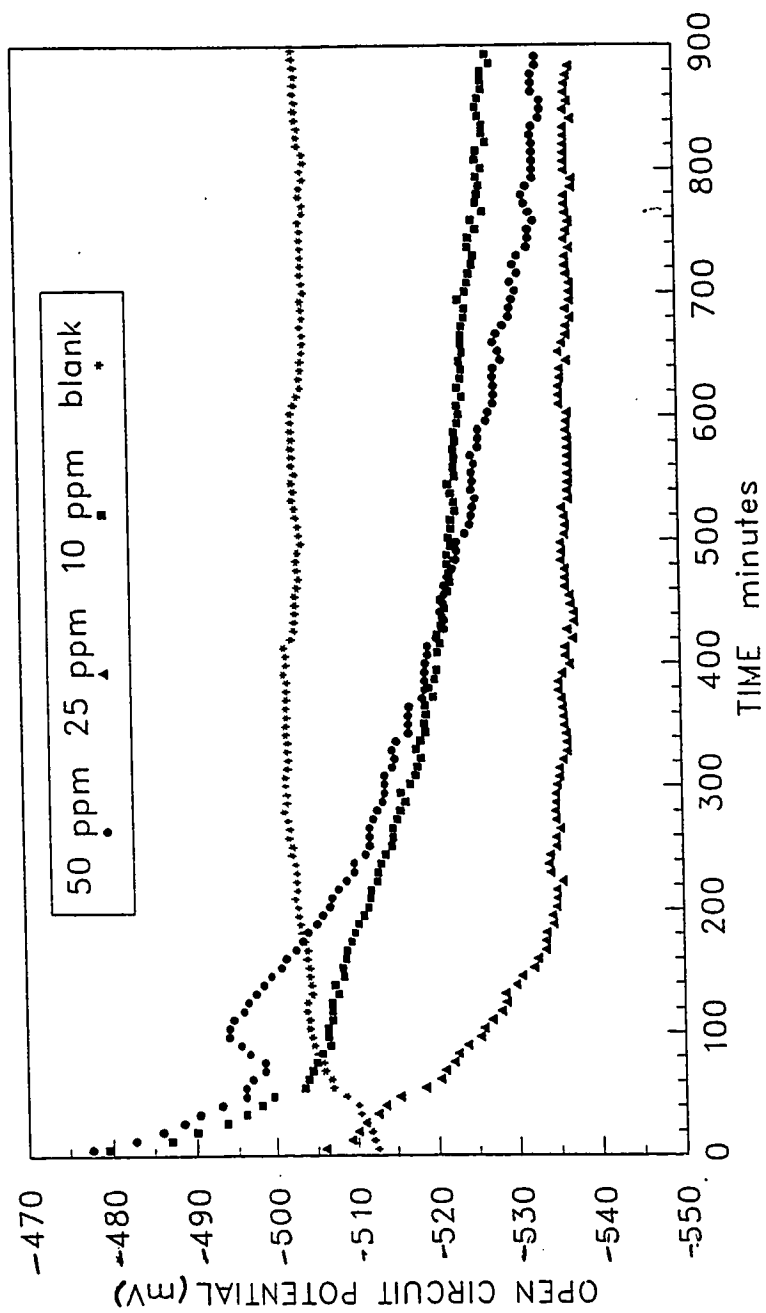


FIGURE 34; Potential profiles of 0, 10, 25, and 50 ppm of 1 (benzyl)-1-H-4,5 dibenzoyl 1,2,3 triazole in 1% deaerated HCl solution using mild steel rotating electrode at 1000 rpm.

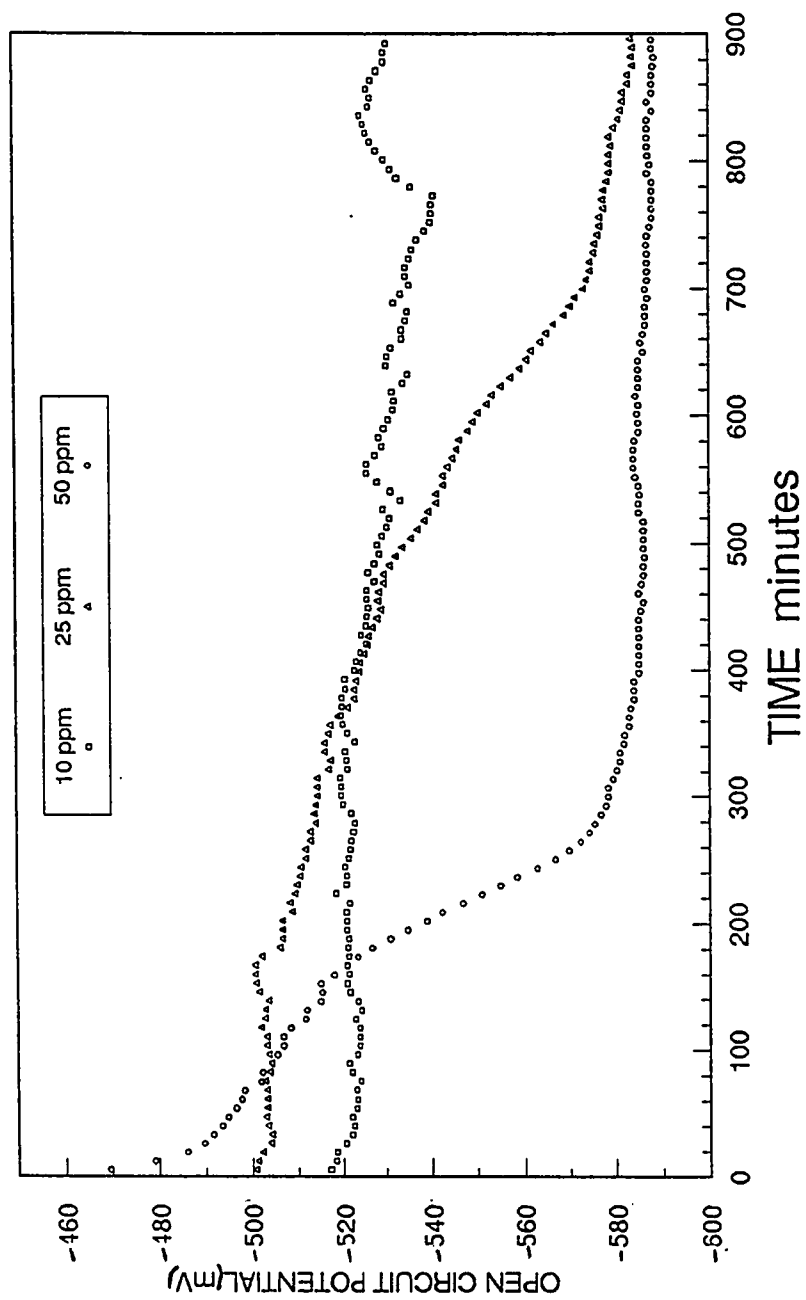


FIGURE 35; Potential profiles of 10, 25, and 50 ppm of 1 (4-bromobenzyl)-1-H-4,5 dibenzoyl 1,2,3-triazole in 1% deaerated HCl solution using mild steel rotating electrode at 1000 rpm.

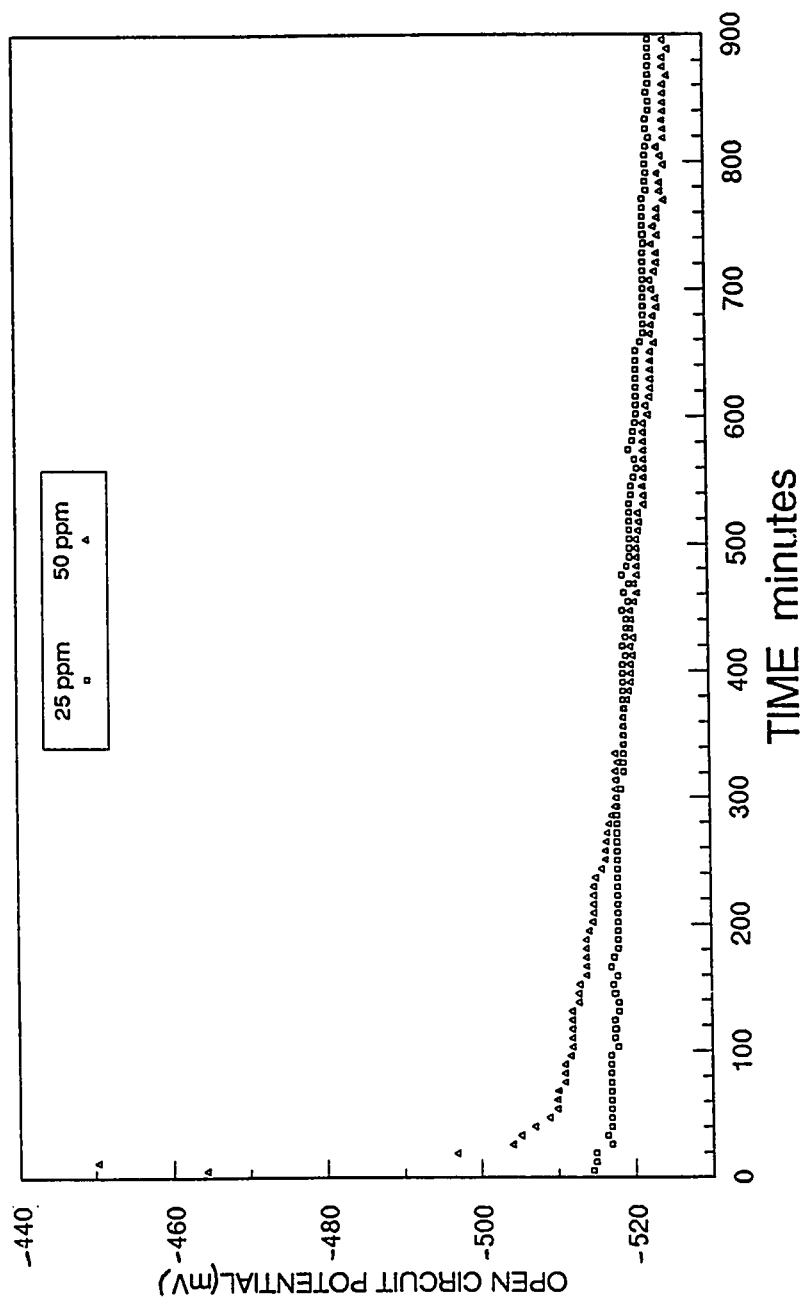


FIGURE 36; Potential profiles of 25, and 50 ppm of 1-(4-methylbenzyl)-1H-4,5 dibenzoyl-1,2,3-triazole in 1% deaerated HCl solution using mild steel rotating electrode at 1000 rpm.

5.2.1.3 Results of Tafel Polarization

The Tafel polarization plots of both anodic and cathodic scans of these compounds showed that E_{corr} has shifted to more negative direction compared to the uninhibited solution with increasing concentrations as shown in Figures 37, 38, and 39. Chemical addition resulted in interfering with both side of the reactions and predominating the cathodic one. Hence, these compounds can be classified as cathodic inhibitors. This classification is related to their reactions at the metal surface and how the potential on the electrode is affected. A potential independent region was observed only in the anodic scans of the 1 (benzyl)-1-H-4,5 dibenzoyl 1,2,3 triazole. Some of the calculated results obtained from the Tafel plots are summarized in Tables 9a to 9c and their diagrams are presented in the above mentioned figures.

Table 9a

1 (benzyl)-1-H- 4,5 dibenzoyl 1,2,3 triazole

CONC.	E_{corr} †	E at I=0 *	β_a ^	β_c ^	I_{corr} uA/cm ²
10 ppm	-528 mV	-509 mV	136	137	50.7
25 ppm	-533 mV	-509 mV	176	95	13.4
50 ppm	-537 mV	-523 mV	136	91	3.7

† Measured open circuit potential

* Calculated open circuit potential

^ Calculated at the end of the experiment

Table 9b

1 (4- bromobenzyl)-1-H- 4,5 dibenzoyl 1,2,3 triazole

CONC.	E_{corr}'	E at I=0 *	β_a ^	β_c ^	I_{corr} uA/cm ²
10 ppm	-529 mV	-527 mV	137	122	94.7
25 ppm	-586 mV	-582 mV	252	292	29.5
50 ppm	-588 mV	-584 mV	220	268	50.0

' Measured open circuit potential

* Calculated open circuit potential

^ Calculated at the end of the experiment

Table 9c

1 (4- methylbenzyl)-1-H- 4,5 dibenzoyl 1,2,3 triazole

CONC.	E_{corr}'	E at I=0 *	β_a ^	β_c ^	I_{corr} uA/cm ²
25 ppm	-525 mV	-518 mV	243	238	84.0
50 ppm	-523 mV	-513 mV	199	139	44.4

' Measured open circuit potential

* Calculated open circuit potential

^ Calculated at the end of the experiment

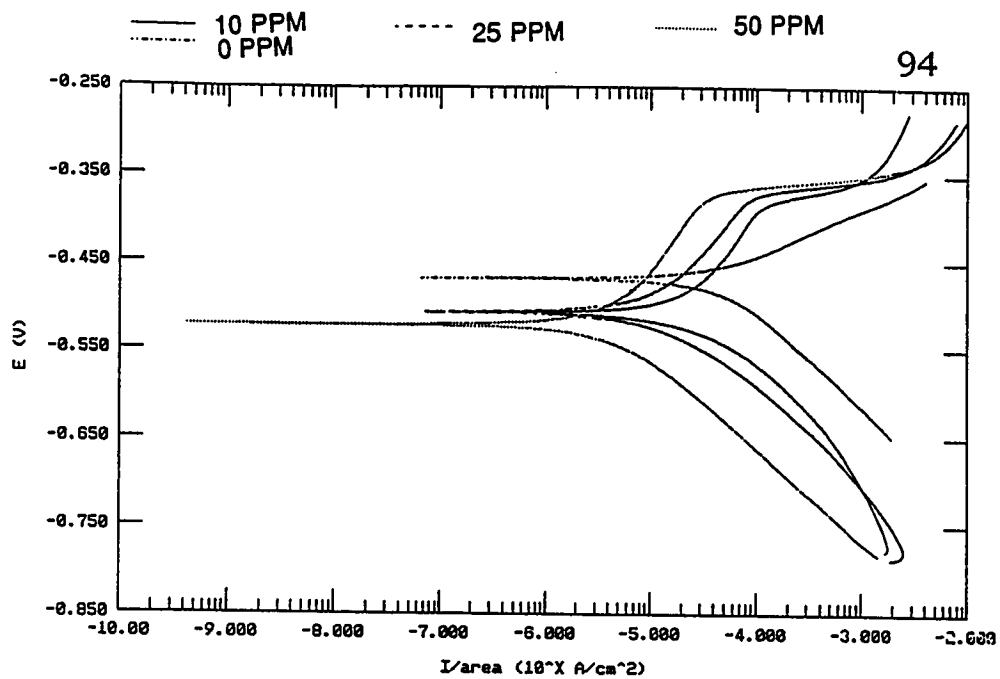


FIGURE 37; Polarization diagrams of Tafel plot at 0, 10, 25, and 50 ppm of 1 (benzyl)-1-H-4,5 dibenzoyl 1,2,3 triazole in 1% deaerated HCl solution using mild steel rotating electrode at 1000 rpm. The scanning rate was 0.25 mV/s with scanning increments of 0.5 mV.

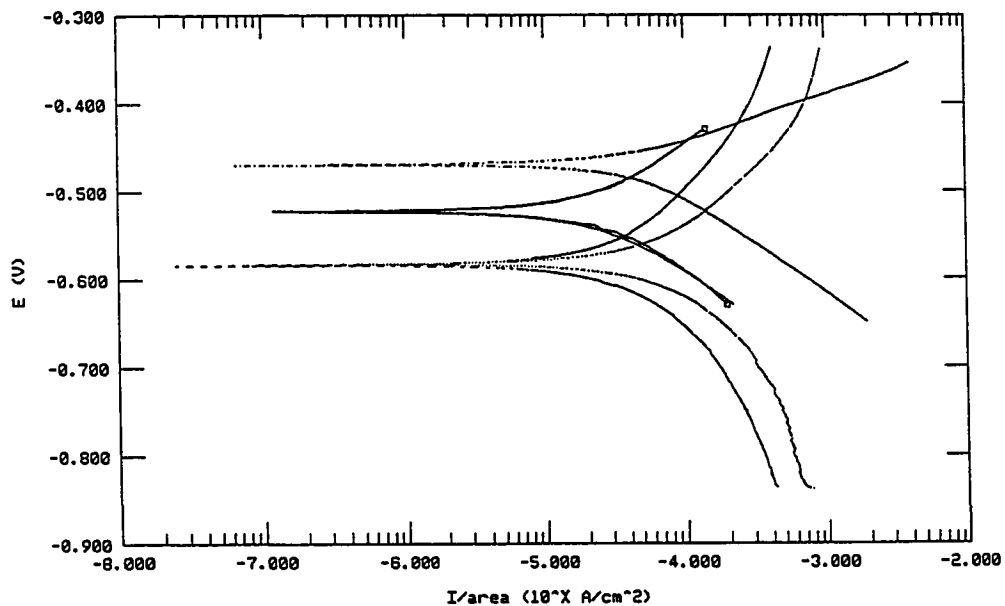


FIGURE 38; Polarization diagrams of Tafel plot at 0, 10, 25, and 50 ppm of 1 (4-bromobenzyl)-1-H-4,5 dibenzoyl-1,2,3 triazole in 1% deaerated HCl solution using mild steel rotating electrode at 1000 rpm. The scanning rate was 0.25 mV/s with scanning increments of 0.5 mV.

— 10 PPM - - - 25 PPM - · - · 50 PPM
 ····· 0 PPM

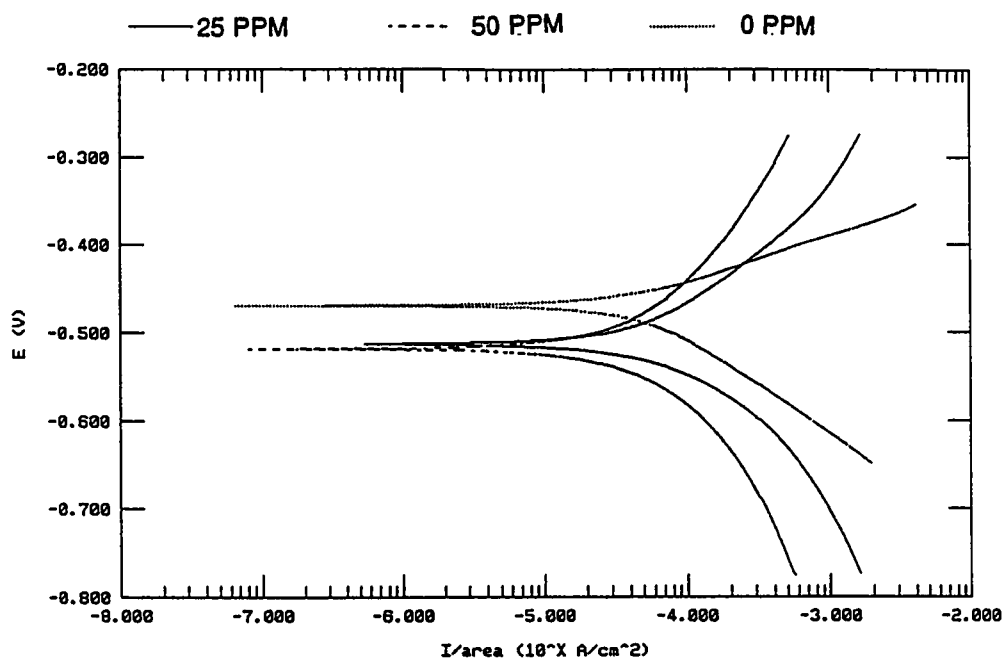
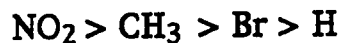


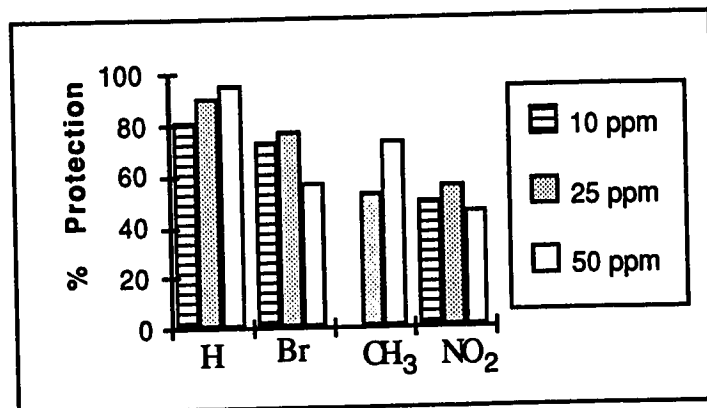
FIGURE 39; Polarization diagrams of Tafel plot at 0, 25, and 50 ppm of 1 (4-methylbenzyl)-1-H-4,5 dibenzoyl 1,2,3 triazole in 1% deaerated HCl solution using mild steel rotating electrode at 1000 rpm. The scanning rate was 0.25 mV/s with scanning increments of 0.5 mV.

5.2.1.4 Discussion

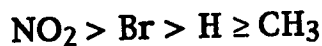
The corrosion rate profiles obtained from the on-line linear polarization technique showed that the inhibition capacity of these compounds are increased as follow :



This sequence is in good agreement with the results obtained from AC impedance and Tafel polarization. The graphical representation of the inhibition efficiency obtained from on-line linear polarization technique is shown below.



The bromo group is expected to be next in the previous sequence as follow:



But actually it appeared after the methyl group which can be explained by the dual actions of the electron withdrawing capacity as well as the strong effect of the counter interaction of the inductive effect of the halogen atom.

Introducing electron withdrawing groups on 1 (benzyl)-1-H-4,5 dibenzoyl 1,2,3 triazole compound is accompanied by a decrease in corrosion protection. As these groups or atoms are introduced, the

electron donation ability of the reacting center atom or atoms decreases. So, the strength of the adsorption bond and the inhibition efficiency will be decreased due to the decreasing of the electron density around the triazole ring.

Nitro group has the strongest electron withdrawing capacity among the tested compounds, so it showed the lowest protection value. Figure 33 shows that as the chemical concentration increases the corrosion rate will decrease. However, at 50 ppm an increase in concentration was followed by an increase in corrosion rate due to most probably to precipitation of the inhibitor. This again confirms the AC impedance trend shown in Figure 29.

Methyl group which is an electron releasing group is expected to behave better than H, and Br substituents. Unfortunately, it gave lower protection than bromo substituents. This is probably due to the induction effects of bromine on the aromatic ring which acts as an enrichment power on the triazole group. This may give the 1 (4-bromobenzyl)-1-H- 4,5 dibenzoyl 1,2,3 triazole the higher protection value at 10 and 25 ppm compared to methyl derivative. It is more likely that the efficiency of the methyl substituent in the triazole compound is influenced by the low solubility of the 1 (4-methylbenzyl)-1-H- 4,5 dibenzoyl 1,2,3 triazole in the diluted hydrochloric acid solution even after changing the solvent to toluene. The latter reason may be the most effective factor influencing its inhibitive influence.

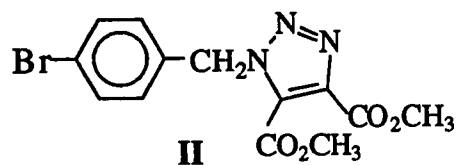
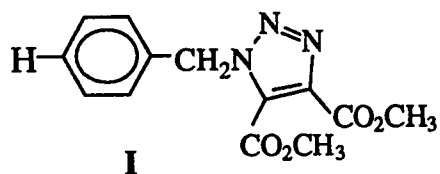
5.2.2 Substituents At 4,5 Positions Of The Triazole Cycle.

Four compounds were studied in an attempt to investigate the role and the effect of different substituents on the corrosion rate.

These compounds were :

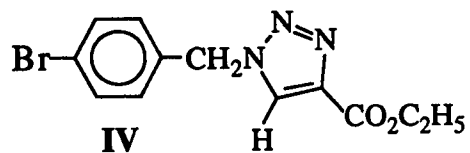
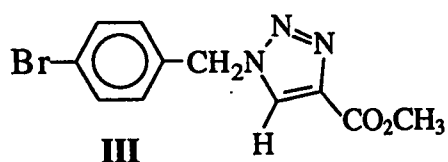
I-Dimethyl 1 (benzyl)-1-H-1,2,3 triazole 4,5- dicarboxylate

II-Dimethyl 1 (4- bromobenzyl)-1-H-1,2,3 triazole 4,5 dicarboxylate



III-Methyl 1 (4- bromobenzyl)1-H-1,2,3 triazole 4- carboxylate

IV-Ethyl 1 (4- bromobenzyl)1-H-1,2,3 triazole 4- carboxylate



The chain length, group effects, and mono versus di substituents comparison were covered in this part of study. Two techniques were used namely; on-line linear polarization and Tafel plot techniques. The experimental conditions and the setup were all the same as applied before. The stock solutions of the above chemicals were dissolved in ethanol.

5.2.2.1 Results of continuous Linear Polarization Resistance

The corrosion rate obtained from the on-line linear polarization technique and the calculated inhibition efficiency are summarized in the following Tables 10, 11, 12, and 13.

Table 10
dimethyl 1 (benzyl)-1-H- 1,2,3 triazole 4,5 dicarboxylate

Conc.	Final E	Corrosion Rate *	Inhibition Efficiency
10 ppm	- 511 mV	14.1 mpy	84%
25 ppm	- 511 mV	9.9 mpy	88.8%

* represent the average of the last hour readings

Table 11
dimethyl 1 (4- bromobenzyl)-1-H- 1,2,3 triazole 4,5 dicarboxylate

Conc.	Final E	Corrosion Rate *	Inhibition Efficiency
10 ppm	- 507 mV	71 mpy	19.3%
25 ppm	- 584 mV	16.6 mpy	81.1%

* represent the average of the last hour readings

Table 12
methyl 1 (4- bromobenzyl)-1-H- 1,2,3 triazole 4-
carboxylate

Conc.	Final E	Corrosion Rate *	Inhibition Efficiency
10 ppm	- 512 mV	60.6 mpy	31.1%
25 ppm	- 525 mV	10.2 mpy	88.4%

* represent the average of the last hour readings

Table 13
ethyl 1 (4- bromobenzyl)-1-H- 1,2,3 triazole 4-carboxylate

Conc.	Final E	Corrosion Rate *	Inhibition Efficiency
10 ppm	- 517 mV	65 mpy	26.1%
25 ppm	- 532 mV	26 mpy	70.5%

* represent the average of the last hour readings

The corrosion rate profiles of these compounds at 10 and 25 ppm are shown in Figures 40, 41, 42, and 43 respectively versus the corrosion rate of the uninhibited solution. Also, the behavior of the open circuit potential which was measured versus SCE during the experimental period applying the formerly mentioned sequence are illustrated in Figures 44, 45, 46, and 47. It is obvious from these graphs that the substitution at 4 and 5 positions of the triazole ring exhibited low protection at a concentration of 10 ppm. This is particularly true in the presence of bromine substituents. This is due to the lower coverage capabilities of these compounds at low concentrations.

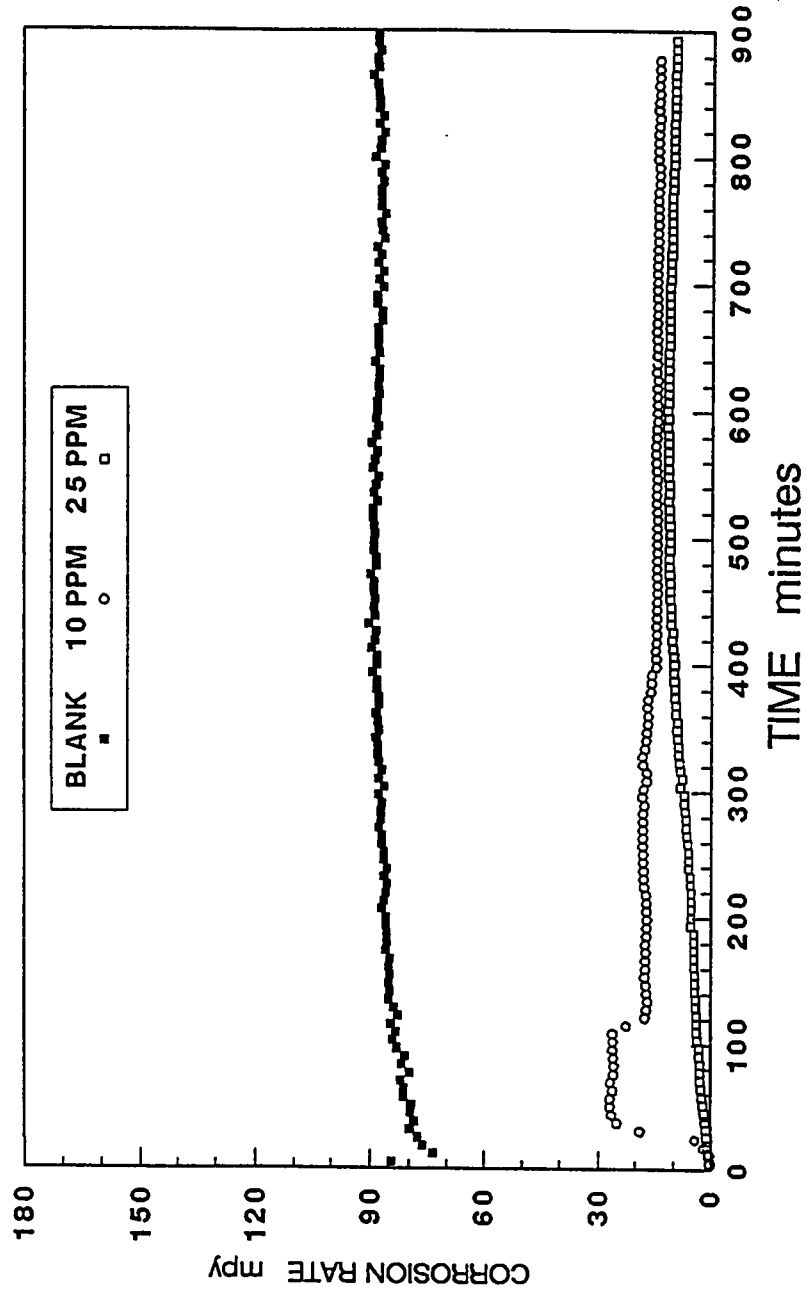


FIGURE 40; 0, 10, and 25 ppm of dimethyl 1 (benzyl)-1-H-1,2,3 triazole 4,5 dicarboxylate in 1% HCl deaerated solution using mild steel rotating electrode at 1000 rpm.

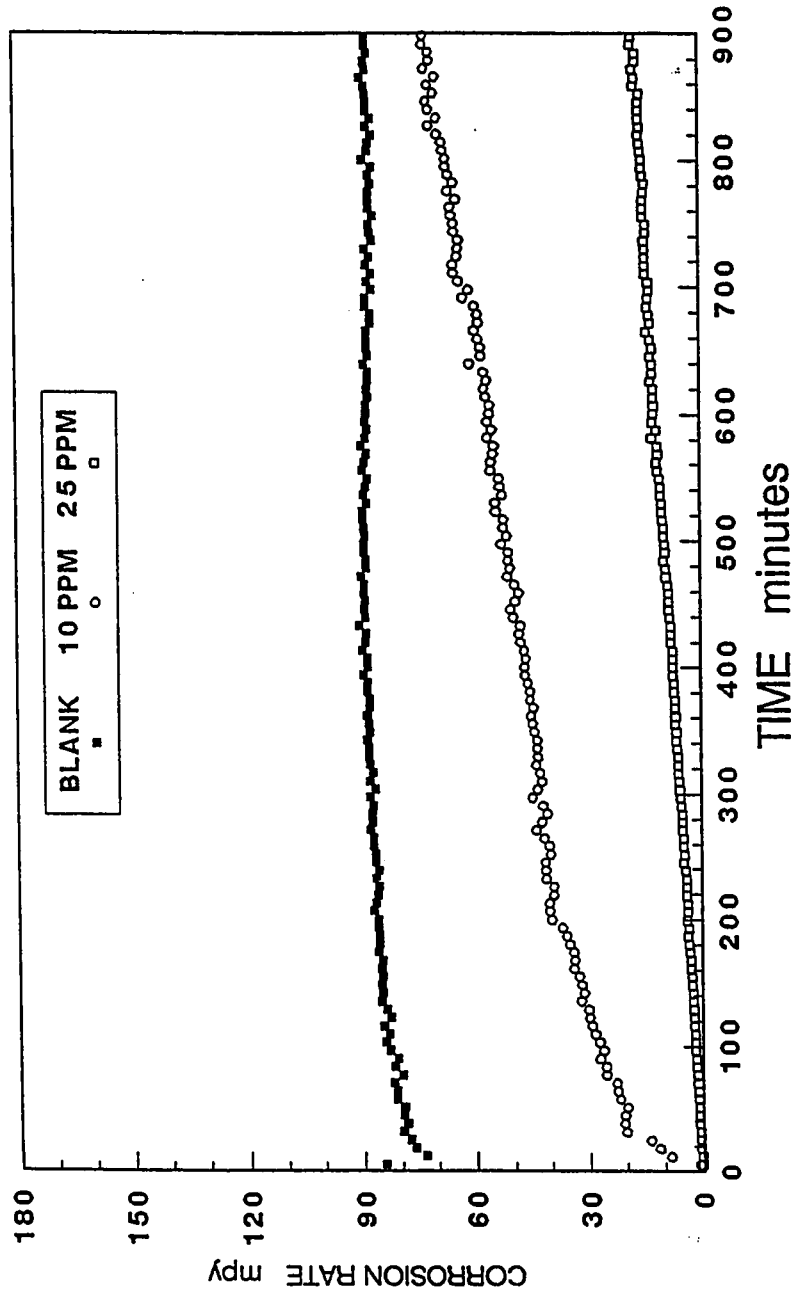


FIGURE 41; 0, 10, and 25 ppm of dimethyl 1-(4-bromobenzyl)-1-H-1,2,3 triazole 4,5 dicarboxylate in 1% HCl deaerated solution using mild steel rotating electrode at 1000 rpm.

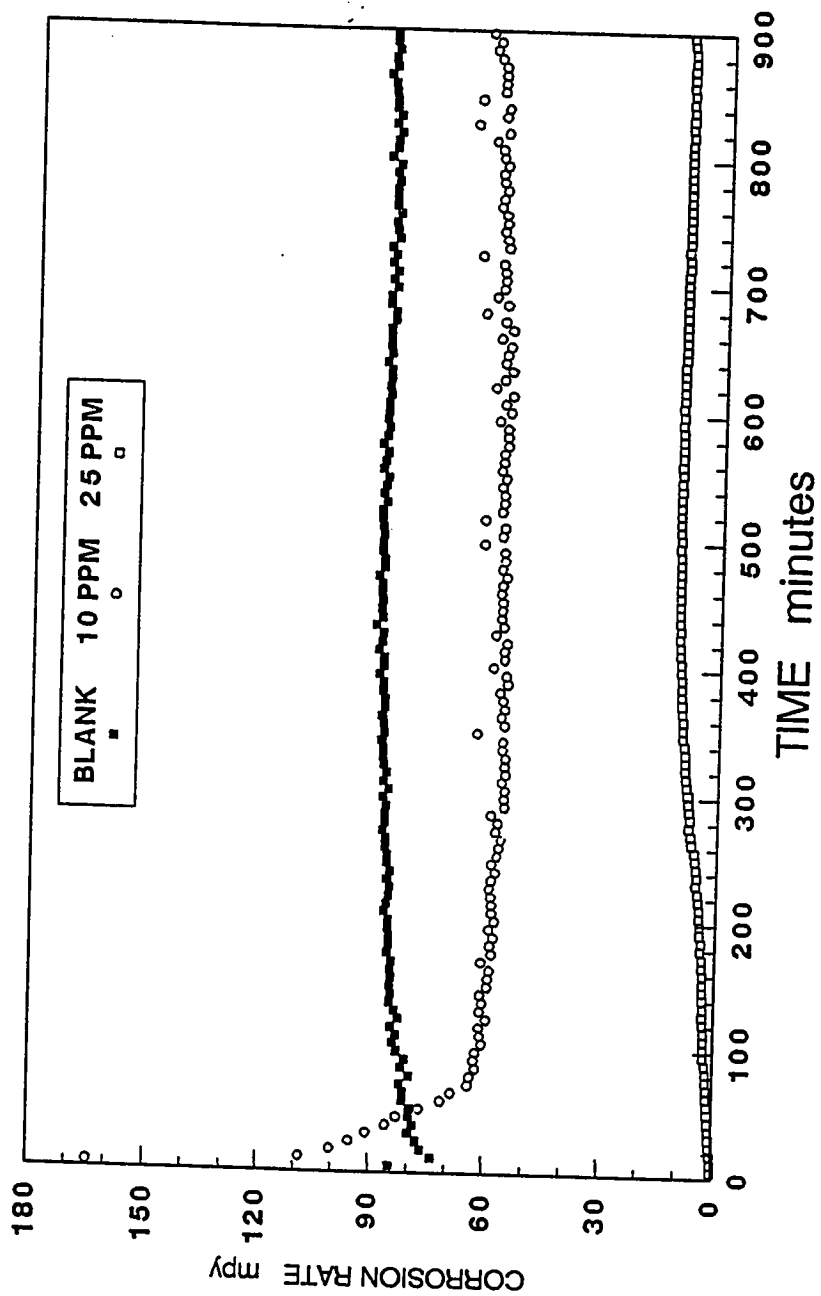


FIGURE 42; 0, 10, and 25 ppm of methyl 1 (4-bromobenzyl)-1-H-1,2,3-triazole 4-carboxylate in 1% HCl deaerated solution using mild steel rotating electrode at 1000 rpm.

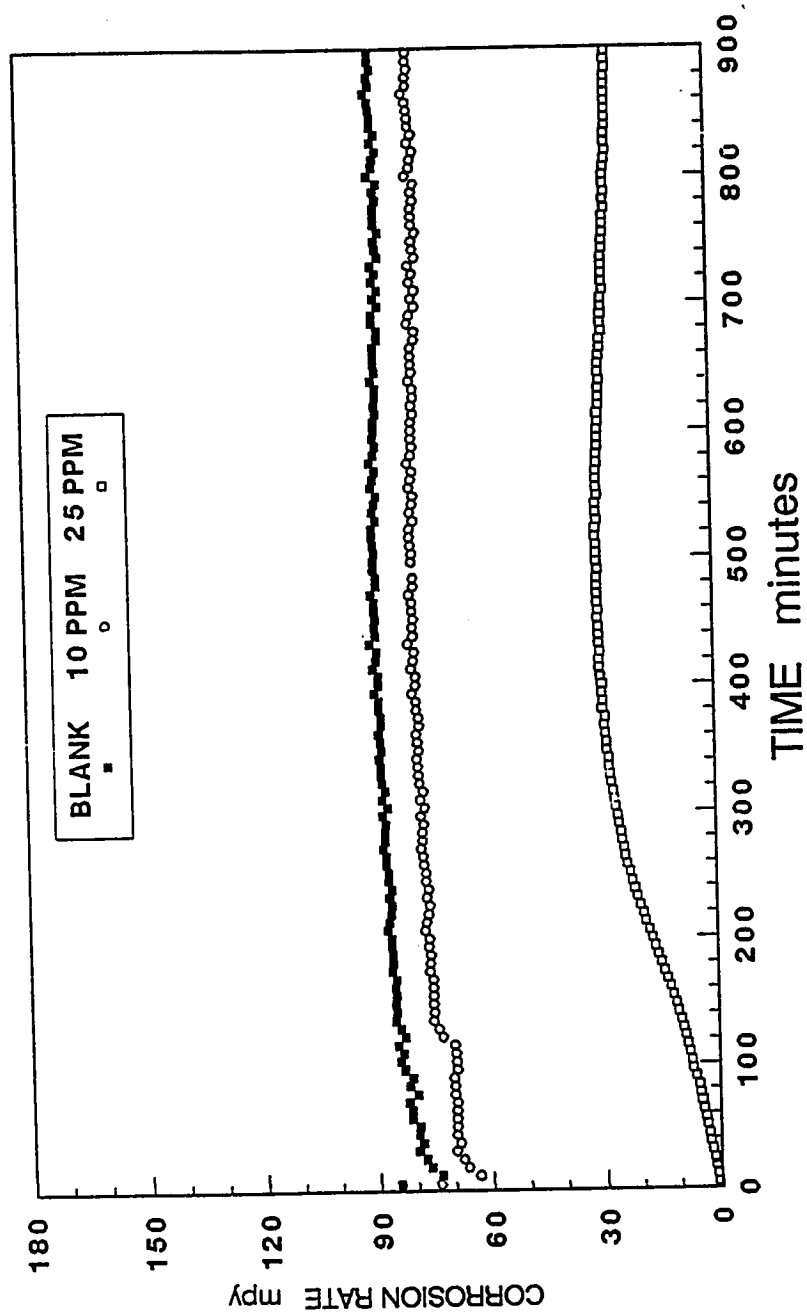


FIGURE 43; 0, 10, and 25 ppm of ethyl 1 (4-bromobenzyl)-1-H-1,2,3 triazole 4- carboxylate in 1% HCl deaerated solution using mild steel rotating electrode at 1000 rpm.

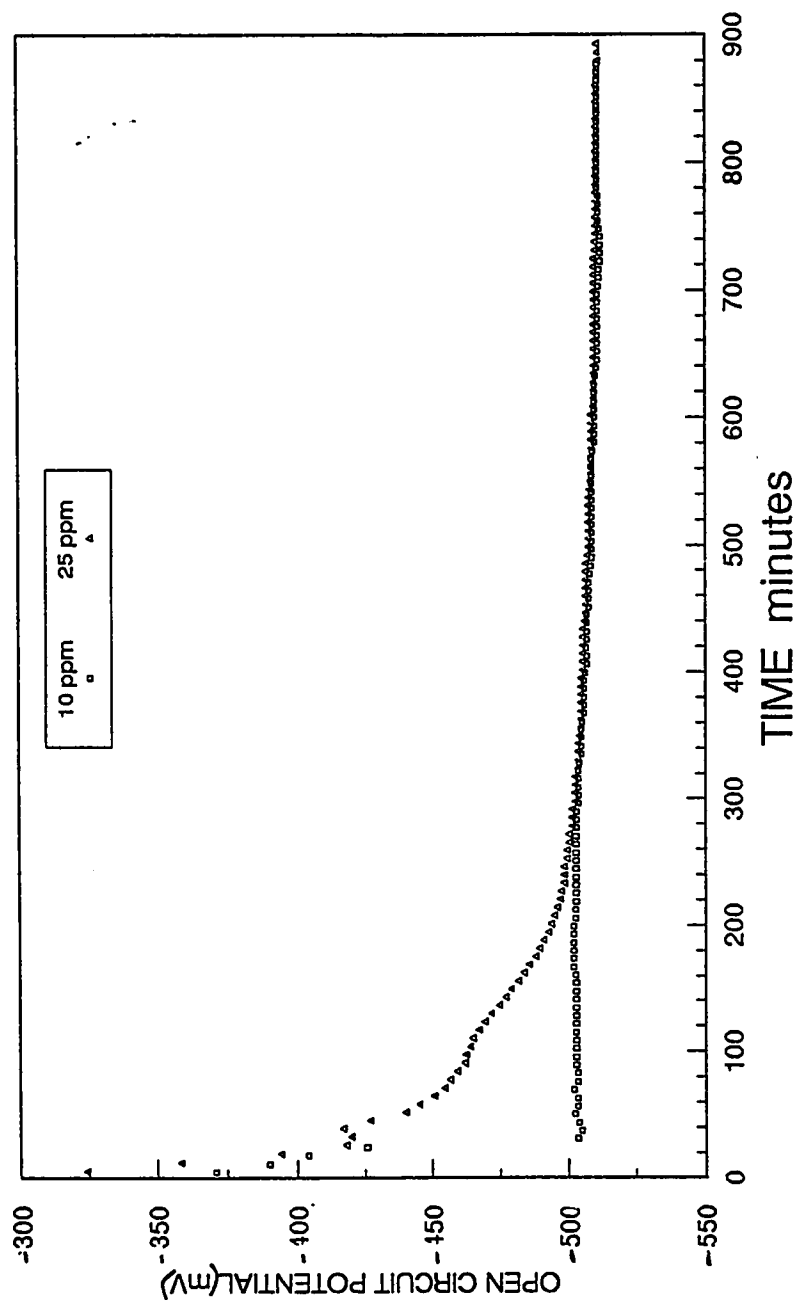


FIGURE 44; Potential behaviors of 10 and 25 ppm of dimethyl 1 (benzyl)-1H-1,2,3-triazole-4,5-dicarboxylate in 1% HCl deaerated solution using mild steel rotating electrode at 1000 rpm.

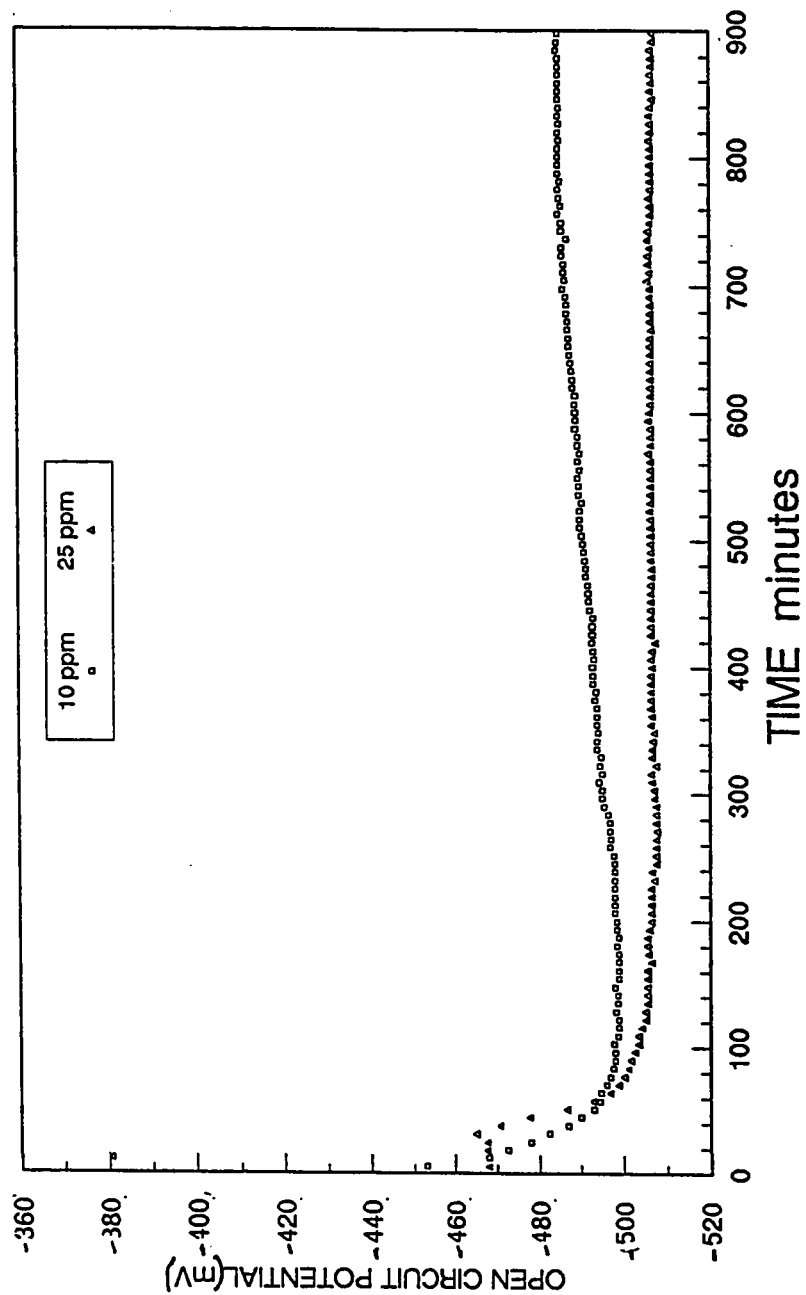


FIGURE 45; Potential behaviors of 0,10 and 25 ppm of dimethyl 1 (4-bromobenzyl)-1-H-1,2,3-triazole-4,5-dicarboxylate in 1% HCl deaerated solution using mild steel rotating electrode at 1000 rpm.

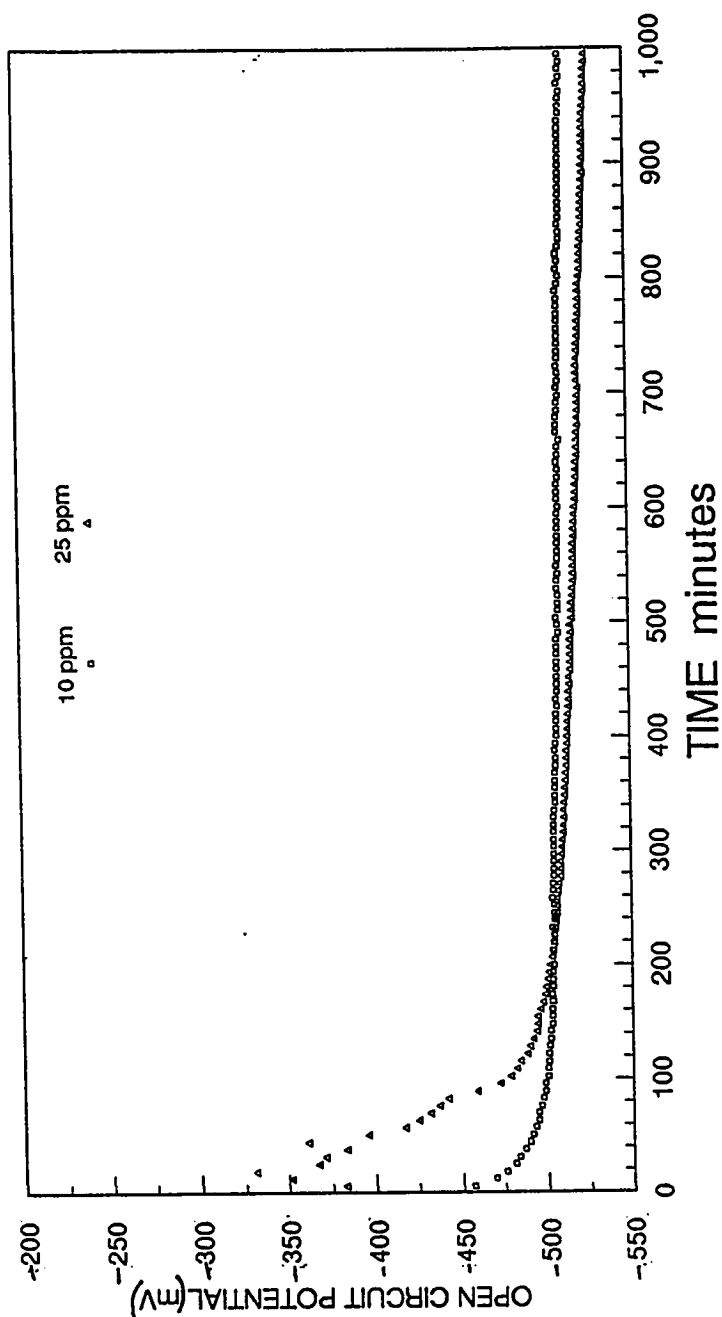


FIGURE 46; Potential behaviors of 10, and 25 ppm of methyl 1(4-bromobenzyl) -1-H- 1,2,3 triazole 4- carboxylate in 1% HCl deaerated solution using mild steel rotating electrode at 1000 rpm.

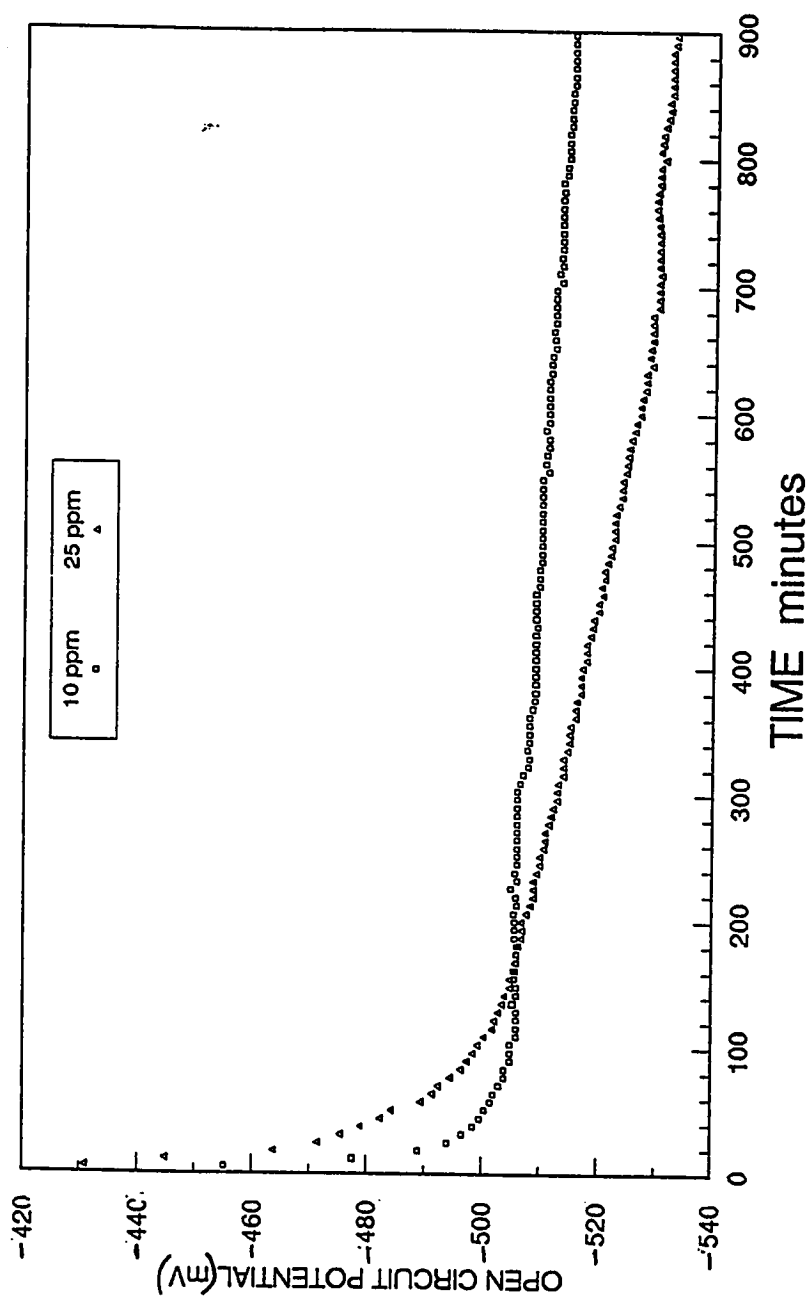


FIGURE 47; Potential behaviors of 10 and 25 ppm of ethyl 1-(4-bromobenzyl)-1H-1,2,3-triazole-4-carboxylate in 1% HCl deaerated solution using mild steel rotating electrode at 1000 rpm.

5.2.2.2 Results of Tafel Polarization:

Tafel polarization scans were also performed in the 1% HCl deaerated solution in the presence of these compounds where the potential was scanned from ± 250 mV versus the E_{corr} . The Tafel plots of these compounds at 10 and 25 ppm are presented in Figures 48 to 51. Addition of these compounds were resulted in shifting the E_{corr} of the electrode to the more negative direction. Some of the calculated results obtained from these plots are summarized in Tables 14a to 14d.

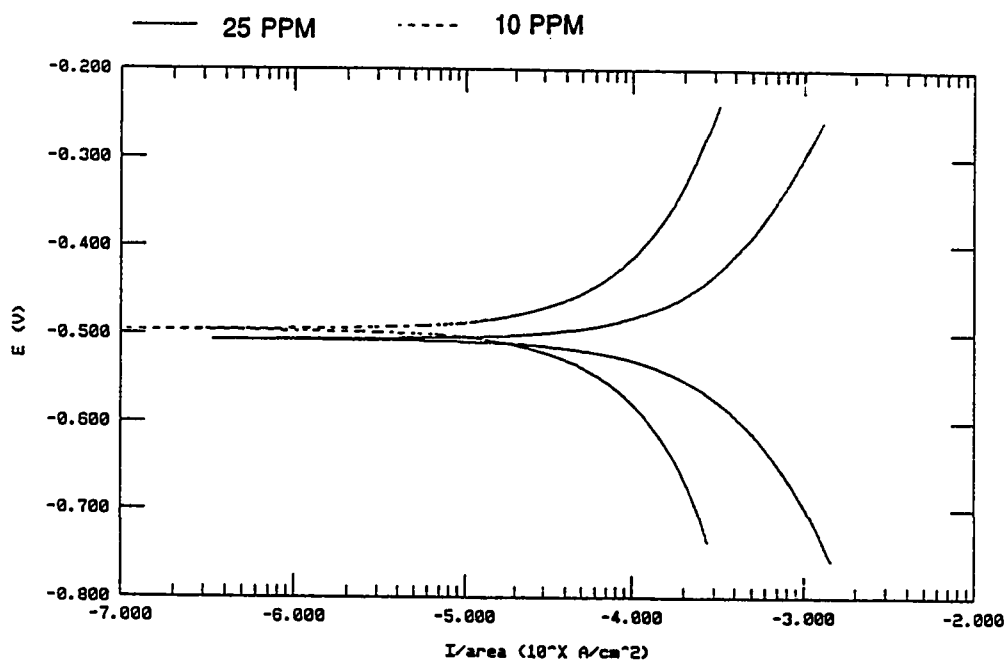


FIGURE 48; Tafel plots at 10 and 25 ppm of dimethyl 1 (benzyl)-1-H-1,2,3 triazole 4,5 dicarboxylate. The scanning rate was 0.25 mV/s with scanning increments of 0.5 mV.

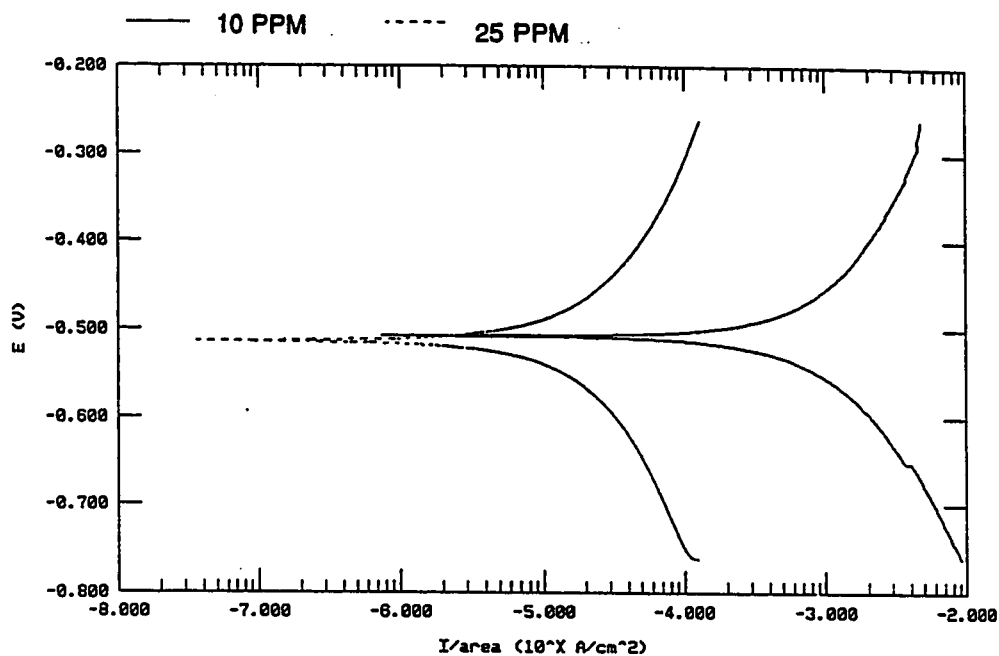


FIGURE 49; Tafel plots at 10 and 25 ppm of dimethyl 1 (4-bromobenzyl) -1-H- 1,2,3 triazole 4,5 dicarboxylate. The scanning rate was 0.25 mV/s with increments of 0.5 mV.

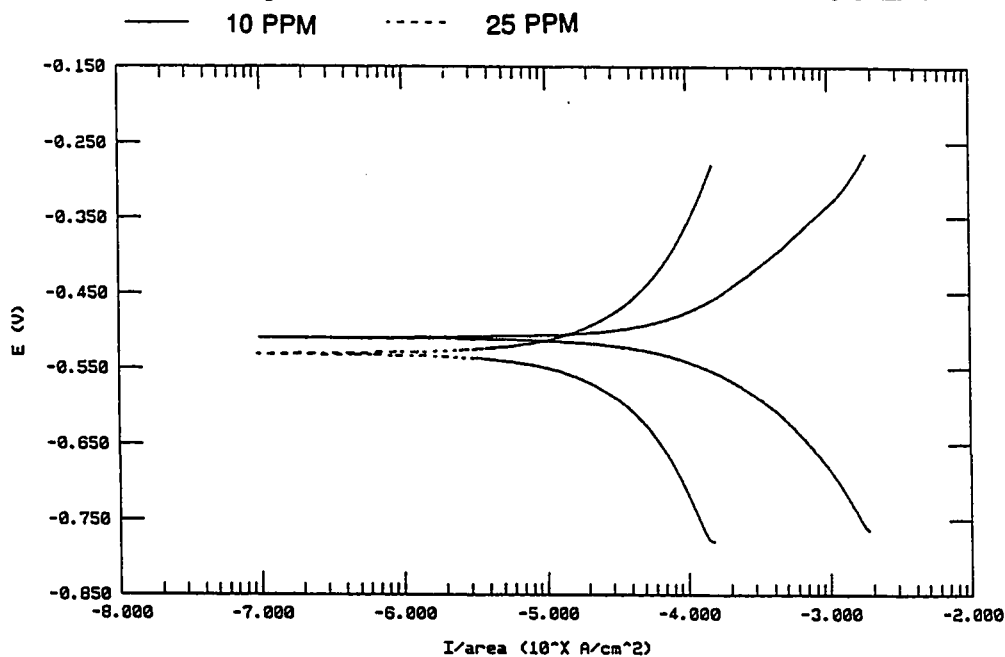


FIGURE 50: Tafel plots at 10, and 25 ppm of methyl 1- (4-bromobenzyl) -1-H- 1,2,3 triazole 4- carboxylate . The scanning rate was 0.25 mV/s with increments of 0.5 mV.

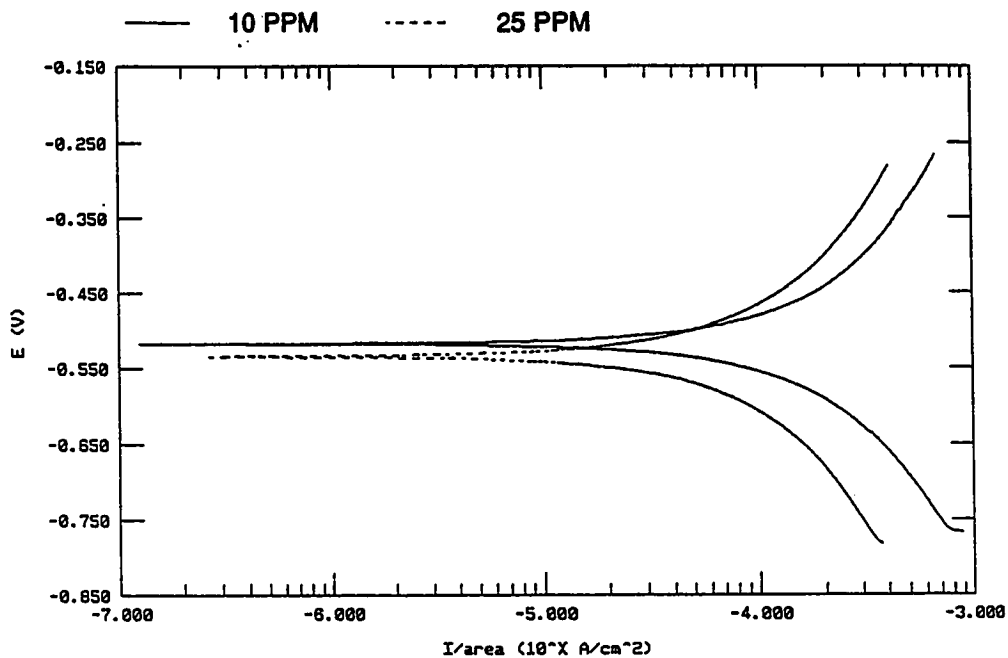


FIGURE 51: Tafel plots at 10, and 25 ppm of ethyl 1-(4-bromobenzyl)-1-H- 1,2,3 triazole 4- carboxylate. The scanning rate was 0.25 mV/s with increments of 0.5 mV.

Table 14a
dimethyl 1 (benzyl)-1-H- 1,2,3 triazole 4,5 dicarboxylate

CONC.	E_{corr} †	E at $I=0^*$	β_a ^	β_c ^	I_{corr} $\mu\text{A}/\text{cm}^2$
10 ppm	-510 mV	-509 mV	172	137	56.5
25 ppm	-511 mV	-510 mV	166	170	22.5

† Measured open circuit potential

* Calculated open circuit potential

^ Calculated at the end of the experiment

Table 14b
dimethyl 1-(4- bromobenzyl)-1-H- 1,2,3 triazole 4,5
dicarboxylate

CONC.	E_{corr} †	E at I=0 *	β_a ^	β_c ^	I_{corr} uA/cm ²
10 ppm	-486 mV	-496 mV	312	319	176
25 ppm	-508 mV	-507 mV	219	194	77.7

† Measured open circuit potential

* Calculated open circuit potential

^ Calculated at the end of the experiment

Table 14c
methyl 1 (4-bromobenzyl)-1-H- 1,2,3 triazole 4-carboxylate

CONC.	E_{corr} †	E at I=0 *	β_a ^	β_c ^	I_{corr} uA/cm ²
10 ppm	-514 mV	-510 mV	116	103	54.7
25 ppm	-529 mV	-531 mV	229	270	52.2

† Measured open circuit potential

* Calculated open circuit potential

^ Calculated at the end of the experiment

Table 14d
ethyl 1 (4-bromobenzyl)-1-H- 1,2,3 triazole 4-carboxylate

CONC.	E_{corr} †	E at I=0 *	β_a ^	β_c ^	I_{corr} uA/cm ²
10 ppm	-517 mV	-518 mV	260	284	165
25 ppm	-532 mV	-535 mV	172	137	77.2

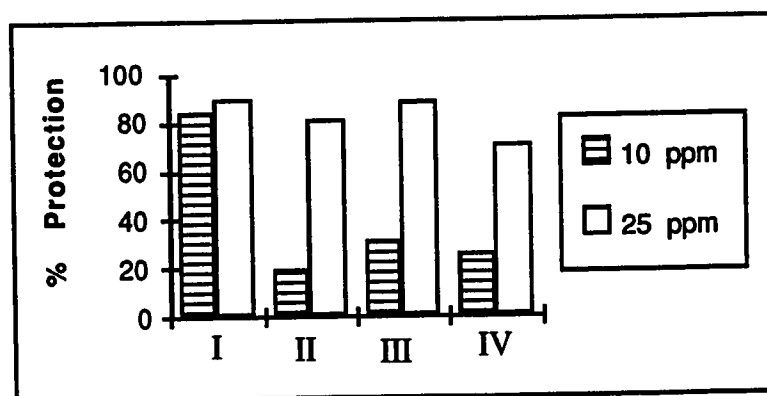
† Measured open circuit potential

* Calculated open circuit potential

^ Calculated at the end of the experiment

5.2.2.3 Discussion:

The graphical representation of the protection percentage of these compounds which obtained from continuous linear polarization are shown below.



The performance ranking of these compounds are as follow:

$$I > III > II > IV .$$

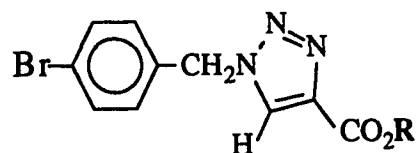
Replacing the keto groups, COC_6H_5 , of 1 (benzyl)-1-H- 4,5 dibenzoyl 1,2,3 triazole at 4 and 5 positions with an ester groups, CO_2CH_3 , resulted in similar behavior. Very close corrosion rates were obtained as shown in Table 15. This probably indicates that both substituents, the keto and ester groups, have the same effect on the electron density around the triazole cycle. Also most likely that, both covered the electrode surface completely resulting in a good reduction in the corrosion rate.

Table 15
Inhibition comparison of the keto and ester groups of the 1
(benzyl)-1-H- 1,2,3 triazole compound

TYPE OF G	Corrosion Rate mpy		Inhibition Efficiency	
	10 ppm	25 ppm	10 ppm	25 ppm
Keto	16.9 mpy	8.5 mpy	81%	90.3%
Ester	14.1 mpy	9.9 mpy	84%	88.8%

An increase in the carbon chain length of an inhibitor is expected to enhance the inhibition efficiency [6,28,51, 54]. This could be attributed to an increase in the electronic density at the nitrogen atoms due to inductive effects[52], an increase in the coverage ability [30], hydrophobicity [51], and polarizability [4,52] and a decrease in the solubility [51] of the inhibitor.

Unfortunately, the corrosion retardation ability of the triazole compound shown below decreases as the chain length increases from methyl to ethyl.



R can be either CH₃ or C₂H₅

This might be due to a decrease in the adsorbability of the triazole compound which was observed as the chain length gets longer. This also can be attributed to an increase in the hydrophilic character of the molecule causing a higher interaction between the adsorbed molecules at the metal- solution interface and the bulk solution. Some results of the effects of chain length on corrosion rate is given in Table 16. Also, Figures 52 and 53 show the behavior of these compounds using on-line monitoring program.

TABLE 16

Results Of The Effects Of Chain Length On Corrosion Rate

Type of R	Corrosion Rate mpy		Inhibition Efficiency	
	10 ppm	25 ppm	10 ppm	25 ppm
Methyl	60.6 mpy	10.2 mpy	31%	88.4%
Ethyl	65 mpy	26 mpy	26%	70.5%

Finally, compound III displays better performance compared to compound II. Disubstituents at 4 and 5 positions expect to perform better than at position 4 only due to the higher bonds conjugation. However, disubstituents revealed on lowering the inhibition activities. One factor can be considered her is the geometric hindrance factor which may be involved.

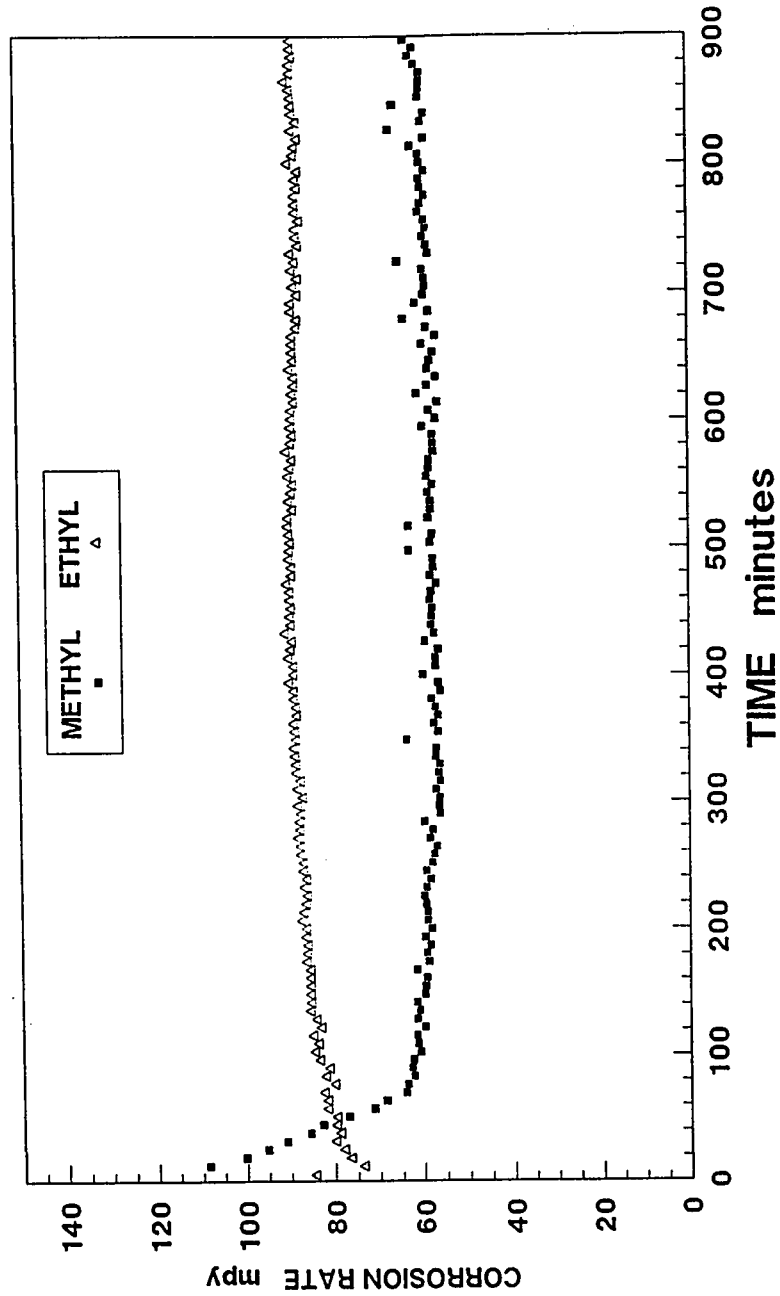


FIGURE 52: Corrosion behavior of 10 ppm of both methyl and ethyl 1-(4-bromobenzyl)-1-H-1,2,3 triazole 4- carboxylate in 1% HCl deaerated solution using mild steel rotating electrode at 1000 rpm.

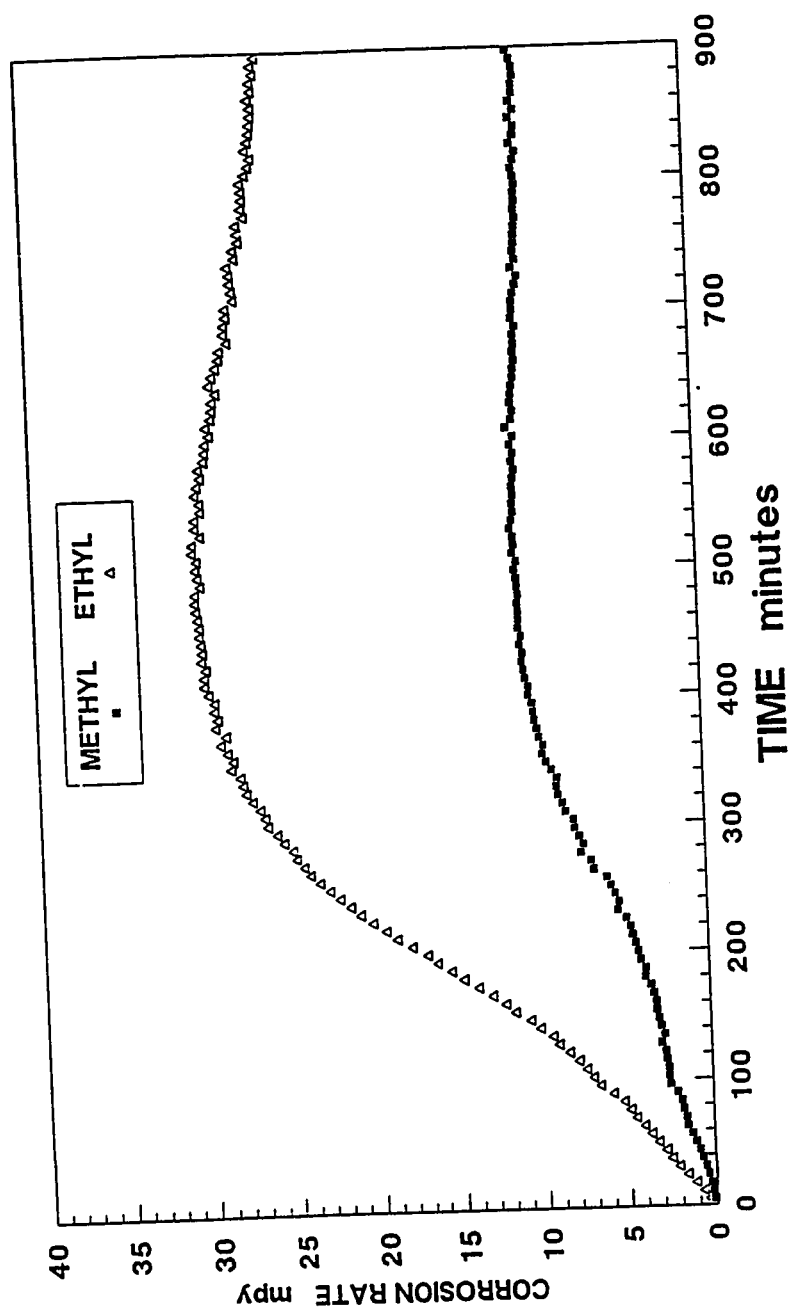


FIGURE 53: Corrosion behavior of 25 ppm of both methyl and ethyl 1 (4-bromobenzyl)-1-H- 1,2,3 triazole 4- carboxylate in 1% HCl deaerated solution using mild steel rotating electrode at 1000 rpm.

5.3 FILM PERSISTENCE TEST OF 1 (BENZYL)-1-H- 4,5 DIBENZOYL 1,2,3 TRIAZOLE

The objective of this part of the study is to investigate the extent of film persistency of the compound which was found to be the most efficient inhibitor as a function of exposure time. This approach represents the batch chemical treatment which has short chemical treatment followed by a long protection period.

The testing specimen was exposed at 10000 ppm of the stock solution at stagnant condition for 30 and 60 minutes while nitrogen gas was bubbled at a low rate. During the exposure period, a film on the electrode surface is expected to be formed. Then, the exposed rotating cylinder electrode was immersed in a deaerated 1% HCl solution and the corrosion monitoring was initiated for 4000 minutes ,67 hours, using continuous linear polarization technique.

Figures 54 and 55 illustrate the effect of exposure time on the corrosion rate of the pretreated electrode. In general, the corrosion rate decreases as the exposure time increases . It is noticed from these graphs that, as the filming exposure time increases the corrosion rate decreases. The corrosion rates after 67 hours exposure for 30 and 60 minutes filming were 10 and 3 mpy. These results indicate that, 1 (benzyl)-1-H- 4,5 dibenzoyl 1,2,3 triazole can be used for batch treatment due to its strong film forming ability.

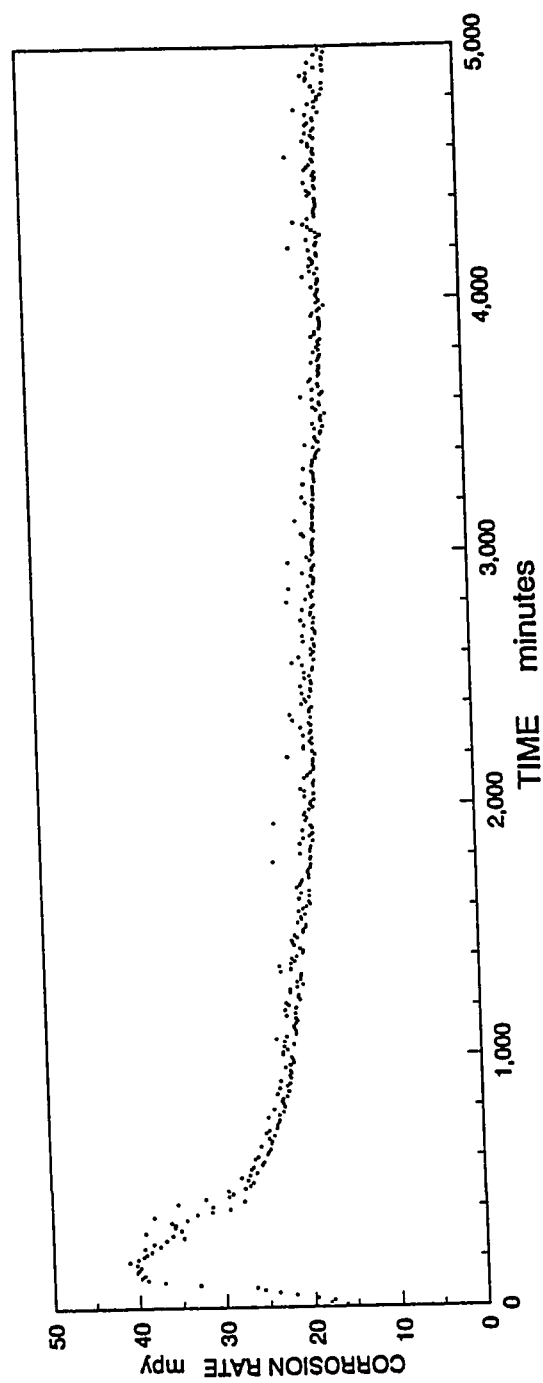


FIGURE 54: Film persistency test of 1 (benzyl)-1-H- 4,5 dibenzoyl 1,2,3 triazole after 30 minutes filming in 10000 ppm.

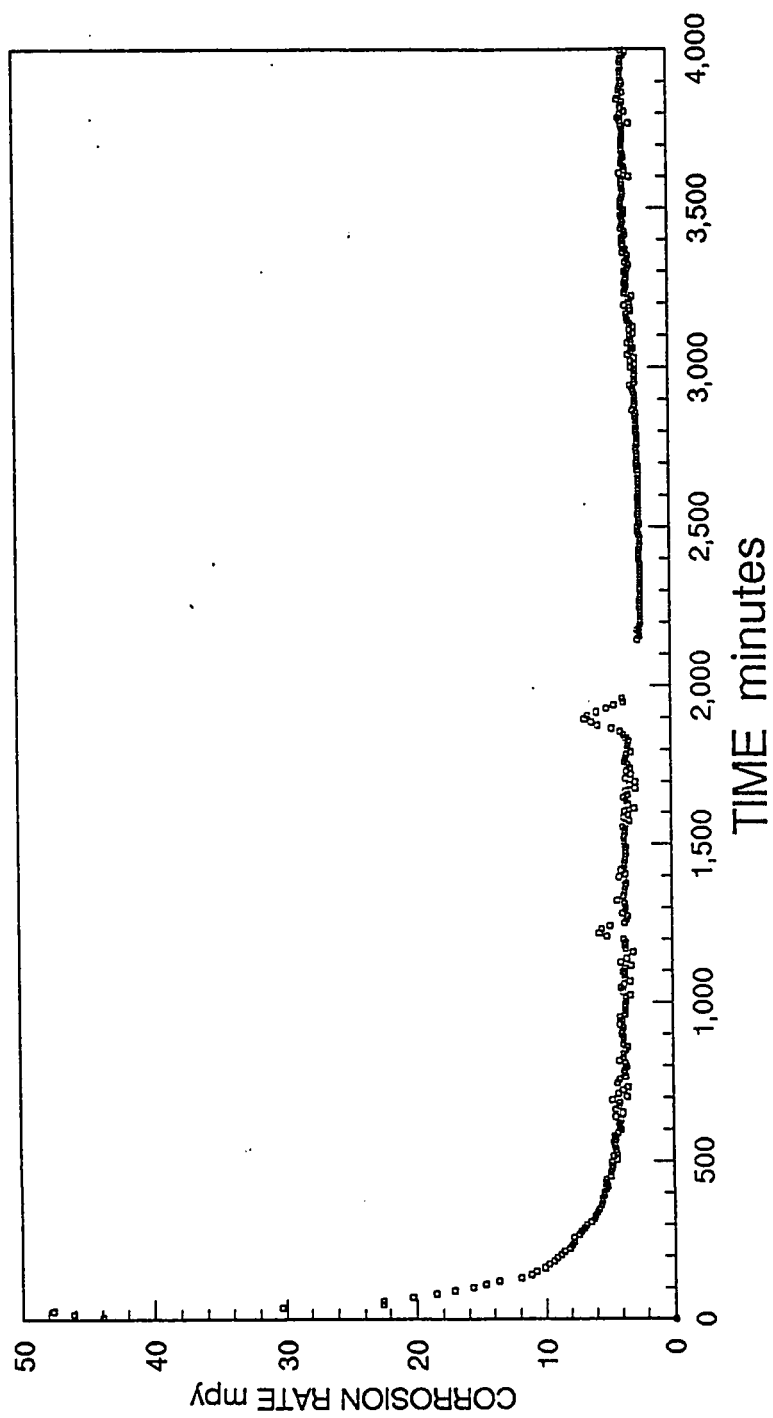


FIGURE 55: Film persistency test of 1 (benzyl)-1-H- 4,5 dibenzoyl 1,2,3 triazole after 60 minutes filming in 10000 ppm.

CHAPTER 6

CONCLUSION

6.1 TRIAZOLE EVALUATION

The comparison under similar conditions of the inhibiting activity of different triazole compounds provides a better elucidation of the effect of their chemical structure. The inhibition activities of the compounds studied in this research are interpreted from the point of view of the electronic structure. The relations found between the parameters of the chemical structure and the inhibiting activity of the compounds provide a way of prognosticating the inhibition behavior of the triazole compounds in the case of corrosion of mild steel in acid media.

The results of this study have shown that corrosion of mild steel electrode in 1% HCl deoxygenated solution can be controlled in the presence of 1(benzyl) 1-H- 4,5 dibenzoyl 1,2,3 triazole. The film persistence test indicates that 1(benzyl) 1-H- 4,5 dibenzoyl 1,2,3

triazole forms a very stable, inert, and long lasting film. Also, substitutions at the benzyl nucleus influence the electron density, and provide some evidence that an increase in the electron density positively influences the inhibition action of these compounds.

Moreover, in the presence of the studied triazole compounds, a noticeable shift in the E_{corr} to more negative direction is observed. This shift indicates a reduction in the rate of hydrogen evolution through the formation of a passive layer as a result of adsorption of inhibitor at the metal surface. This deviation increases in the presence of electron withdrawing substituents or with increasing concentration of the inhibitor.

The final ranking of the derivatives of 1(benzyl) 1-H- 4,5 dibenzoyl 1,2,3 triazole compounds at the para position are as follow:



and in the case of substitution at 4 and 5 positions of the triazole cycle, the performance ranking of these compounds are as follow:



6.2 PROPOSED MECHANISM

According to Lorenz and Mansfeld [43], these triazole compounds inhibited the mild steel electrode by interface inhibition mechanism where two dimensional layers adsorbed on the corroding surface electrode. It presumes a strong interaction between the iron substrate and the inhibitor resulting in reducing the iron dissolution to more than 95% in the case of 1(benzyl) 1-H- 4,5 dibenzoyl 1,2,3 triazole.

Assumption is that, the nitrogen atoms of the inhibitor compound are adsorbed at the interface on the metal surface, where the adsorbed portion is in equilibrium with the dissolved portion present in the solution. The other part of the molecule also expected to be incorporated into the double layer and reinforce the adsorbed film [36].

6.3 FACTORS INFLUENCING THE INHIBITION EFFICIENCY OF THE TRIAZOLE COMPOUNDS

Several structural and chemical factors determine the effectiveness of these inhibitors. For example, as the electron density

[42,50] or electron donation ability of the reacting center atom or atoms increase, the strength of the adsorption bond and the inhibition efficiency will increase [6]. This could be achieved through:

- 1-Increasing the aromaticity and /or conjugated bonding [54].
- 2- Introducing electron donating substituents
- 3- Increase of the heterocyclic aromaticity [28,35,54]
- 4- Adding some substituents that increase the electronic density at the central atom by increasing the inductive effects and polarizability [4,52].

APPENDIX 1

DATA OBTAINED FROM ON- LINE LINEAR POLARIZATION

File name: SECOND25.DAT

Inhibitor:	2nd at 25ppm in 1%HCl
Experimental Duration:	906 Minutes
Corrosion Technique:	Linear Polarization Resistance
Measurement Procedure:	Normal
Cathodic Tafel Constant:	170.0 mV
Anodic Tafel Constant:	170.0 mV
Electrode Type:	Rotating Cylinder
Exposed Diameter:	1.22 cm
Exposed Length:	1.22 cm
Exposed Surface Area:	4.599 cm²
Metal Type:	MILDSTEEL
Molecular Weight:	55.847 grams/mole
Density:	7.860 grams/cc
Electrode Lost:	2

File Name: SECOND25.DAT

CORROSION RATE mpy	CORROSION RATE STATISTICAL FIT R ²	OPEN - CIRCUIT ELECTRODE POTENTIAL mV	CORRODING ELECTRODE AREA cm ²	CORROSION RATE measurement s TIME minutes
0.359955	0.999515	-431.1	4.599602	5.283333
0.710177	0.999911	-445	4.599602	11.75
1.149653	0.998992	-463.8	4.599602	18.216667
1.640918	0.999672	-471.5	4.599601	24.683333
2.099127	0.998321	-475.5	4.5996	31.15
2.476529	0.999487	-479	4.5996	37.6
2.768533	0.998433	-482.5	4.5996	44.066667
3.205623	0.999899	-484.5	4.599599	50.533333
3.596799	0.999563	-489.5	4.599598	57
4.006341	0.996682	-491.5	4.599597	63.466667
4.478324	0.999364	-492.5	4.599596	69.933333
4.834608	0.99949	-494.5	4.599595	76.4
5.200992	0.999248	-496.5	4.599593	82.866667
5.8502	0.998653	-497.5	4.599593	89.333333
6.6298	0.999286	-498.5	4.599591	95.783333
7.043017	0.999418	-499.4	4.599589	102.24167
7.43787	0.998742	-500.5	4.599588	108.7
7.897	0.999266	-502	4.599586	115.16667
8.45714	0.999539	-502.3	4.599584	121.633333
9.081559	0.999249	-503	4.599581	128.1
9.448866	0.997727	-503.6	4.59958	134.56667
10.183477	0.998631	-504.1	4.599577	141.033333
10.761984	0.998211	-505	4.599574	147.5
11.680249	0.999407	-505	4.599572	153.96667
12.249577	0.998957	-506	4.599569	160.433333
13.01174	0.999089	-506	4.599566	166.9
13.865732	0.999606	-506.1	4.599562	173.36667

14.701359	0.999679	-506.5	4.599559	179.83333
15.390067	0.99992	-507	4.599555	186.3
16.308342	0.999761	-507.1	4.599551	192.76667
16.932774	0.999998	-507	4.599547	199.23333
17.869419	0.999897	-507.8	4.599543	205.7
18.778517	0.999996	-508.5	4.599539	212.15
19.430504	0.99996	-509	4.599534	218.61667
20.192686	0.999938	-509	4.59953	225.06667
20.927321	0.999998	-509	4.599524	231.53333
21.515036	0.999785	-509.5	4.59952	237.99167
22.139483	0.999903	-510	4.599515	244.45
22.736385	0.999928	-510	4.599509	250.91667
23.324106	0.999716	-510.7	4.599504	257.38333
23.88428	0.999765	-511	4.599498	263.85
24.269985	0.999945	-511	4.599493	270.3
24.719971	0.999986	-511.6	4.599486	276.76667
24.940389	0.999537	-512	4.599481	283.23333
25.482205	0.999754	-512.3	4.599474	289.68333
25.84955	0.999915	-513	4.599469	296.15
26.400553	0.999751	-513	4.599462	302.60833
26.538331	0.99998	-513.2	4.599455	309.06667
26.823035	0.999918	-514	4.59945	315.525
27.254666	0.999995	-514	4.599443	321.98333
27.603652	0.999957	-514	4.599436	328.43333
27.7598	0.999658	-514.7	4.599429	334.9
27.915949	0.999826	-515	4.599424	341.35833
28.430231	0.999919	-515	4.599417	347.81667
28.292529	0.999981	-515.2	4.59941	354.26667
28.595607	0.999819	-516	4.599403	360.73333
28.97215	0.99987	-516.1	4.599396	367.18333
28.659973	0.999726	-516.2	4.59939	373.65
29.247725	0.999788	-517	4.599383	380.10833
29.110024	0.999965	-517	4.599376	386.56667
29.284544	0.999995	-517	4.599369	393.01667
29.25704	0.99995	-517.2	4.599362	399.48333
29.587673	0.999987	-518	4.599355	405.93333

29.817294	0.999644	-518	4.599348	412.4
29.826523	0.999931	-518	4.599341	418.85
29.707189	0.999967	-518.6	4.599334	425.31667
29.945994	0.99994	-519	4.599327	431.76667
29.881759	0.999993	-519.1	4.599319	438.23333
29.92772	0.999883	-520	4.599312	444.68333
30.037964	0.99993	-520	4.599305	451.15
29.992095	0.999861	-520.8	4.599298	457.6
30.093156	0.999935	-520.5	4.599291	464.06667
30.185034	0.999881	-521	4.599284	470.525
30.249363	0.999804	-521	4.599277	476.98333
30.212678	0.999768	-521.5	4.599269	483.43333
29.872946	0.99997	-522	4.599262	489.9
30.03829	0.999247	-522.3	4.599255	496.35
30.139352	0.999858	-522.7	4.599248	502.81667
30.047567	0.999293	-522.7	4.599241	509.275
30.313928	0.999469	-522.7	4.599234	515.73333
30.286426	0.999823	-523	4.599227	522.19167
29.781392	0.999837	-523.4	4.59922	528.65
30.09367	0.999991	-524	4.599212	535.11667
30.1029	0.999986	-524	4.599205	541.56667
29.735614	0.999856	-524.1	4.599198	548.03333
29.763209	0.999542	-524.7	4.599191	554.48333
30.020389	0.998708	-524.8	4.599184	560.95
29.882685	0.999737	-525	4.599177	567.40833
29.671513	0.999656	-525.2	4.59917	573.86667
29.754209	0.99967	-525.5	4.599163	580.325
29.442019	0.999811	-526	4.599156	586.78333
29.359413	0.999986	-526.3	4.599149	593.25
29.31354	0.999627	-527	4.599142	599.7
29.047264	0.999822	-527	4.599135	606.15833
29.240161	0.99995	-527.2	4.599128	612.61667
28.918782	0.999987	-527.8	4.599121	619.08333
28.854541	0.99964	-528	4.599114	625.53333
28.808667	0.999829	-528	4.599108	631.99167
28.569938	0.99995	-528.9	4.599101	638.45

28.955688	0.999731	-528.5	4.599094	644.90833
28.781244	0.999568	-528.7	4.599087	651.36667
28.551698	0.999854	-528.9	4.59908	657.83333
28.340518	0.999976	-529	4.599073	664.28333
28.26709	0.999971	-529	4.599067	670.74167
27.817135	0.999487	-529	4.59906	677.2
28.019214	0.99988	-530	4.599054	683.66667
27.964153	0.999783	-530	4.599047	690.11667
27.826439	0.999828	-530	4.59904	696.575
27.844846	0.999975	-530	4.599034	703.03333
27.367335	0.999902	-530.3	4.599027	709.5
27.440843	0.999867	-530	4.599021	715.95
27.523535	0.999936	-530	4.599014	722.40833
27.551125	0.999895	-530	4.599008	728.86667
27.643002	0.999822	-530	4.599001	735.33333
27.211405	0.999066	-530	4.598995	741.79167
27.27573	0.999918	-529.9	4.598988	748.25
26.972704	0.999176	-529.6	4.598982	754.70833
27.000293	0.999975	-529.5	4.598975	761.16667
27.04625	0.999959	-529.4	4.598969	767.63333
26.596281	0.999921	-529.6	4.598963	774.08333
26.734075	0.999825	-530	4.598956	780.54167
26.660641	0.999746	-530	4.59895	787
26.679045	0.999943	-530.1	4.598944	793.45833
26.743369	0.999858	-530.9	4.598937	799.91667
26.458707	0.999936	-530.1	4.598931	806.375
26.238329	1	-530.4	4.598925	812.83333
26.100607	0.999985	-530.5	4.598919	819.29167
26.376159	0.99995	-530.9	4.598912	825.75
26.220068	0.999878	-531.4	4.598906	832.21667
26.11908	0.999889	-531.7	4.5989	838.66667
26.08238	0.9998	-531.6	4.598894	845.13333
26.008943	0.999924	-532	4.598888	851.59167
25.981426	0.999992	-532	4.598881	858.04167
26.128405	0.999877	-532	4.598875	864.5
25.935576	0.999952	-532	4.598869	870.95833

25.972347	0.999429	-532.1	4.598863	877.41667
25.788702	0.999821	-532	4.598857	883.875
25.88976	0.999969	-532.5	4.598851	890.33333
25.660194	0.999904	-532.8	4.598844	896.8
25.917381	0.99952	-532.8	4.598838	903.25
25.696998	0.999855	-532.5	4.598832	909.71667

NOMENCLATURE

α	Symmetry Coefficient
β_a	Anodic Tafel Constant
β_c	Cathodic Tafel Constant
δ	Thickness of the Diffusion Layer
η	Overpotential or Overvoltage
η_a	Activation Polarization
η_c	Concentration Polarization
ω	Angular Frequency
A	Area
a	Activities
C_o	Corrosion Rate in the Absence of the Inhibitor
C_i	Corrosion Rate in the Presence of the Inhibitor
d	Density
E	Half-cell Potential
E_o	Standard Half-cell Potential
E_{app}	Apply Potential
E_{Corr}	Corrosion Potential
E.W	Equivalent Weight
F	Faraday Constant
I_{anodic}	Anodic Current
I_{cathodic}	Cathodic Current

I_{Corr}	Corrosion Current
I_{MEAS}	Measured Current
I_0	Exchange Current and equal to I_{Corr}
$I_{\text{O.M}}$	Oxidation Current of the Metal
$I_{\text{R.Z}}$	Reduction Current of the Z
mpy	Miles Per Year
n	Number of Electrons Transferred
R	Gas Constant
R_s	Solution Resistance or Uncompensated Electrolyte Resistance
R_p	Polarization Resistance
T	Absolute Temperature
Z'	Real impedance
Z''	Imaginary Impedance

REFERENCES

1. Padwa, Albert "1,3 Dipolar Cycloaddition chemistry" Vol. 1 & 2 John Wiley & sons, 1984.
2. Hackerman N., **Materials Performance**, Vol. 29, No. 2, pp;44-47, 1990.
3. Chadwick D., and Hashemi T., **Corrosion Science**, Vol. 18, pp 39-51, 1978.
4. Stupnisek-Lisac E., Metikos-Hukovic M., Lencic D., Vorkapic-Furac J., and Berkovic K., **Corrosion** , Vol. 48, No.11, pp; 924-930, 1992.
5. Antropov L. I., **Corrosion Science**, Vol. 7, pp; 607-620, 1967.
6. Abd-El-Nabey B., shaban M., and Essa M., **6th European Symposium on Corrosion Inhibitors**, Ferrara, Italy, 16th-20th September, 1985, pp;295-315.
7. Thibault S., **Corrosion Science**, Vol. 17, pp;701-709, 1977.
8. Aramaki K., and nishihara H., **6th European Symposium on Corrosion Inhibitors**, Ferrara, Italy, 16th-20th September, 1985.
9. Abu Orabi S.T., Jibril J., Ali A., Shahateet S., and Atfah M., **J. Heterocyclic Chem.**, submitted for publication.
10. Keij F., de Graaff A., Haasnoot J., and Reedijk J., **J. Chem. Soc. Dalton Trans.**, pp;2093-2097, 1984.
11. Ogle I.C.G and Poling G.W., **Canadian Metallurgical Quarterly**, Vol. 14, No. 1, pp;37-46, 1975.

12. Youda R., Nishihara H., and Aramaki K., **Corrosion Science**, Vol. 28, pp. 87-96, 1988.
13. AbdelRahman A.H., **Corrosion**, Vol. 47, No. 6, pp: 424-428, 1991.
14. Lewis G., **Br. Corrosion. J.**, Vol. 16, No. 3, pp; 169-171, 1981.
15. Mansfeld F., Smith T., and Parry E.P., **Corrosion**, Vol. 27, No. 7, pp; 289-294, 1971.
16. Walker R., **Corrosion**, Vol. 31, No. 3, pp; 97-100, 1975.
17. Fox P.G., and Bradley, **Corrosion Science**, Vol 20, pp 643-649, 1980.
18. Wu J.S. and Nobe Ken, **Corrosion**, Vol. 37, No. 4, pp; 223-225, 1981.
19. El-Taib Heakal F., and Haruyama S., **Corrosion Science**, Vol. 20, pp. 887-898, 1980.
20. Al-Kharafi F.M., Al-Hajjar F.H., and Katrib A., **Corrosion Science**, Vol. 26, No. 4, pp 257-264, 1986.
21. Aramaki K., Kiuchi T., Sumiyoshi T., and Nishihara H., **Corrosion Science**, Vol. 32, No. 5/6, pp 593-607, 1991.
22. da Costa S., Agostinho s., Chagas H., and Rubim J., **Corrosion**, Vol. 43, No. 3, pp; 149-153, 1987.
23. Wippermann K., Schultze J., Kessel R., and Penninger J., **Corrosion Science**, Vol. 32, No. 2, pp; 205-230, 1991.
24. Chin R.J., Altura D., and Nobe K., **Corrosion**, Vol. 29, No. 5, pp; 185-187, 1973.
25. Al-Hajjar F.H., **Corrosion Science**, Vol. 28, No. 2, pp. 163-171, 1988.

26. Ohsawa M, and Suetaka W. , **Corrosion Science**, Vol. 19, pp. 709-722, 1979.
27. S. Kertit J. ,A. Srhiri A., El-kacemi K., and Etman m. , **J. of Applied Electrochemistry**, Vol. 23, pp; 835-840, 1993.
28. Granese S.L., Rosales B.M., Oviedo C., and Zerbino J.O., **Corrosion Science**, Vol. 33, No. 9, pp. 1439-1453, 1992.
29. El-Anadouli Bahgat E., **Corrosion Science**, Vol. 34, No. 5, pp. 779-784, 1993.
30. Raicheva S.N. Aleksiev B. V., and Sokolova E.I., **Corrosion Science**, Vol. 34, No. 2, pp. 343-350, 1993.
31. Subramanyam N. C. Sheshadri B.S., and Mayanna S.M., **Corrosion Science**, Vol. 34, No. 4, pp. 563-571, 1993.
32. Banerjee G., and Malhotra S.N., **Corrosion**, Vol. 48, No.1, pp; 10-15, 1992.
33. Al-Abdallah M.M., and Abu-Orabi S.T., **Anti-Corrosion**, Oct., pp;4-6, 1989.
34. Al-Abdallah M.M., Tashtoush H., Al-Talib M., and Al-Omari M., **Corrosion**, Vol.47, No.6, pp;449-452, 1991.
35. Al-Abdullah M. M., and Abu- Orabi, **Korrosion**, Vol. 22, pp; 150-154, 1991
36. Gad Allah A.G. and Tamous H., **J. of Applied Electrochemistry**, Vol.20, pp;488-493, 1990.
37. Barbosa M. A., **6th European Symposium on Corrosion Inhibitors**, Ferrara, Italy, 16th-20th September, 1985,pp;613-625.
38. Botta A., Kuron D., and Rother H., **6th European Symposium on Corrosion Inhibitors**, Ferrara, Italy, 16th-20th September, 1985, pp;105-115.

39. Mercer, A. D., **6th European Symposium on Corrosion Inhibitors**, Ferrara, Italy, 16th-20th September, 1985 , pp:729-740.
40. Mitchell, John Jr., " **Applied Polymer Analysis and Characterization** " vol. 2, hanser, 1991.
41. Sayed S. M., Ashour E. A., and Ateya B. G., **Corrosion Science**, Vol. 36, No. 2, pp. 221- 230, 1994.
42. Aramaki Kunitsugu, **5th European Symposium on Corrosion Inhibitors**, Ferrara, Italy,15th- 19th September,1980 , pp:267- 285.
43. Lorenz W.,and Mansfeld F., **6th European Symposium on Corrosion Inhibitors**, Ferrara, Italy, 16th-20th September, 1985 , pp:23-40.
44. Dean S. W., Derby R., and Von dem Bussche G., **Corrosion/81**, Toronto, Ontario, Canada, April 6-10, 1981, Paper # 253.
45. Robinson J. S., "Corrosion inhibitors; recent developments" Chemical technology review No. 132, Noyes data corporation, Newjersey, USA 1979.
46. Mansfeld F., Kendig M.W., and Lorenz W., **J. Electrochem. Soc.**, Vol.132, No.2, 1985, pp:290-296.
47. Stern M. and Geary A., **J. Electrochem. Soc.**, Vol.104, No.1, 1957, pp:56-63.
48. Stern Milten, **J. Electrochem. Soc.**, Vol.104, No.11, 1957, pp:645-650.
49. Abdel Wanees S., **Anti-corrosion methods and materials**, Vol. 41, No. 1, 1994, pp: 3-7.
50. Kaesche H., and Hackerman N., **J. Electrochem. Soc.**, Vol.105, 1958, pp:191

51. Dupin P., Vilorio D.A., deSavignac A., Lattes A., Sutter B., and Haicour Ph., **5th European Symposium on Corrosion Inhibitors**, Ferrara, Italy, 15th- 19th September, 1980 , pp;301-
52. TrabANELLI G., and Carassiti V., " Mechanism and phenomenology of organic inhibitors" , *Advances in corrosion science and technology*, Vol. 1, M. G. Fontanna and R. W. Stachle, Ed., Plenum Press, New York, 1970, pp-147-228.
53. Cox P. F., Every R. L., and riggs, Jr. O. L., *Corrosion*, Vol.20 , No.9, pp;299t , 1964.
54. Nathan C. C., " Corrosion Inhibitors " Ed., NACE, Texas, 1973, pp: 1- 33.
55. Szklarska Z. Smialowska, "Corrosion Inhibition " Hausler R. H., Ed., NACE, Texas, 1988, pp: 1-6.
56. Thomas Edward O' Loughlin., "Determination of Tafel constants in nonlinear polarization curves. " ,Naval Postgraduate School, Monterey, CA., Dec. 1987.
57. Uhlig Herbert H., and Revie R. Winston., "Corrosion and corrosion control; An introduction to corrosion science and engineering" 3rd Ed., Awiley- Interscience Publication, John Wiley & sons, Inc. 1985.
58. Fontana Mars G., "Corrosion Engineering" 3rd Ed., Mc Graw- Hill, Inc, 1986.
59. Pourbaix M., "Lectures on electrochemical corrosion" , Plenum Press, New York, 1973.
60. West J. M., " Basic Corrosion and Oxidation" Ellis Horwood Limited, 1980, Chichester, England.
61. Lorenz W.,and Mansfeld F., *Corrosion Science*, Vol. 21, No. 9, pp. 647- 672, 1981.

62. Donahue Francis M., **Corrosion/81**, Toronto, Ontario, Canada, April 6-10, 1981, Paper # 249.
63. Kuznetsov Yu, Oleynik S., Andreev N., and Vesely S., **6th European Symposium on Corrosion Inhibitors**, Ferrara, Italy, 16th-20th September, 1985 , pp;567-577.
64. Baboian R., " Electrochemical Techniques" Ed., NACE, Texas, 1986.
65. " Corrosion Basics: An Introduction" Ed., NACE, Texas, 1984.
66. Webster S., Harrop D., McMahon A., and Partridge G., **CORROSION/ 93** , NACE, paper # 109.
67. Rocchini Gabriele, **Corrosion Science**, Vol. 33, No. 11, pp. 1759-1771, 1992.
68. Annand Robert, **Corrosion**, Vol. 22, No. 8, pp. 215- 228, 1966.
69. " Operating and service manual of model 350A corrosion measurement system" EG&G Princeton Applied Raserarch, 1980.
70. Schweitzer Phill A, P.E., " Corrosion and corrosion protection handbook" 2nd Ed., Marcel Dekker, Inc., new York, 1989.
71. Dawson J., Rothwell A.N., Walsh T.G., Lawson K., and Palmer W., **CORROSION/ 93** , NACE, paper # 108.
72. Grauer R., Moneland P.J., and Pinic, ' A literature review of polarization resistance constant b values for the measurement of corrosion rate" ed. NACE, Texas, 1982.
73. Atkinson J.T.N.and vanDroffelaar H.," corrosion and its control; an introduction to the subject' Ed by NACE, Texas, 1982.

74. EG&G Princeton Applied Research " Application Note Corr -4 ; electrochemistry & corrosion overview and techniques"
75. Abu Orabi S., Adnan Atfah M., Jibril I., Marii F., and Al- Sheikh Ali A., J. Heterocyclic Chem., Vol. 26, Sept, - Oct. , 1989, pp; 1461- 1468.
76. Abu Orabi S., Adnan Atfah M., Jibril I., Marii F., and Al- Sheikh Ali A., **Gazzetta Chimica Italiana.**, Vol. 122, 1992, pp; 29- 33.
77. Rocctin G., **Corrosion**,Vol. 43,No. 6, pp; 326-331, 1987.
78. Bard Allen J. and Faulkner Larry R.," **Electrochemical Methods: Fundamentals & Applications**" John Willey & Sons, New York, 1980.
79. Al- Abdulhadi A. and Boah J., The international conference on chemistry in industry, Organized by ACSAIG and BSE, Bahrain 14-16, Nov. 1992, Vol.2, pp; 659-675.
80. Mansfeld F. **Corrosion**, Vol. 36, No. 5, pp. 301- 307, 1981.
81. Mansfeld F., Kendig M. W.,and Tsai S., **Corrosion**, Vol. 38, No. 11, pp. 570-580, 1982
82. Walter G.W., **Corrosion Science**, Vol. 26, No. , pp. 681-703, 1986.
83. Macdonald D. and Mckuber M. C. H., ' **Electrochemical impedance techniques in corrosion science.**" **Electrochemical corrosion testing**, STP 727, ASTM, Phil. Pa., 1981.
84. Silverman D. C. and Carrico J. E., **CORROSION/ 87** , NACE, Sanfrancisco, Ca., paper # 269, 1987.